

IMPLEMENTATION OF COMB FILTERS
BY SAMPLED ANALOG TECHNIQUES

Bruce Richard Freund

DUDLEY KNOX LIBRARY
NAVAL POSTGRADUATE SCHOOL
MONTEREY, CALIFORNIA 93940

NAVAL POSTGRADUATE SCHOOL

Monterey, California



THESIS

IMPLEMENTATION OF COMB FILTERS
BY
SAMPLED ANALOG TECHNIQUES

by

Bruce Richard Freund

June 1975

Thesis Advisor:

T.F. Tao

Approved for public release; distribution unlimited.

9602
T168500

| REPORT DOCUMENTATION PAGE | | READ INSTRUCTIONS BEFORE COMPLETING FORM |
|--|-----------------------|---|
| 1. REPORT NUMBER | 2. GOVT ACCESSION NO. | 3. RECIPIENT'S CATALOG NUMBER |
| 4. TITLE (and Subtitle) Implementation of Comb Filters by Sampled Analog Techniques | | 5. TYPE OF REPORT & PERIOD COVERED Master's Thesis; June 1975 |
| 7. AUTHOR(s) Bruce Richard Freund | | 6. PERFORMING ORG. REPORT NUMBER |
| 9. PERFORMING ORGANIZATION NAME AND ADDRESS Naval Postgraduate School Monterey, California 93940 | | 8. CONTRACT OR GRANT NUMBER(s) |
| 11. CONTROLLING OFFICE NAME AND ADDRESS Naval Postgraduate School Monterey, California 93940 | | 10. PROGRAM ELEMENT, PROJECT, TASK AREA & WORK UNIT NUMBERS |
| 14. MONITORING AGENCY NAME & ADDRESS (if different from Controlling Office) | | 12. REPORT DATE June 1975 |
| | | 13. NUMBER OF PAGES 154 |
| | | 15. SECURITY CLASS. (of this report) Unclassified |
| | | 15a. DECLASSIFICATION/DOWNGRADING SCHEDULE |
| 16. DISTRIBUTION STATEMENT (of this Report) Approved for public release; distribution unlimited. | | |
| 17. DISTRIBUTION STATEMENT (of the abstract entered in Block 20, if different from Report) | | |
| 18. SUPPLEMENTARY NOTES | | |
| 19. KEY WORDS (Continue on reverse side if necessary and identify by block number) Comb Filters Sampled Analog Filters | | |
| 20. ABSTRACT (Continue on reverse side if necessary and identify by block number) The design of sampled analog filters using Z-transform techniques developed in digital filter theory is studied. Both recursive and non-recursive algorithms are implemented and analyzed. Some deviations from theoretical frequency responses are noted. An analog Fourier transformer is | | |

(20. ABSTRACT Continued)

constructed by cascading a recursive comb filter and a non-recursive bandpass filter.

Implementation of Comb Filters
by
Sampled Analog Techniques

by

Bruce Richard Freund
Ensign, United States Navy
B.S., Oregon State University, 1974

Submitted in partial fulfillment of the
requirements for the degree of

MASTER OF SCIENCE IN ELECTRICAL ENGINEERING

from the

NAVAL POSTGRADUATE SCHOOL
June 1975

Thesis

ABSTRACT

The design of sampled analog filters using Z-transform techniques developed in digital filter theory is studied. Both recursive and non-recursive algorithms are implemented and analyzed. Some deviations from theoretical frequency responses are noted. An analog Fourier transformer is constructed by cascading a recursive comb filter and a non-recursive bandpass filter.

TABLE OF CONTENTS

| | | |
|------|---|----|
| I. | INTRODUCTION ----- | 12 |
| II. | SAMPLED ANALOG RECURSIVE FILTER ----- | 18 |
| | A. THEORY ----- | 18 |
| | 1. Standard Z-Transform ----- | 20 |
| | a. First-Order Low Pass Filter ----- | 20 |
| | b. Second-Order Low Pass Filter ----- | 22 |
| | c. First-Order High Pass Filter ----- | 23 |
| | d. Second-Order High Pass Filter ----- | 24 |
| | 2. Bilinear Z-Transform ----- | 25 |
| | a. First-Order Low Pass Filter ----- | 26 |
| | b. Second-Order Low Pass Filter ----- | 27 |
| | c. High Pass Filters ----- | 28 |
| | d. Advantages of Bilinear Z-Transform ----- | 28 |
| | 3. Sampling Effects ----- | 29 |
| | B. EXPERIMENT ----- | 31 |
| | 1. System Configuration ----- | 31 |
| | 2. Experimental Frequency Response ----- | 32 |
| III. | SAMPLED ANALOG NON-RECURSIVE FILTER ----- | 70 |
| | A. THEORY ----- | 70 |
| | B. EXPERIMENT ----- | 74 |
| | 1. System Configuration ----- | 74 |
| | 2. Observations ----- | 76 |
| IV. | SAMPLED ANALOG FOURIER TRANSFORMER ----- | 90 |
| | A. THEORY ----- | 90 |
| | B. EXPERIMENT ----- | 91 |

| | | |
|------------|---|-----|
| V. | CONCLUSIONS ----- | 96 |
| APPENDIX A | Derivation of Filter Transfer Function --- | 97 |
| APPENDIX B | Recursive Filter Design ----- | 99 |
| APPENDIX C | Derivation of Calibration Curve for Recursive Filter Coefficients ----- | 121 |
| APPENDIX D | Determination of Transfer Function Coefficients from Unit Step Response ----- | 124 |
| APPENDIX E | Programs to Calculate the Recursive Filter Coefficients from the Unit Step Response ----- | 130 |
| APPENDIX F | Computer Generation of Theoretical Recursive Filter Frequency Response ----- | 133 |
| APPENDIX G | Non-Recursive Filter Design ----- | 136 |
| APPENDIX H | Computer Calculation of Coefficients and Tapping Resistances for the Non-Recursive Filter ----- | 141 |
| APPENDIX I | Computer Calculation of Non-Recursive Filter Frequency Response ----- | 145 |
| APPENDIX J | Effects of Hamming Weighting ----- | 149 |
| | LIST OF REFERENCES ----- | 153 |
| | INITIAL DISTRIBUTION LIST ----- | 154 |

LIST OF TABLES

| | | |
|-------|--|-----|
| I. | Summary of Recursive Filter Cut-Off Frequencies - | 69 |
| II. | Non-Recursive Filter Coefficients and Tapping Resistance Values ----- | 77 |
| III. | Summary of Observed Non-Recursive Filter Parameters ----- | 77 |
| IV. | Theoretical and Observed Q ----- | 88 |
| V. | Fourier Component Isolation ----- | 95 |
| VI. | First-Order Standard Z Low Pass Filter ----- | 104 |
| VII. | b_1 Versus μ ----- | 106 |
| VIII. | First-Order Standard Z High Pass Filter ----- | 107 |
| IX. | Second-Order Standard Z Low Pass Filter ----- | 110 |
| X. | First-Order Bilinear Z Filters ----- | 113 |
| XI. | Second-Order Bilinear Z Filters ----- | 117 |
| XII. | First-Order Filter Design Summary ----- | 120 |
| XIII. | Recursive Coefficient Calibration Curve ----- | 123 |
| XIV. | Unit Step Response ----- | 126 |

LIST OF FIGURES

| | | |
|------|--|----|
| 1.1 | Signal to Noise Ratio Improvement by Use of a Comb Filter ----- | 13 |
| 1.2 | Sampled Low Pass Filter ----- | 14 |
| 1.3 | Sampled High Pass Filter as a Canceller ----- | 15 |
| 2.1 | Second-Order Recursive Filter ----- | 18 |
| 2.2 | ω_c vs b_1 ----- | 21 |
| 2.3 | ω_c vs b_1 ----- | 23 |
| 2.4 | ω_c' vs b_1 ----- | 27 |
| 2.5 | ω_c' vs b_1 ----- | 28 |
| 2.6 | Repetitious Frequency Response ----- | 30 |
| 2.7 | First-Order Recursive Filter ----- | 31 |
| 2.8 | Coefficient Calibration Curve ----- | 32 |
| 2.9 | b_1 vs μ ----- | 34 |
| 2.10 | Theoretical and Observed Frequency Response of Standard Z Low Pass Filter; $b_1 = -0.3$ ----- | 39 |
| 2.11 | Theoretical and Observed Frequency Response of Standard Z Low Pass Filter; $b_1 = -0.7$ ----- | 42 |
| 2.12 | Theoretical and Observed Frequency Response of Standard Z High Pass Filter; $b_1 = 0.3$ ----- | 45 |
| 2.13 | Theoretical and Observed Frequency Response of Standard Z High Pass Filter; $b_1 = 0.7$ ----- | 48 |
| 2.14 | Theoretical and Observed Frequency Response of Bilinear Z Low Pass Filter; $b_1 = -0.7$ ----- | 51 |
| 2.15 | Theoretical and Observed Frequency Response of Bilinear Z Low Pass Filter; $b_1 = 0.0$ ----- | 54 |
| 2.16 | Theoretical and Observed Frequency Response of Bilinear Z Low Pass Filter; $b_1 = 0.3$ ----- | 57 |
| 2.17 | Theoretical and Observed Frequency Response of Bilinear Z Low Pass Filter; $b_1 = 0.7$ ----- | 60 |

| | | |
|------|--|----------|
| 2.18 | Theoretical and Observed Frequency Response of Bilinear Z High Pass Filter; $b_1 = -0.3$ | ----- 63 |
| 2.19 | Theoretical and Observed Frequency Response of Bilinear Z High Pass Filter; $b_1 = -0.7$ | ----- 66 |
| 3.1 | Implementation of a Non-Recursive Filter | ----- 72 |
| 3.2 | Rectangular Bandpass Filter Response | ----- 73 |
| 3.3 | TAD-12 Delay Configuration | ----- 74 |
| 3.4 | Non-Recursive Filter Set-Up | ----- 75 |
| 3.5 | Theoretical and Observed Frequency Response; $f_o = \frac{1}{4}f_s, f_c = 50$ kHz | ----- 78 |
| 3.6 | Theoretical and Observed Frequency Response; $f_o = \frac{1}{4}f_s, f_c = 50$ kHz, Magnitude in dB | ----- 79 |
| 3.7 | Theoretical and Observed Frequency Response; $f_o = \frac{1}{4}f_s, f_c = 100$ kHz | ----- 80 |
| 3.8 | Theoretical and Observed Frequency Response; $f_o = \frac{1}{4}f_s, f_c = 100$ kHz, Magnitude in dB | ----- 81 |
| 3.9 | Theoretical and Observed Frequency Response; $f_o = \frac{1}{2}f_s, f_c = 50$ kHz | ----- 82 |
| 3.10 | Theoretical and Observed Frequency Response; $f_o = \frac{1}{2}f_s, f_c = 50$ kHz, Magnitude in dB | ----- 83 |
| 3.11 | Theoretical and Observed Frequency Response; $f_o = \frac{1}{2}f_s, f_c = 100$ kHz | ----- 84 |
| 3.12 | Theoretical and Observed Frequency Response; $f_o = \frac{1}{2}f_s, f_c = 100$ kHz, Magnitude in dB | ----- 85 |
| 3.13 | Two-Sided Impulse Response | ----- 87 |
| 4.1 | Sampled Analog Fourier Transformer | ----- 90 |
| 4.2 | Observed Frequency Response | ----- 94 |
| A-1 | Filter System | ----- 97 |
| C-1 | Coefficient Circuit | -----121 |
| G-1 | Rectangular Passband Filter | -----136 |
| H-1 | Coefficient Implementation | -----142 |

| | | |
|-----|---|-----|
| J-1 | Fourier Transform of Hamming Function ----- | 149 |
| J-2 | Equal Impulses ----- | 150 |

ACKNOWLEDGEMENT

The author expresses his sincere appreciation to Dr. T.F. Tao for his guidance and assistance in this study, LCDR Stacy Holmes for his assistance, and the other members of the research team for their time and support.

Special recognition is made of the invaluable help of Alicia, Albert, and Alfred Tao.

The cooperation of the technical staff of Reticon Corporation is also recognized.

I. INTRODUCTION

Whether one is extracting information, such as separating signals from noise in a communications system, detecting targets in a radar system, or preparing signals for transmission or display, signal processing is a major portion of system design. This processing may be accomplished by several means, ranging from simple RLC circuits to complex digital computers. Several factors will influence the choice of processing scheme, among these are nature of the signal and noise, desired results, weight, power consumption, cost, and convenience. Each scheme has its own advantages and liabilities.

One such type of signal processing scheme is the discrete time or sampled signal processing. This method utilizes a signal which is sampled at regular intervals. The sampled values are combined with previous and subsequent samples by some algorithm to produce the processed output. Implementations of these algorithms are referred to as sampled filters. Basic Fourier analysis indicates that periodic sampling in time makes the filter response periodic in frequency [1]. Busiginies and Dishal report a sampled filter, developed by Clark, in 1949 [2]. The repetitious nature of the frequency response became useful with the development of radar systems.

A pulsed radar signal has a discrete spectrum, with spectral lines spaced from the carrier frequency at multiples

of the pulse repetition frequency (PRF) [3]. The signal to noise ratio of a received signal could be improved by passing the signal with the noise through a filter with a series of narrow passbands also spaced at the PRF. The signal components would all be passed by the filter while only the noise components close to the signal frequencies would pass. The remaining noise is attenuated by the filter. Such a filter is called a "comb" filter due to the appearance of the passbands as teeth of a comb. Figure 1.1 illustrates the use of a comb filter.

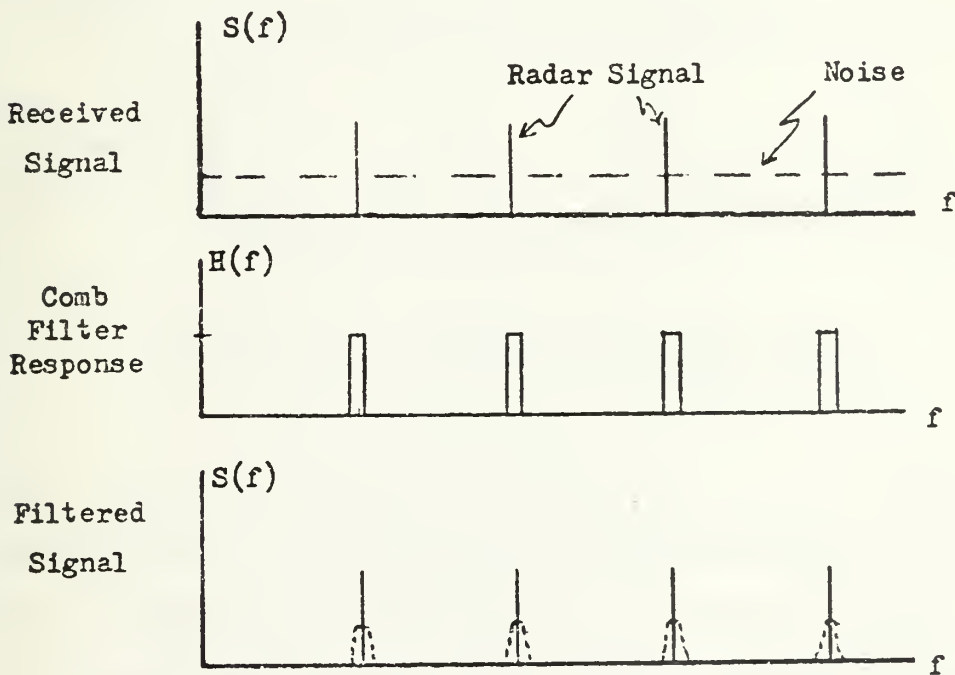


FIGURE 1.1. Signal to Noise Ratio Improvement by Use of a Comb Filter

While it is theoretically possible to build a comb filter out of many individual bandpass filters, maintaining the proper harmonic spacing between them is difficult. A sampled filter will have a frequency response which is periodic at a constant frequency defined as the repetition period, f_s . A low pass sampled filter, as shown in Figure 1.2, will be repeated as a bandpass filter centered at multiples of f_s , hence the sampled low pass filter forms a comb filter.

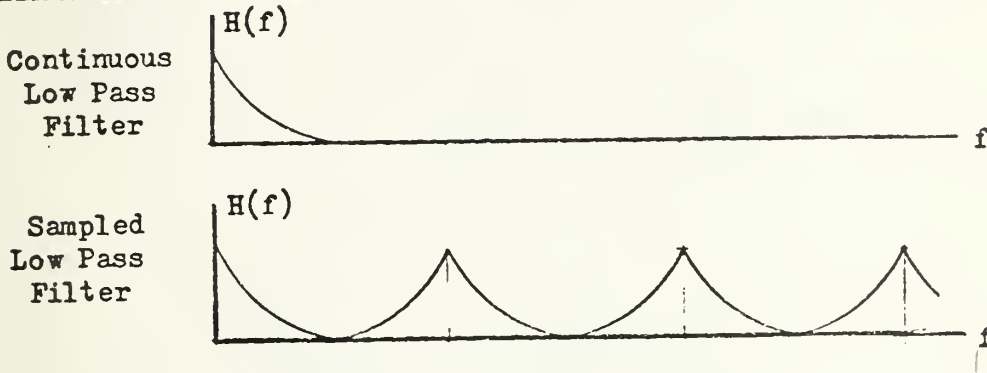


FIGURE 1.2. Sampled Low Pass Filter

For a given continuous low pass filter with a cut-off frequency of f_c , the resulting derived sampled filter will have a bandpass bandwidth of $2f_c$. Since a narrower 'tooth' will reject more noise, the cut-off frequency of the sampled filter should be a small fraction of the repetition period.

Another application for comb filters is found in radar systems which use Doppler shift to detect moving targets.

Moving Target Indicator (MTI) radar uses a repetitious filter to suppress the 'clutter' returns from stationary targets while allowing shifted returns from moving targets to pass. This canceller filter can be implemented by a sampled high pass filter, as illustrated in Figure 1.3.

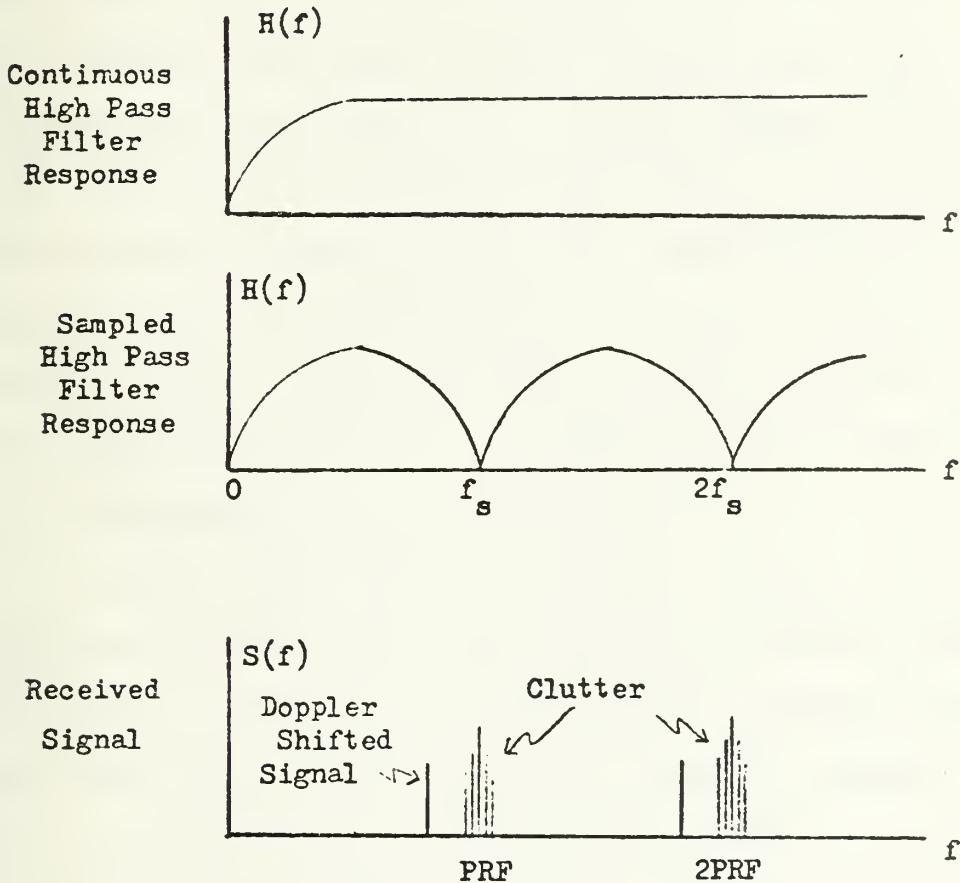


FIGURE 1.3 Sampled High Pass Filter as a Canceller

The sampled implementation of comb filters may be accomplished by a recursive technique where the previous inputs and outputs are weighted and fed-back to the input. The results of recursive algorithms are treated in great

detail by Gold and Rader in Reference 1. The values of the weighting coefficients determine the filter cut-off frequency. Chapter II of this study looks at the details of the relationships between the coefficients and the filter response.

Current literature suggests areas other than radar where comb filters are applicable. Arndt suggests the use of a comb filters for TV signal enhancement in noisy channels [4]. Illetschko and Mavrodieva utilize comb filters in color TV processing of chrominance, luminance, and brightness components [5],[6]. Uses for comb filters in digital controllers are suggested by White [7]. Other areas of application will no doubt emerge with time.

Since a comb filter effectively 'samples' the frequency spectrum of the input signal with its uniformly spaced passbands, information of the signal's spectral content is available in each comb tooth. A tunable bandpass filter used in conjunction with a comb filter would make it possible to isolate the spectral content of a single tooth. Observation of the behavior of that signal spectral component in 'real time' would be possible. Webb indicates that cases where short time variations in spectral components is of interest arise in the aerospace discipline [8].

As will be shown in Chapter III, a tunable bandpass filter can be implemented by sampled techniques. By taking the impulse response of the desired continuous bandpass filter response, sampling it at an interval equal to the

delay between filter outputs, and setting coefficients for weighting the signal samples proportional to the impulse response sample values, one may approximate the continuous filter response. Such a technique is non-recursive. Filters implemented by the non-recursive method are called transversal or finite impulse response (FIR) filters.

The algorithms used in sampled signal processing techniques require the operations of delay (storage), multiplication (weighting), and addition. The sampled signal values may be stored digitally or by analog means. The weighting coefficients must also be stored by one of these means. Either analog or digital methods may be used to implement the arithmetic operations. Until the recent development of charge transport devices (CTD), only sampled digital signals could be stored. Since digital storage and logic hardware has been increasingly available and inexpensive, a great deal of study has been done on the digital implementation of sampled filters, or simply, digital filters. Now analog 'shift registers' are available for implementing sampled analog filters. This study will show that the various Z-transform design methods developed for digital filter theory may be equally well applied to sampled analog signal processors. As a demonstration, a recursive comb filter and a non-recursive bandpass filter will be implemented and cascaded to form an analog Fourier transformer.

II. SAMPLED ANALOG RECURSIVE FILTER

A. THEORY

The block diagram of a recursive sampled filter is illustrated in Figure 2.1. Since this diagram has two delays in that particular configuration, it is referred to as a second-order recursive filter.

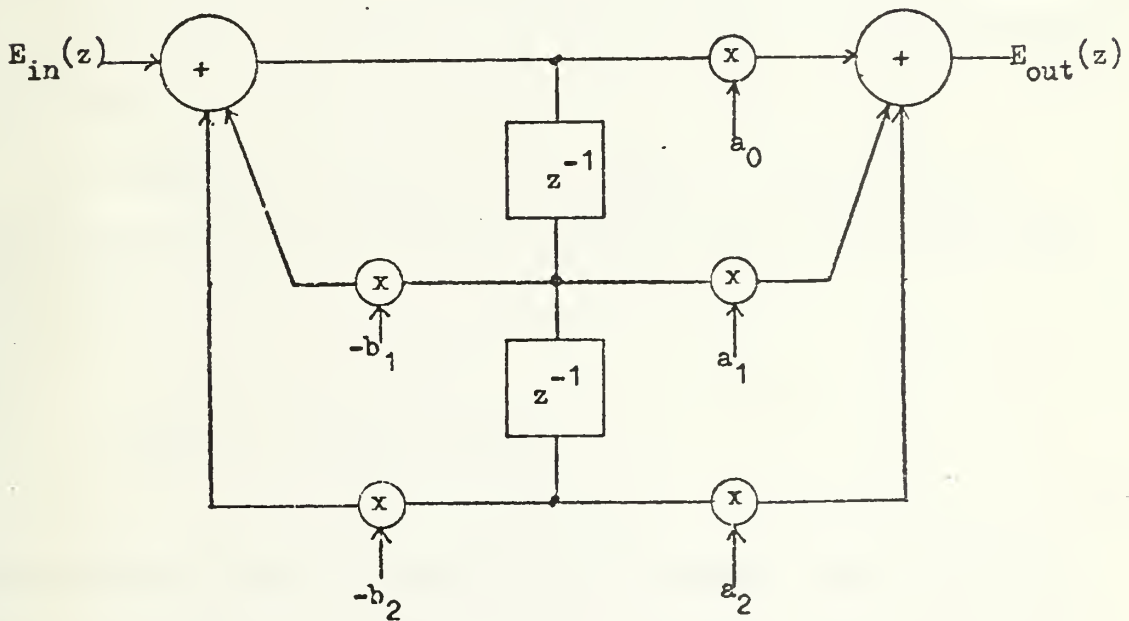


FIGURE 2.1 Second-Order Recursive Filter

Analysis of such a system, performed in Appendix A, indicates that the transfer function, $H(z)$, for this configuration is given by,

$$H(z) = \frac{V_{\text{out}}(z)}{V_{\text{in}}(z)} = \frac{a_0 + a_1 z^{-1} + a_2 z^{-2}}{1 + b_1 z^{-1} + b_2 z^{-2}} ,$$

where z is defined as $e^{j\omega T}$ and T is the time delay.

For the special case where $a_2 = b_2 = 0$, the system becomes a first-order filter. Higher order filters may be obtained by paralleling, cascading, or both, first and second-order sections.

The frequency response of a sampled filter can be determined from its transfer function, $H(z)$, by using the definition of z ,

$$H(j\omega) = H(z) \Big|_{z = e^{j\omega T}} .$$

Analysis performed in Appendix B indicates that the delay terms introduce sine and cosine variations in the frequency response, $H(j\omega)$, which yield a periodic nature. The 'period' of the repetitive response is defined as f_s , where

$$f_s = \frac{1}{T} .$$

Two major design methods are available for determining the transfer function coefficients: the standard Z-transform and the bilinear Z-transform. Both methods will be studied.

1. Standard Z-Transform

The basis for the standard Z-transform comes from the impulse response of the desired filter response, $h(t)$. The impulse response is sampled at the regular interval, T , one time delay, which corresponds to z^{-1} in the Z-domain. The Z-transform is simply a power series in z^{-1} where the coefficients of the series are the sampled impulse response values, or

$$H(z) = \sum_{k=0}^{\infty} h(kT) z^{-k} .$$

For many impulse responses of interest this series can be expressed in closed form. Tables listing these closed forms are called the Z-transform tables. Since the designer often knows the Laplace transfer function, $H(s)$, of the desired filter, some tables are constructed to allow one to bypass the actual impulse response and go directly from $H(s)$ to $H(z)$.

a. First-Order Low Pass Filter

For a simple RC low pass filter, the impulse response is known,

$$h(t) = \omega_c e^{-\omega_c t} ,$$

where $\omega_c = \frac{1}{RC}$, the cut-off frequency. This impulse response has a Z-transform,

$$H(z) = \frac{\omega_c}{1 - e^{-\omega_c T} z^{-1}} .$$

The 3 dB corner frequency, ω_c , is found in Appendix B to be related to the feedback coefficient, b_1 , by the following equation,

$$\frac{\omega_c}{\omega_s} = \frac{1}{2\pi} \cos^{-1} \left(\frac{1 + b_1^2 - 4b_1}{2b_1} \right) ,$$

where $\omega_s \triangleq \frac{2\pi}{T}$. Figure 2.2 illustrates this equation.

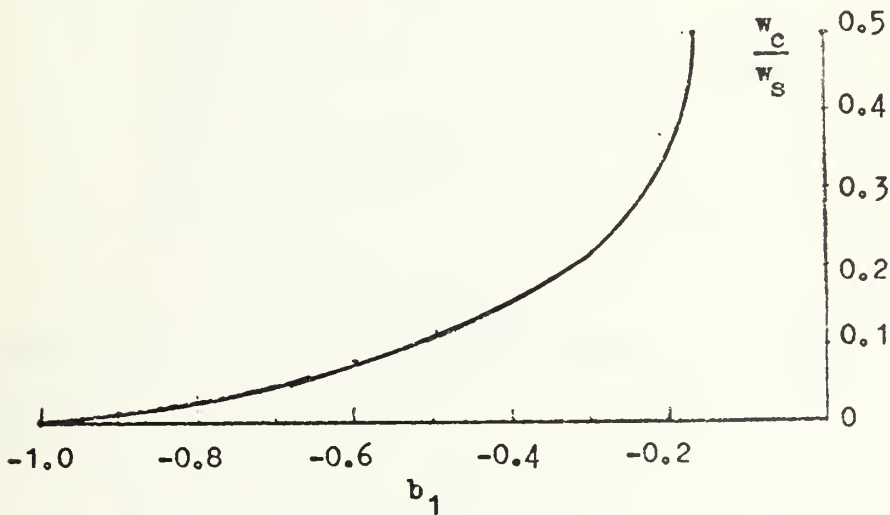


FIGURE 2.2 ω_c vs b_1

For a normalized transfer function, $a_0 = 1$ and $a_1 = 0$.

b. Second-Order Low Pass Filter

The impulse response for a second-order LC low pass filter is,

$$h(t) = \omega_c \sin \omega_c t ,$$

where $\omega_c = (LC)^{-1/2}$. The resulting Z-transform is,

$$H(z) = \frac{\omega_c \sin \omega_c T z^{-1}}{1 - 2\cos \omega_c T z^{-1} + z^{-2}} .$$

For a normalized transfer function,

$$a_0 = 0 ,$$

$$a_1 = 1 ,$$

$$a_2 = 0 ,$$

$$b_1 = -2\cos \omega_c T ,$$

$$b_2 = 1 .$$

ω_c and b_1 are related by the following equation, which is graphed in Figure 2.3,

$$\frac{\omega_c}{\omega_s} = \frac{1}{2\pi} \cos^{-1} \left(\frac{-b_1}{2} \right) .$$

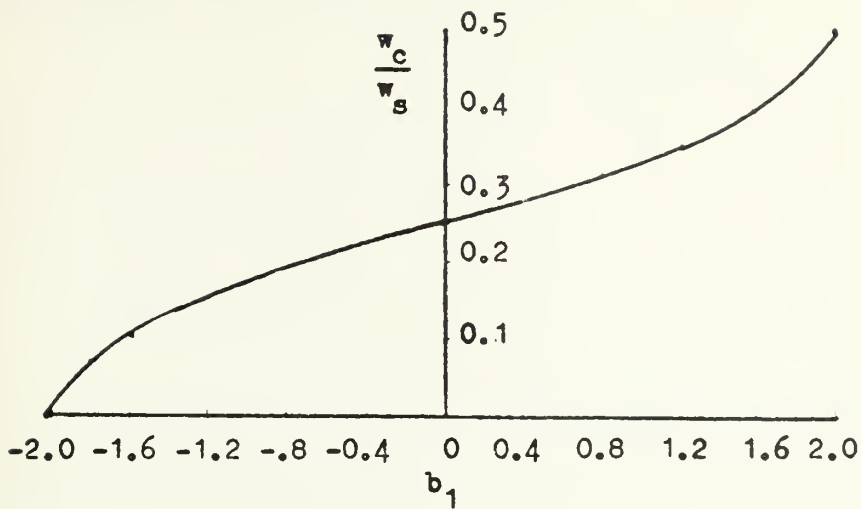


FIGURE 2.3 ω_c vs b_1

c. First-Order High Pass Filter

The impulse response for an RC high pass filter is found in Appendix B to be,

$$h(t) = \delta(t) - \omega_c e^{-\omega_c t} .$$

The resulting Z-transform is,

$$H(z) = \frac{1 - \omega_c e^{-\omega_c T} z^{-1}}{1 - e^{-\omega_c T} z^{-1}} .$$

By inspection, the coefficients are,

$$a_0 = 1 - \omega_c T ,$$

$$a_1 = -e^{-\omega_c T} ,$$

$$b_1 = -e^{-\omega_c T} .$$

Another first-order high pass filter can be constructed from the low pass filter by changing the polarity of b_1 ,

$$H(z) = \frac{1}{1 + e^{-\omega_c T} z^{-1}} .$$

The polarity change has the effect of shifting the response by $\frac{\pi}{T}$, so the new corner frequency is $\frac{\pi}{T} - \omega_c$, where ω_c and b_1 are related by Figure 2.2.

d. Second-Order High Pass Filter

The impulse response for an LC high pass filter is given by,

$$h(t) = (t) - \sin \omega_c t ,$$

where $\omega_c^2 = \frac{1}{LC}$. This yields the following second-order Z-transform,

$$H(z) = \frac{1 - (2\cos \omega_c T + \omega_c \sin \omega_c T) z^{-1} + z^{-2}}{1 - 2\cos \omega_c T z^{-1} + z^{-2}} ,$$

thus,

$$a_0 = 1 ,$$

$$a_1 = -2\cos \omega_c T - \omega_c \sin \omega_c T ,$$

$$a_2 = 1 ,$$

$$b_1 = -2\cos \omega_c T ,$$

$$b_2 = 1 .$$

2. Bilinear Z-Transform

For the bilinear Z-transform, the Laplace transfer function, $H(s)$, is used to determine the Z-transform directly by using the following approximation for s as described in Reference 1,

$$s = \frac{2}{T} \left(\frac{z-1}{z+1} \right) .$$

This formula has the effect of warping the frequency of the desired filter response, $H(j\omega)$, so that,

$$\omega_{\text{bilinear}} = \frac{2}{T} \tan^{-1} \left(\frac{\omega T}{2} \right) .$$

Appendix B shows the precise derivation of this relation.

a. First-Order Low Pass Filter

The transfer function for a single pole low pass filter is,

$$H(s) = \frac{\omega_c}{s + \omega_c} .$$

The result of substitution for s is the bilinear Z-transform,

$$H(z) = \frac{\frac{\omega_c T}{\omega_c T + 2} + \frac{\omega_c T}{\omega_c T + 2} z^{-1}}{1 + \frac{\omega_c T - 2}{\omega_c T + 2} z^{-1}} .$$

A normalized transfer function would have coefficients,

$$a_0 = 1 ,$$

$$a_1 = 1 ,$$

$$b_1 = \frac{\omega_c T - 2}{\omega_c T + 2} .$$

The relationship between the bilinear Z corner frequency, ω_c' , and b_1 is given by the following equation, which is graphed in Figure 2.4,

$$\frac{\omega_c'}{\omega_s} = \frac{1}{\pi} \tan^{-1} \left(\frac{b_1 + 1}{b_1 - 1} \right) .$$

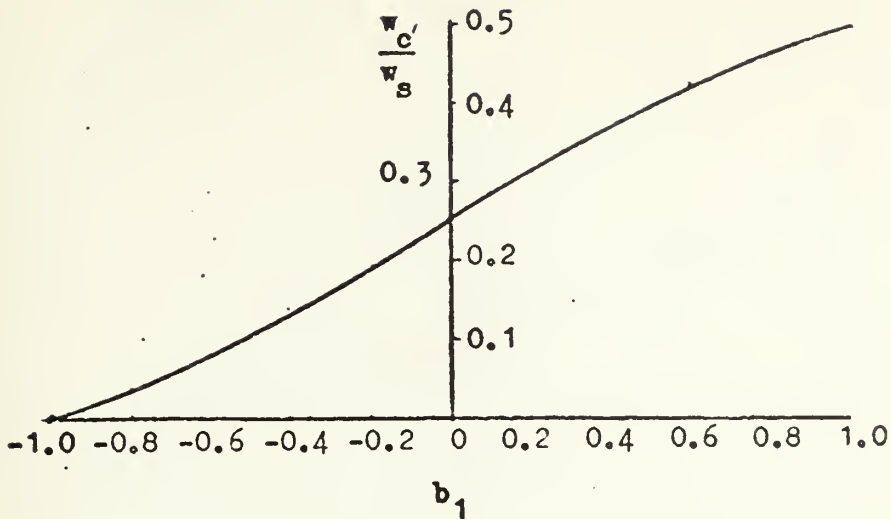


FIGURE 2.4 ω_c , vs b_1

Since $a_0 = a_1$, the bilinear Z low pass filter has a zero for the frequency $\frac{1}{2}\omega_s$, which means the low pass response goes all the way to zero.

b. Second-Order Low Pass Filter

The transfer function for an LC low pass filter is,

$$H(s) = \frac{\omega_c^2}{s^2 + \omega_c^2} ,$$

where $\omega_c = (LC)^{-\frac{1}{2}}$. The resulting normalized bilinear Z-transform is given by

$$H(s) = \frac{1 + 2z^{-1} + z^{-2}}{1 + \left(\frac{2\omega_c^2 T^2 - 8}{\omega_c^2 T^2 + 4} \right) z^{-1} + z^{-2}} .$$

The corner frequency, ω_c , is dependent on b_1 by the following relation, graphed in Figure 2.5,

$$\frac{\omega_{c'}}{\omega_s} = \frac{1}{\pi} \tan^{-1} \left(\frac{2 + b_1}{2 - b_1} \right)^{1/2}$$

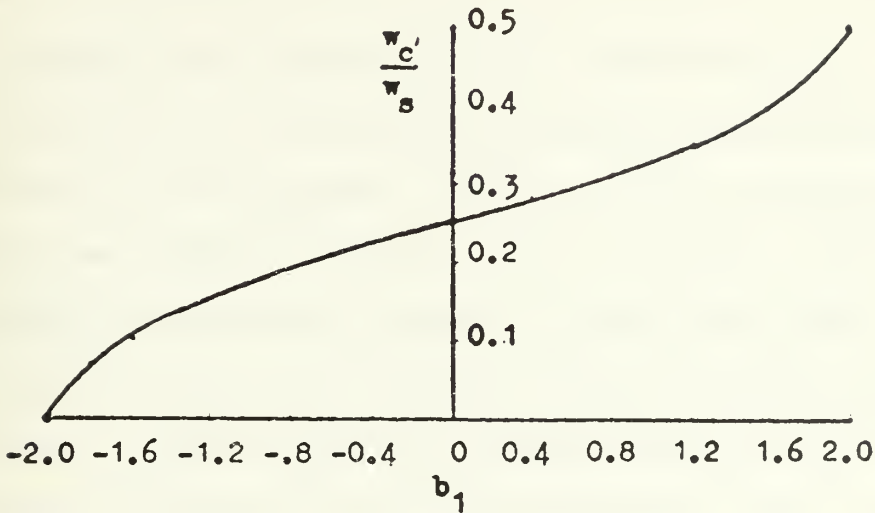


FIGURE 2.5 $\omega_{c'}$ vs b_1

c. High Pass Filters

Analysis performed in Appendix B shows that for the bilinear Z-transform high pass filters, the same form and coefficient values with the exception of the polarity of a_1 as in the low pass case are used. The corner frequencies are found using the same design curves as for the low pass case.

d. Advantages of Bilinear Z-Transform

The bilinear Z-transform design method has advantages over the standard Z-transform. Given a Laplace transfer function, $H(s)$, the Z-transformed transfer function, $H(z)$, can be obtained directly. In addition, the bilinear Z-transform places a zero to force the stop band attenuation

down. The position of this zero may be shifted to transform a high pass filter into a low pass filter, and vice versa, by reversing the polarity of the coefficient, a_1 . The a_i coefficients of a bilinear Z-transform are always integral multiples of one another, reducing design complexity. These advantages occur at a price. The frequency scaling of the bilinear Z-transform response is not linear with the frequency response of $H(s)$, but rather follows a tangent function. As a result of this frequency warping, the bilinear Z-transform frequency response will only approximate that of $H(s)$ for frequencies where,

$$\text{Tan } \frac{\omega}{\omega_s} \cong \frac{\omega}{\omega_s} .$$

The response cut-off frequency may have to be compensated, pre-warped, in order to occur at the desired value.

3. Sampling Effects

For either of the design methods described above, the frequency response will repeat at multiples of the repetition period, f_s , so that the response shape for $0 \leq f \leq \frac{1}{2}f_s$ is mirrored from $\frac{1}{2}f_s \leq f \leq f_s$ and repeated from $kf_s \leq f \leq (k+1)f_s$ for $k = 1, 2, 3, \dots$. Figure 2.6 illustrates the repeated response of an arbitrary filter response.

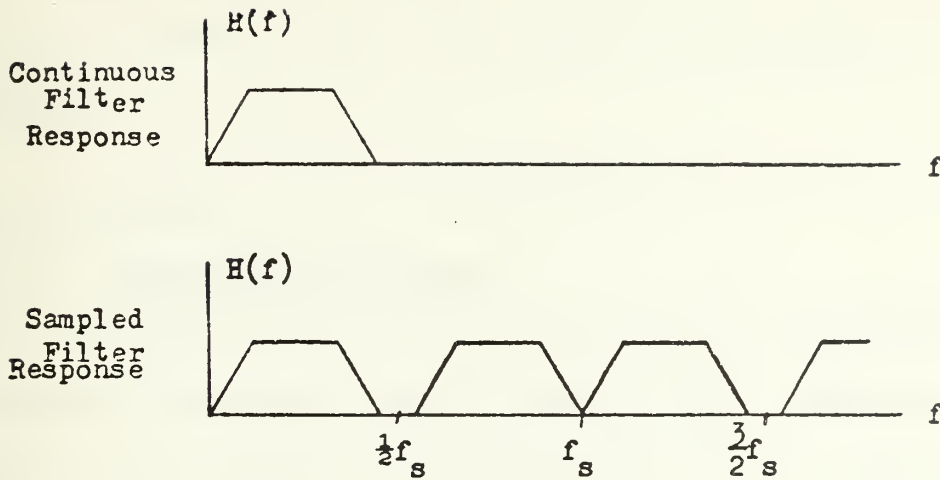


FIGURE 2.6 Repetitious Frequency Response

This repetitious response effect is equivalent to considering an input at an arbitrary frequency, f , such that

$$f - k f_s = f_a \quad , \quad 0 \leq f_a \leq \frac{1}{2} f_s \quad .$$

That is, the input is 'heterodyned' with the particular k^{th} multiple of the repetition period such that the difference frequency, f_a , is less than $\frac{1}{2} f_s$. The filter frequency response $H(f_a)$ is then applied to the input. Therefore, for any input signal frequency, only the filter response from $0 \leq f_a \leq \frac{1}{2} f_s$ is used. If the input frequency meets the Nyquist criterion, i.e. is less than $\frac{1}{2} f_s$, the multiple of the repetition period used to heterodyne the signal, k , is zero. For frequencies

beyond the Nyquist bandwidth of half the repetition period, k is some positive integer. The ambiguity of k is an aliasing effect. For $k = 0$, there is no ambiguity, thus no aliasing.

B. EXPERIMENT

1. System Configuration

A first-order recursive filter was implemented using a Reticon Corporation Serial Analog Delay (SAD-100) device as the delay element. The transfer function coefficients were obtained by potentiometer voltage dividers. The arithmetic operations were implemented using operational amplifiers with feedback. Figure 2.7 illustrates the system.

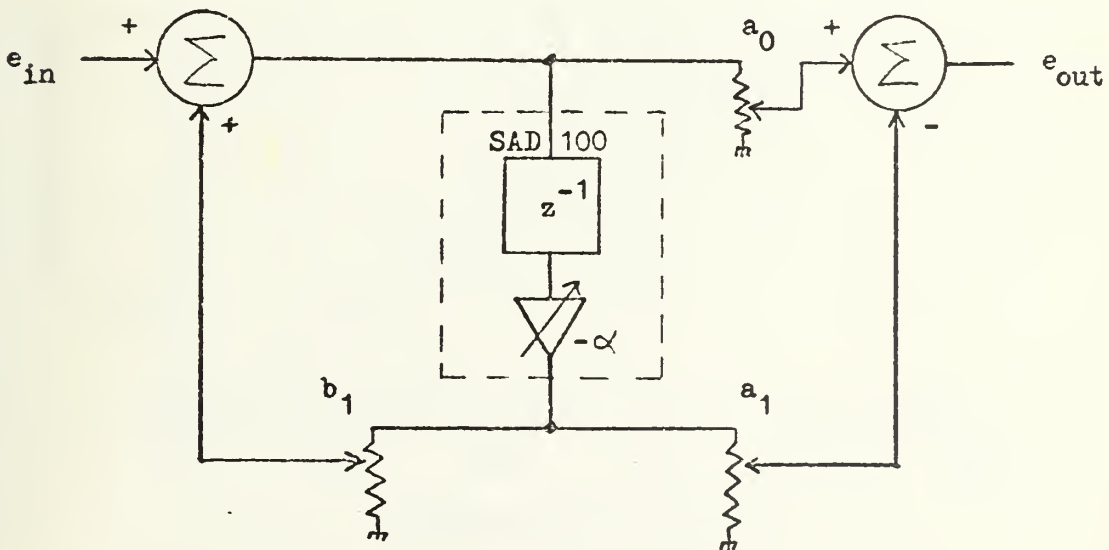


FIGURE 2.7 First-Order Recursive Filter

A variable feedback resistance was installed on the Reticon SAD-100 driver card output amplifier so that the gain of the delay circuit, $-\alpha$, could be adjusted. This factor, α , is important to the setting of the coefficient potentiometers.

Circuit analysis of the coefficient potentiometers, performed in Appendix C, indicates that the maximum coefficient values for a_1 and b_1 is α . In addition, since the input impedance of the summing circuit is finite, the coefficients are determined by a loaded voltage divider relationship graphed in Figure 2.8 for the particular loading used in the system.

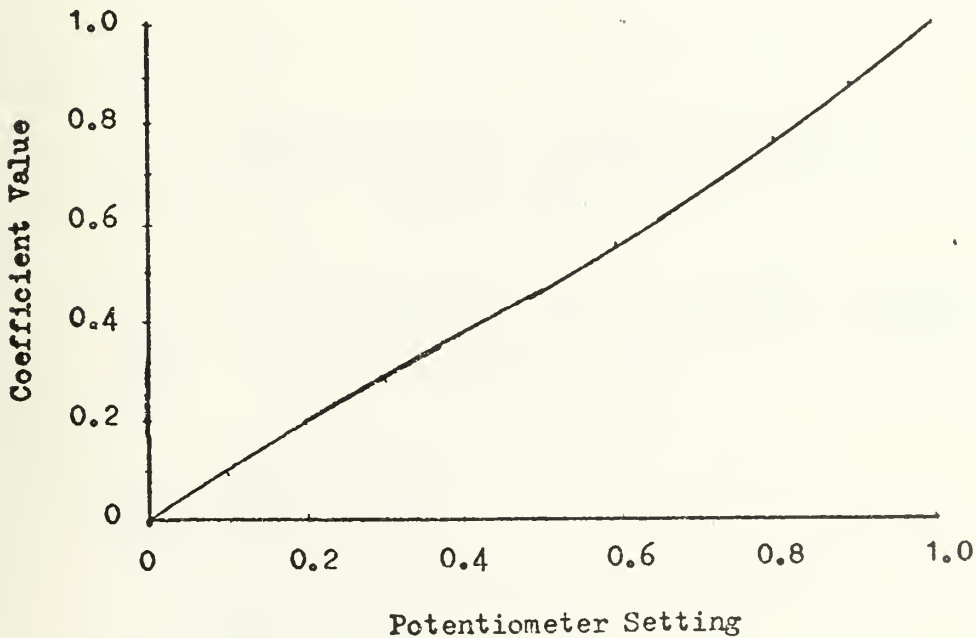


FIGURE 2.8 Coefficient Calibration Curve

The coefficient calibration curve may be experimentally checked by observing the filter response to a unit step input. Appendix D derives the expressions for the coefficients in terms of the differences between successive filter outputs. Figure 2.9 shows the step response for a typical first-order low pass filter. The coefficients are calculated by the following relationships,

$$a_0 = d_1 \quad , \quad a_1 = \frac{d_2^2 - d_1 d_3}{d_2} \quad , \quad b_1 = -\frac{d_k}{d_{k-1}} \quad \text{for } k = 3, 4, 5, \dots .$$

This technique is extended to second-order filters by the use of the following relationships,

$$a_0 = d_1 \quad ,$$

$$a_1 = \frac{d_1 d_2 d_5 - d_2 d_3^2 - d_1 d_3 d_4 - d_2^2 d_4}{d_3^2 - d_2 d_4} \quad ,$$

$$a_2 = \frac{d_3^3 - 2d_2 d_3 d_4 + d_2^2 d_5 + d_1 d_4^2 - d_1 d_3 d_5}{d_3^2 - d_2 d_4} \quad ,$$

$$b_1 = \frac{d_2 d_5 - d_3 d_4}{d_3^2 - d_2 d_4} \quad ,$$

$$b_2 = \frac{d_4^2 - d_3 d_5}{d_3^2 - d_2 d_4} \quad .$$

Appendix E describes the use of the Tektronix 31 programmable calculator to solve these equations.

For first-order standard Z-transform filters of the form,

$$H(z) = \frac{1}{1 + b_1 z^{-1}} ,$$

another method for experimentally determining b_1 is available. As discussed in Appendix B, by taking the ratio between the response minimum and maximum, μ , b_1 is determined by,

$$|b_1| = \frac{1 - \mu}{1 + \mu} ,$$

which is graphed in Figure 2.9.

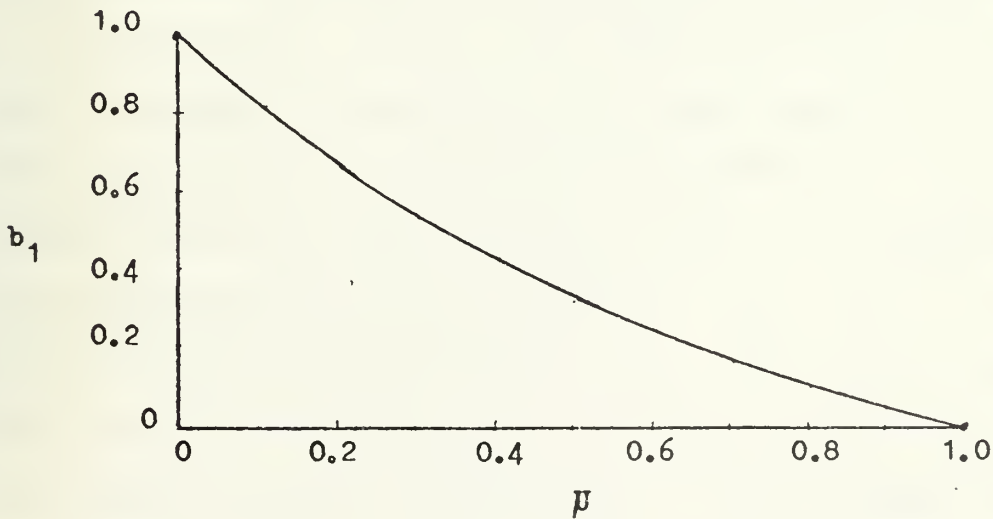


FIGURE 2.9 b_1 vs μ

2. Experimental Frequency Response

Several types of filters were implemented to verify the design theory and observe the characteristics of the repetitious response. For an implementation using a delay time, T , theory indicates that the filter response should repeat exactly at multiples of f_s , where,

$$f_s = \frac{1}{T} .$$

Since the SAD-100 is a 98-bit register, the delay time is 98 times the clock period, T_c ,

$$T = 98T_c .$$

The repetition period would then be the clock frequency, f_c , divided by 98. Since a new input is sampled every clock cycle, the rate of sampling is f_c . The sampling is done at the input gate of the SAD where a transistor is turned on by one of the two clock phases for half of its period. Since the two phase clock operates at $\frac{1}{2}f_c$, the 'on' time, i.e. the sampling pulse width, is T_c . The finite pulse width causes an envelope over the sampled signal spectrum. The envelope follows a $\frac{\sin x}{x}$ shape. This envelope has its first null at $f = \frac{1}{T_c} = f_c$. Since the clock frequency is N times the repetition period, where N is the number of delay bits, N frequency response cycles will occur before

the first sampling envelope null. Because of aliasing from the sampling rate, f_c , only those responses for frequencies less than or equal to $\frac{1}{2}f_c$, i.e. the first $\frac{1}{2}N$, are useful. In this study, only the first twelve cycles are observed, therefore the minimum value of the envelope was,

$$\frac{\sin \pi(\frac{12}{98})}{\pi(\frac{12}{98})} = 0.976 ,$$

which is sufficiently close to unity to be neglected.

Standard Z-transform filters were implemented with,

$$\begin{aligned} a_0 = 1 , \quad a_1 = 0 , \quad b_1 = -0.3, -0.7 \quad \text{low pass,} \\ b_1 = 0.3, 0.7 \quad \text{high pass.} \end{aligned}$$

Bilinear Z-transform filters were implemented with,

$$a_0 = 1 , \quad a_1 = 1 , \quad b_1 = -0.7, 0.0, 0.3, 0.7 \quad \text{low pass,}$$

$$a_0 = 1 , \quad a_1 = -1 , \quad b_1 = -0.3, -0.7 \quad \text{high pass.}$$

Two clock frequencies were used,

$$f_c = 400 \text{ kHz, } 1 \text{ MHz} .$$

Figures 2.10a through 2.19a illustrate the first response period of the various filters implemented. The solid curve represents the calculated response while the points are

the observed response. Figures 2.10b through 2.19c illustrate several response cycles of the filters.

Some significant deviations from the theoretical responses were noticed, especially for the larger values of b_1 . The responses are not mirror images of one another. The reason for this 'skewness' is not clear at present. One possible explanation may center on a frequency varying coefficient, such as a_1 . The values of a_0 and a_1 must stay equal for a zero to appear at multiples of f_s . If one of the values changes differently with frequency than the other, say through a frequency characteristic of the delay device, the zero would not be properly formed, perhaps shifted up or down frequency from kf_s . The other major deviation is the change of the maximum amplitudes of the responses with frequency rather than staying uniform as theory predicts.

For filters with small b_1 , the trend is for decreasing amplitude with increasing frequency, particularly beyond 40 kHz. This effect is probably due to the gain roll-off of the operational amplifiers in the summers. Part of this decrease could be due to the sampling envelope, though it is always greater than 0.97.

For bilinear Z filters with $b_1 = \pm 0.7$, the maxima of the frequency responses increase with frequency, as shown in Figures 2.11 and 2.14. This trend may also be due to deterioration of the zero from a_0 and a_1 varying more

with increased frequency. The effects of frequency varying coefficients need to be pursued.

Measurements of corner frequencies, which are summarized in Table I, indicated good agreement with the design theory.

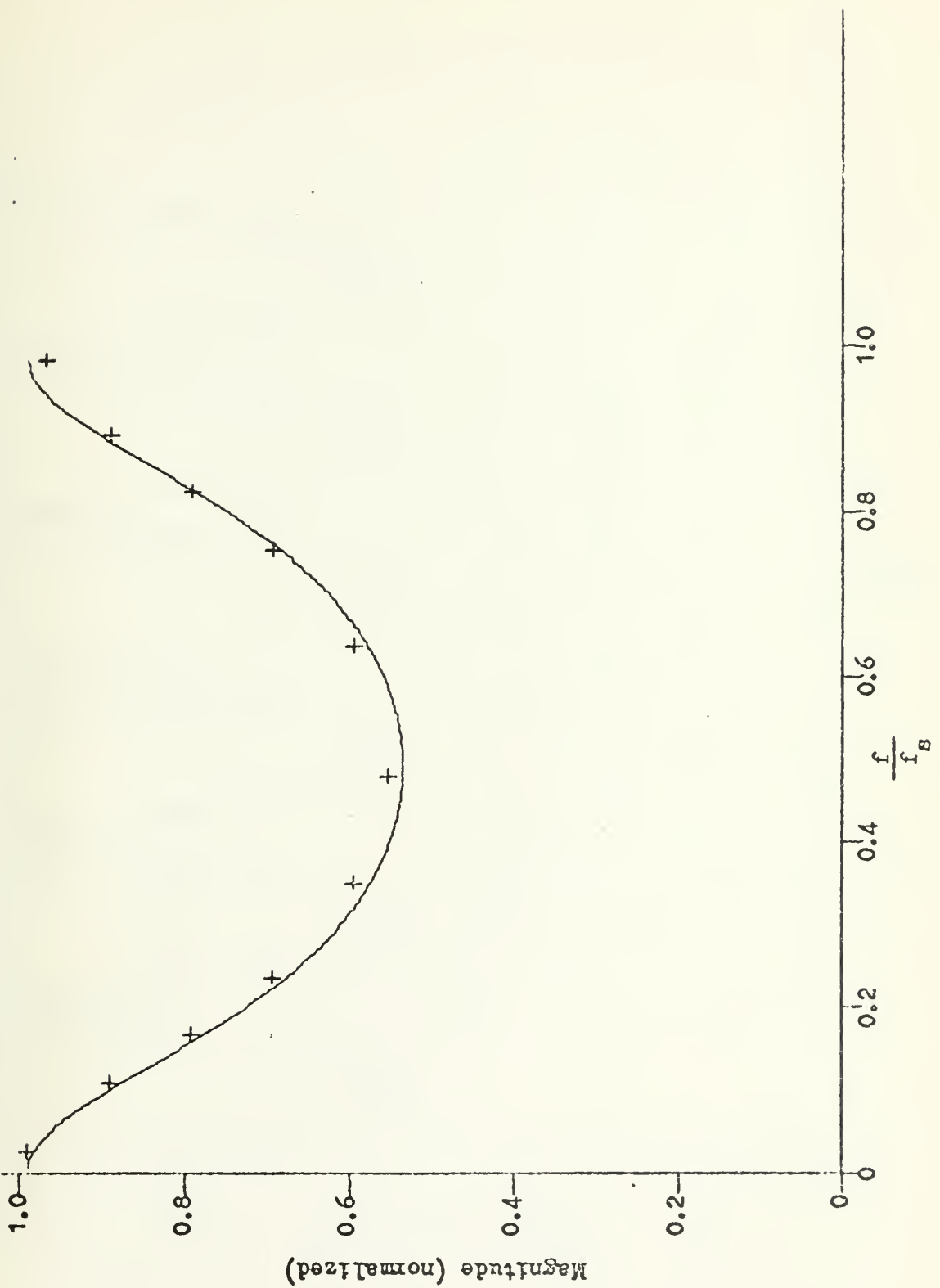


FIGURE 2.10a Theoretical and Observed Frequency Response of Standard Z Low Pass Filter; $b_1 = -0.3$

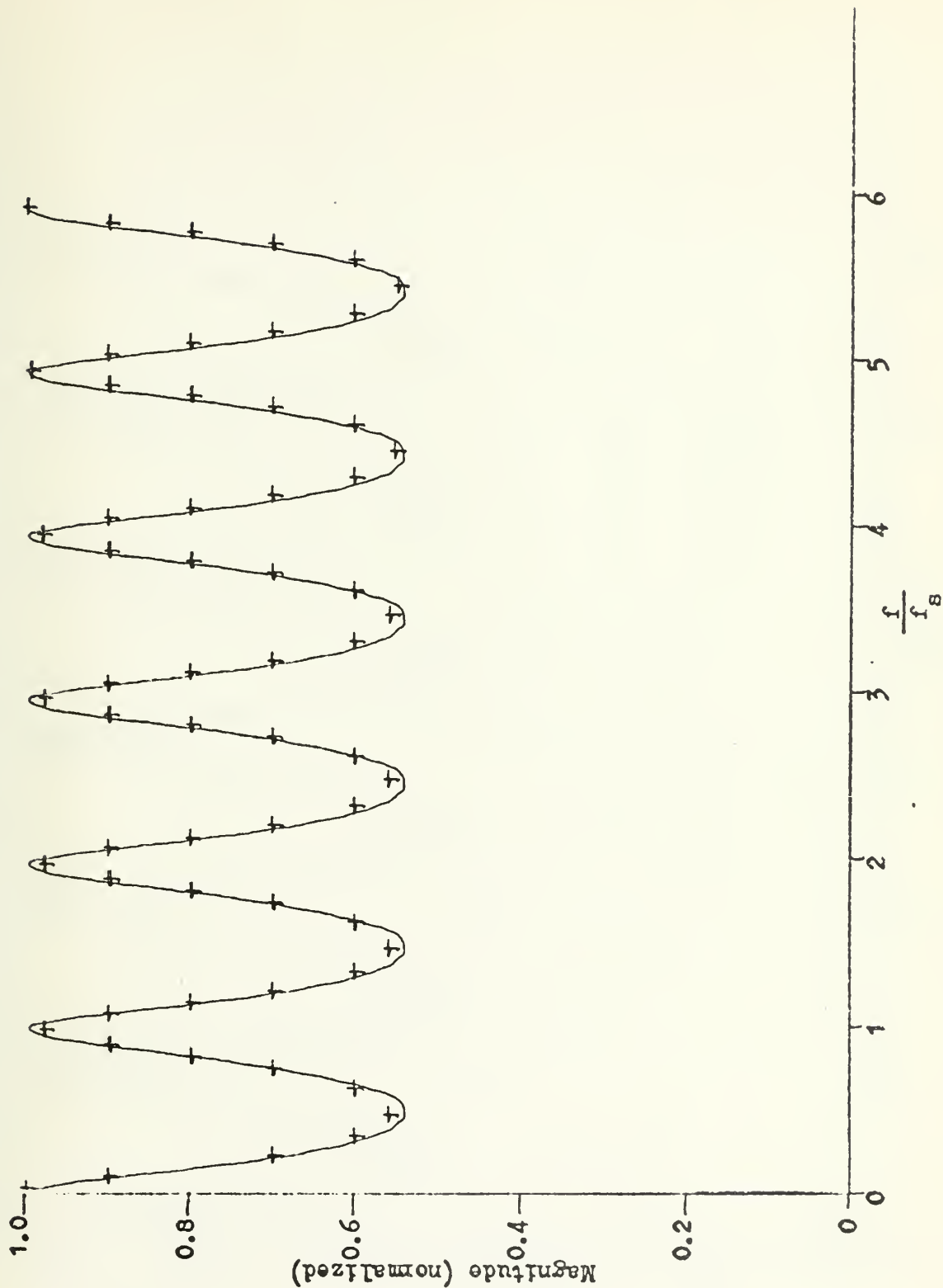


FIGURE 2.10b Theoretical and Observed Frequency Response of Standard Z Low Pass Filter; $b_1 = -0.3$

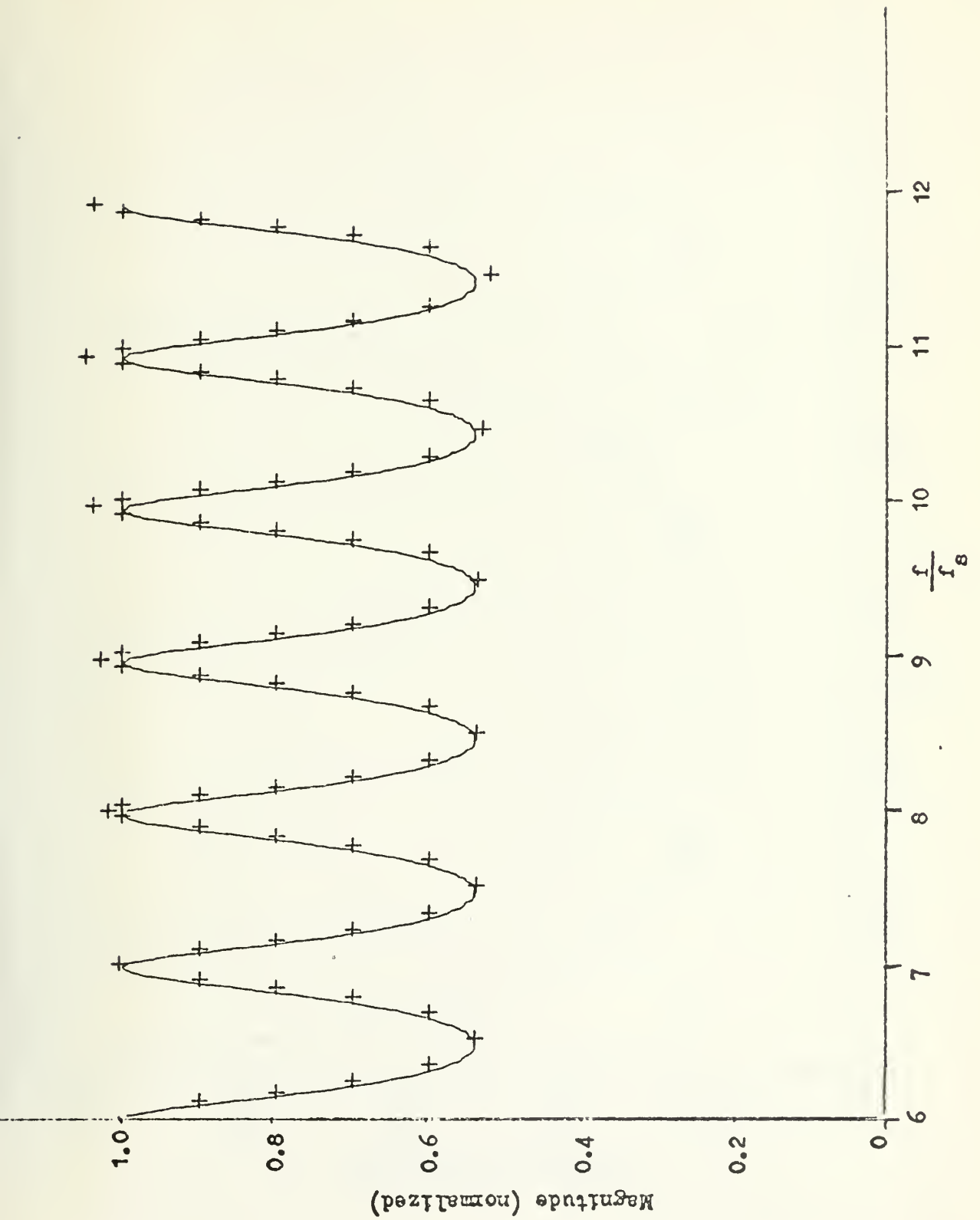


FIGURE 2.10c Theoretical and Observed Frequency Response of Standard Z Low Pass Filter; $b_1 = -0.3$

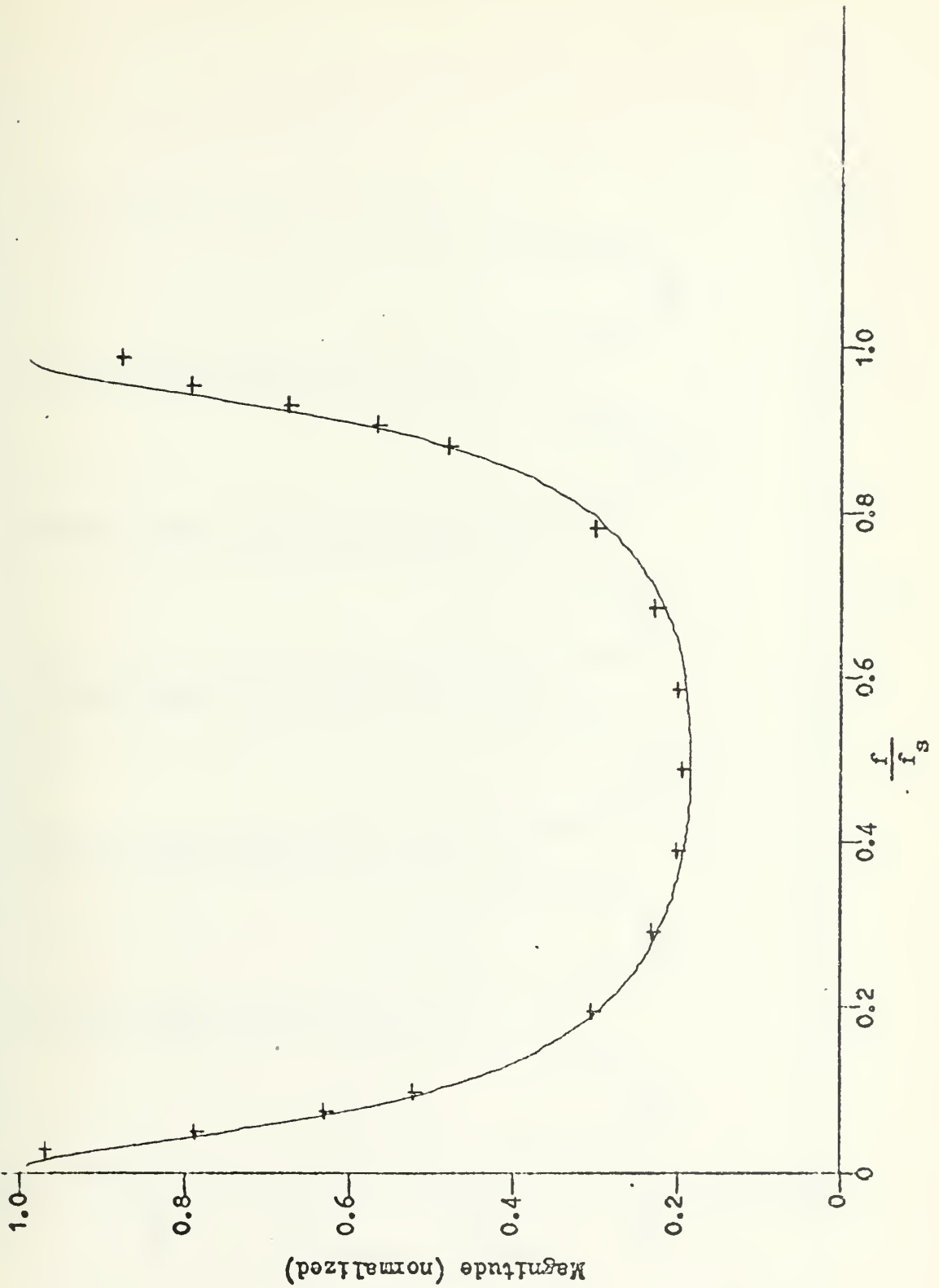


FIGURE 2.11a Theoretical and Observed Frequency Response of Standard Z Low Pass Filter; $b_1 = -0.7$

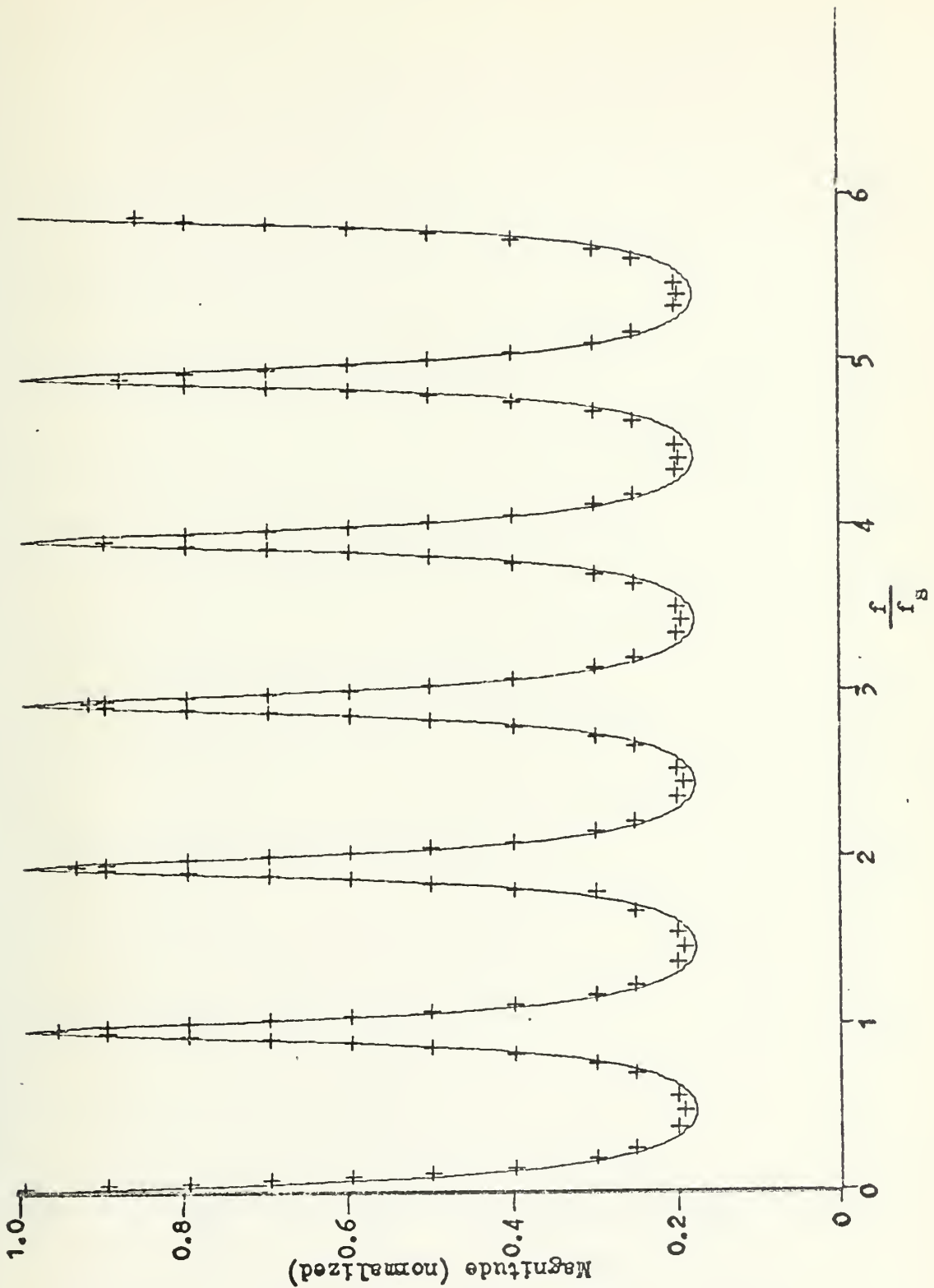


FIGURE 2.11b Theoretical and Observed Frequency Response of Standard Z Low Pass Filter; $b_1 = -0.7$

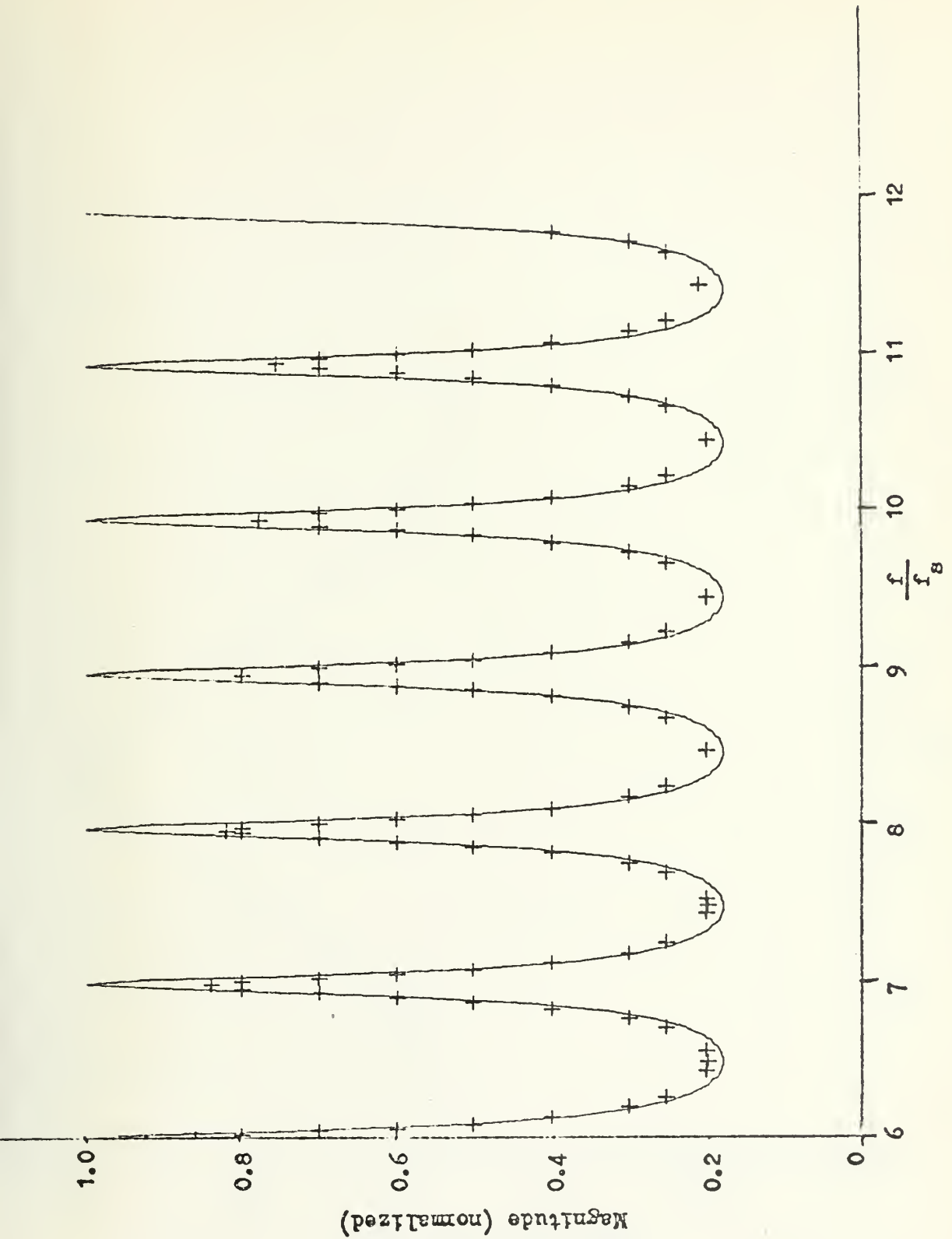


FIGURE 2.11c Theoretical and Observed Frequency Response of Standard Z Low Pass Filter; $b_1 = -0.7$

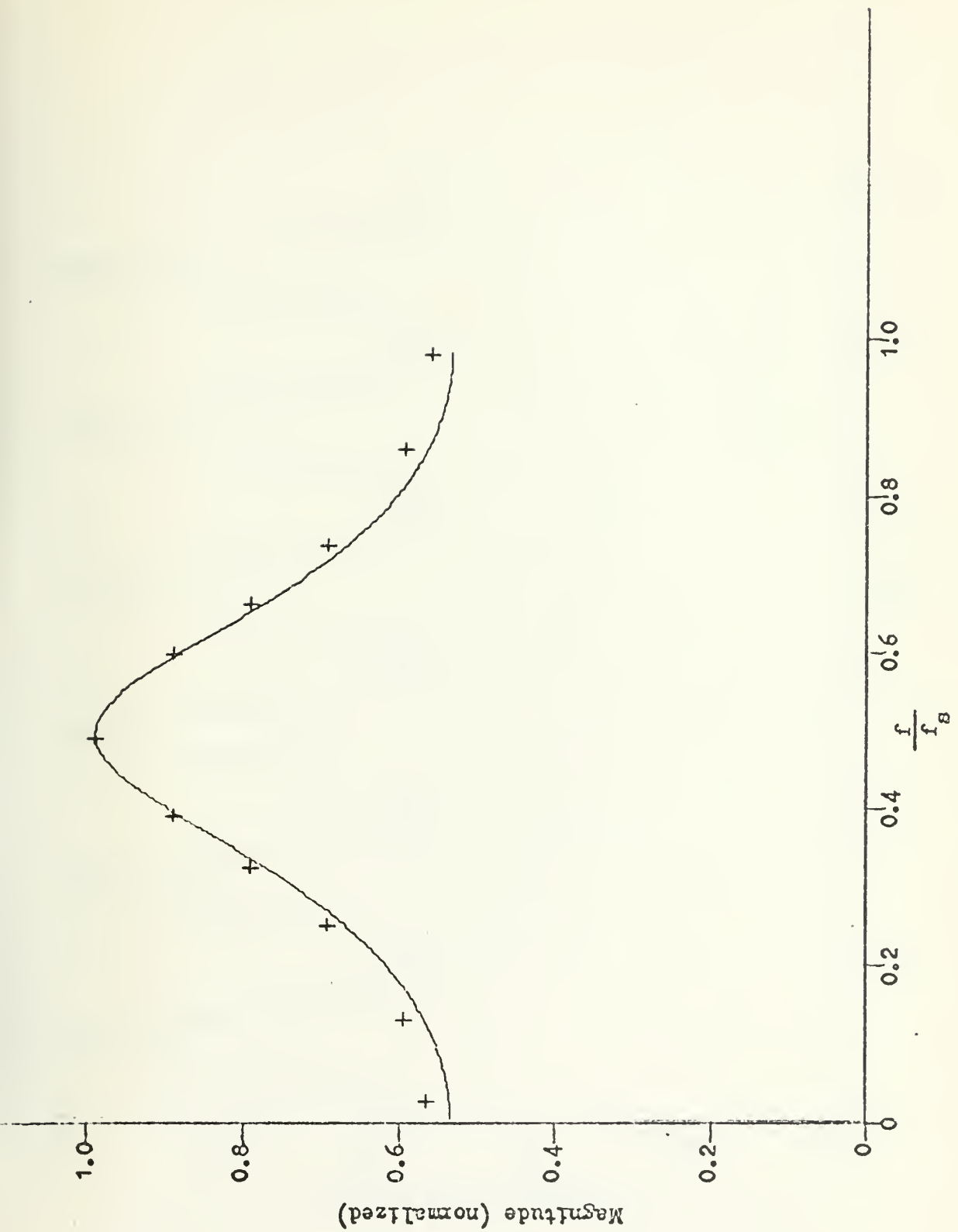


FIGURE 2.12a Theoretical and Observed Frequency Response of Standard Z High Pass Filter; $b_1 = 0.3$

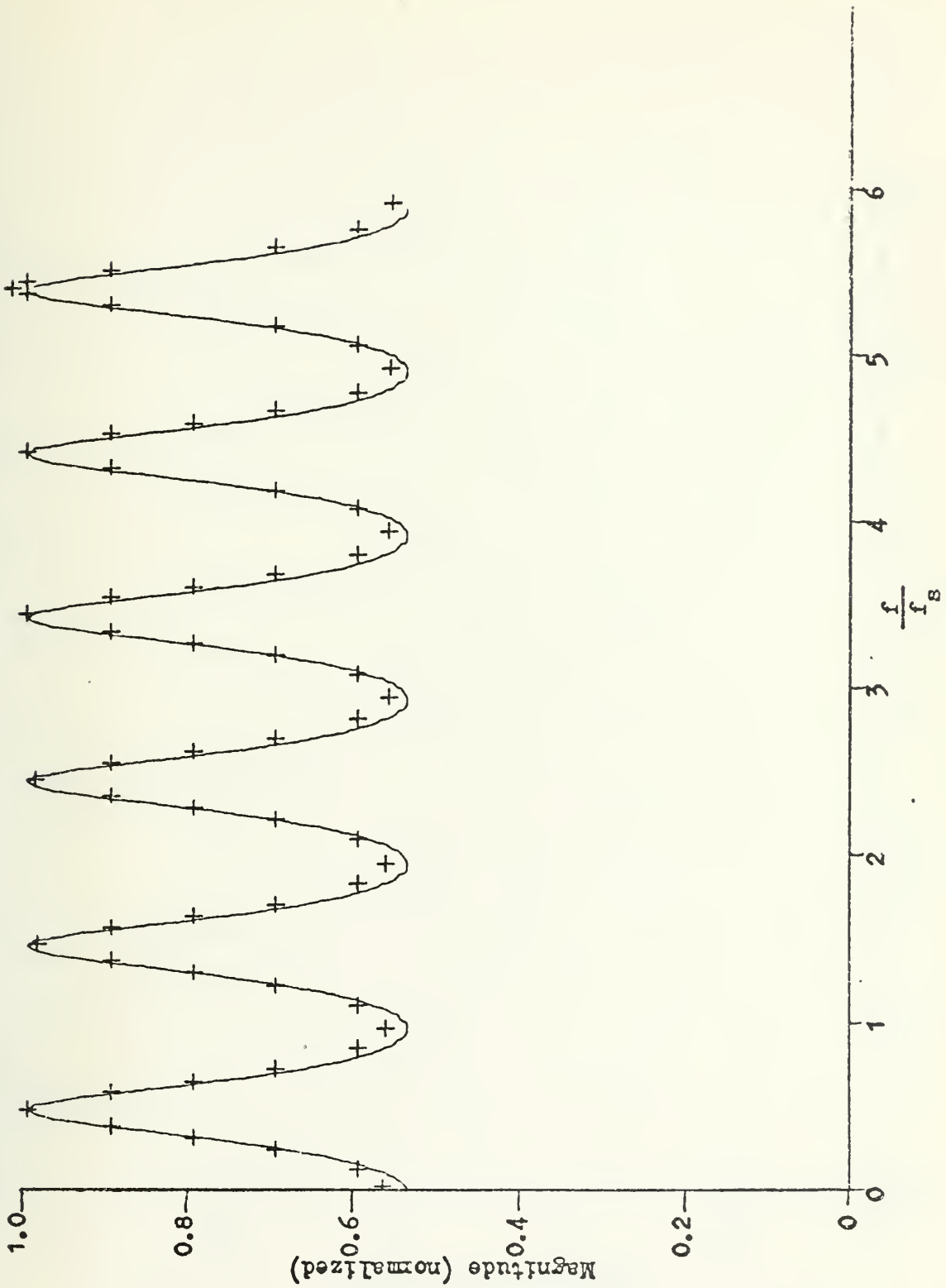


FIGURE 2.12b Theoretical and Observed Frequency Response of Standard Z High Pass Filter; $b_1 = 0.3$

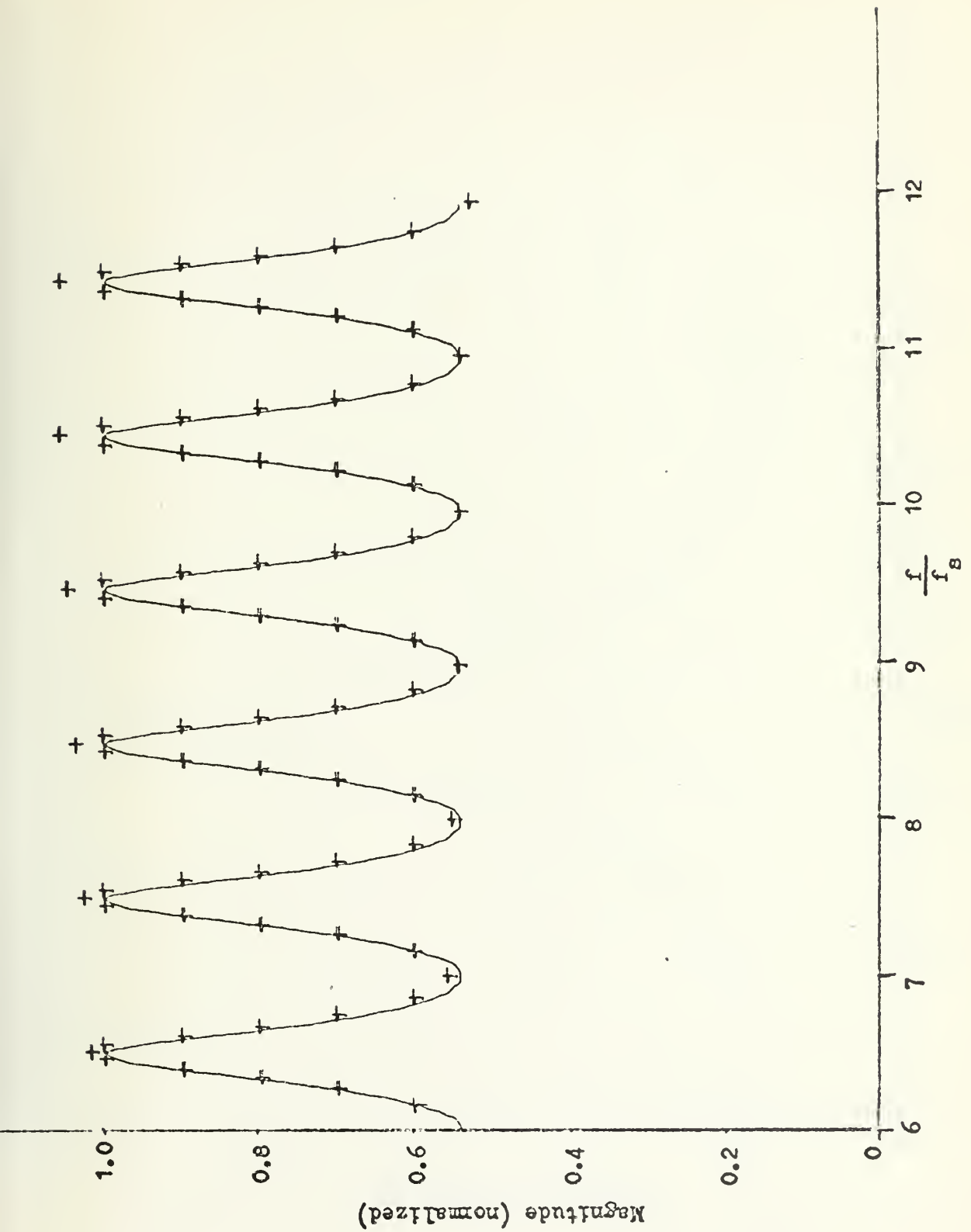


FIGURE 2.12c Theoretical and Observed Frequency Response of Standard Z High Pass Filter; $b_1 = 0.3$

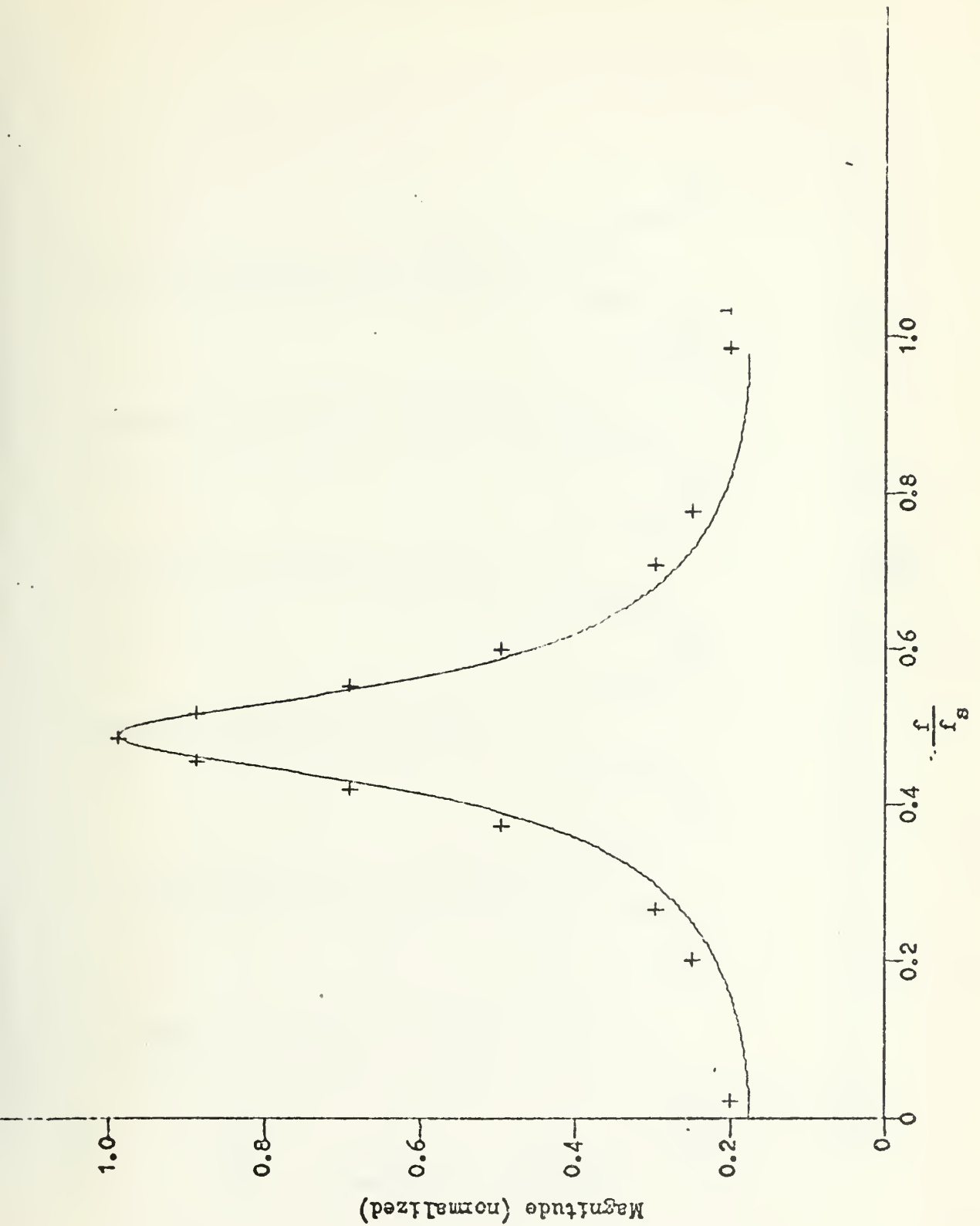


FIGURE 2.13a Theoretical and Observed Frequency Response of Standard Z High Pass Filter; $b_1 = 0.7$

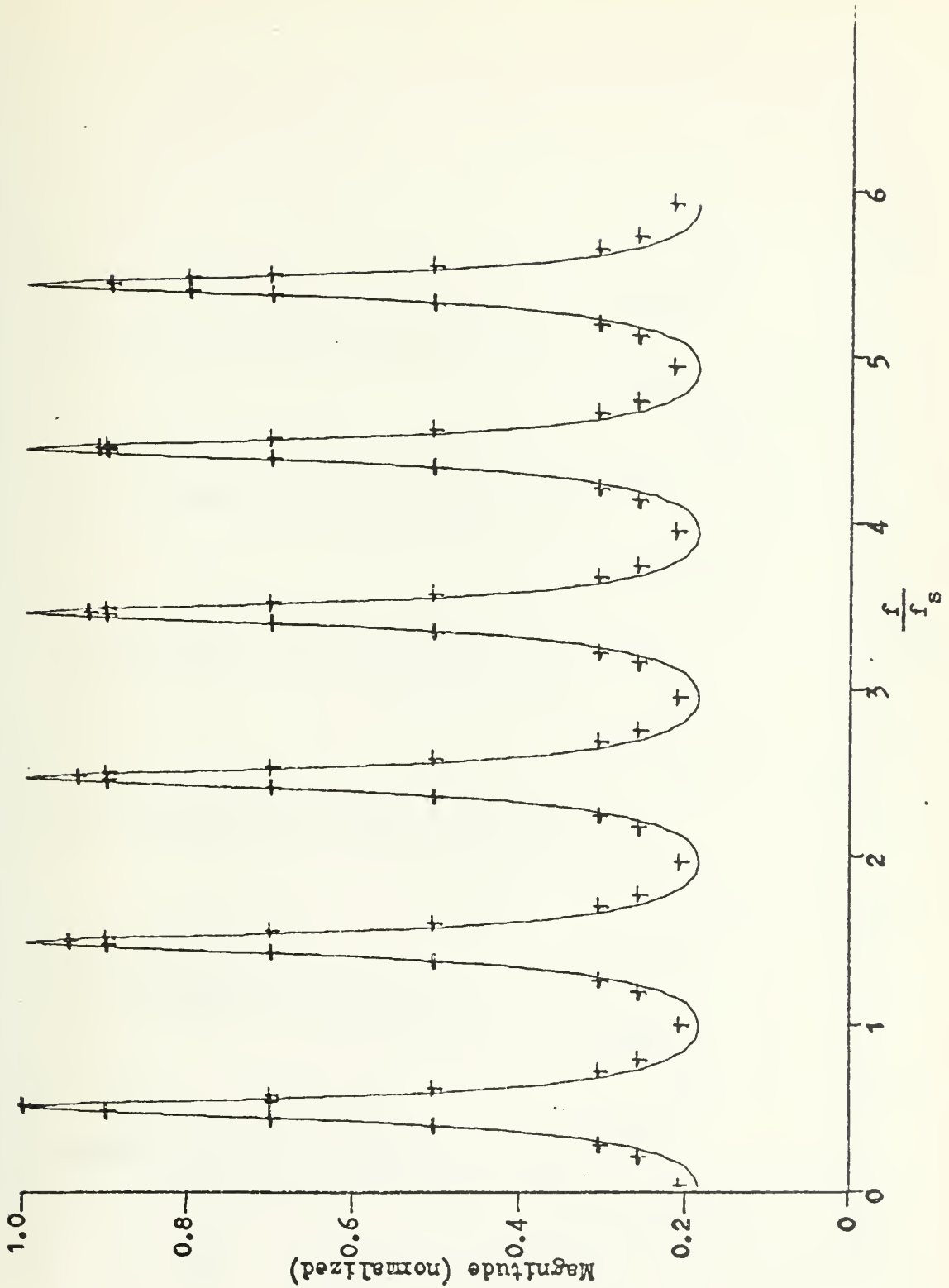


FIGURE 2.13b Theoretical and Observed Frequency Response of Standard Z High Pass Filter; $b_1 = 0.7$

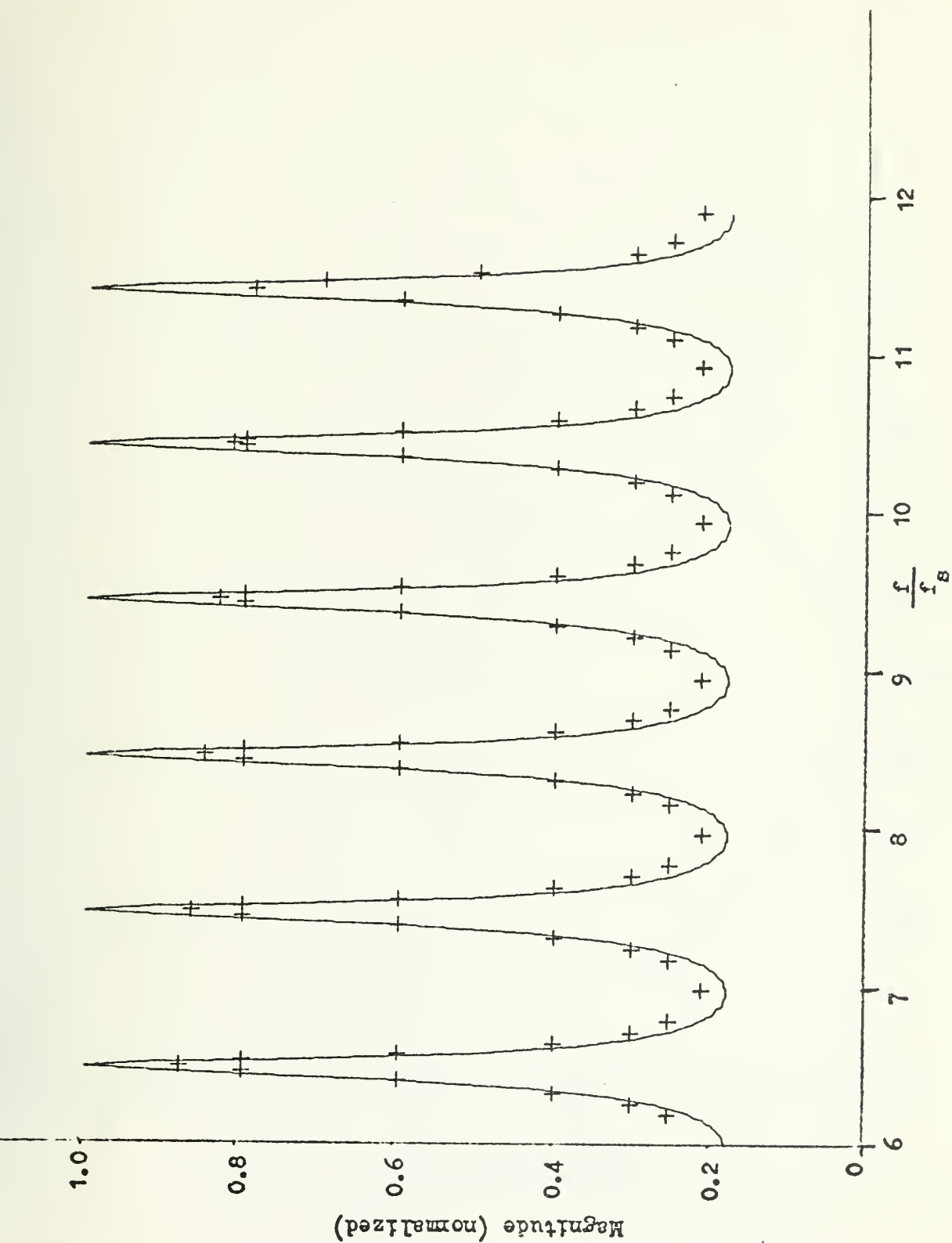


FIGURE 2.13c Theoretical and Observed Frequency Response of Standard Z High Pass Filter; $b_1 = 0.7$

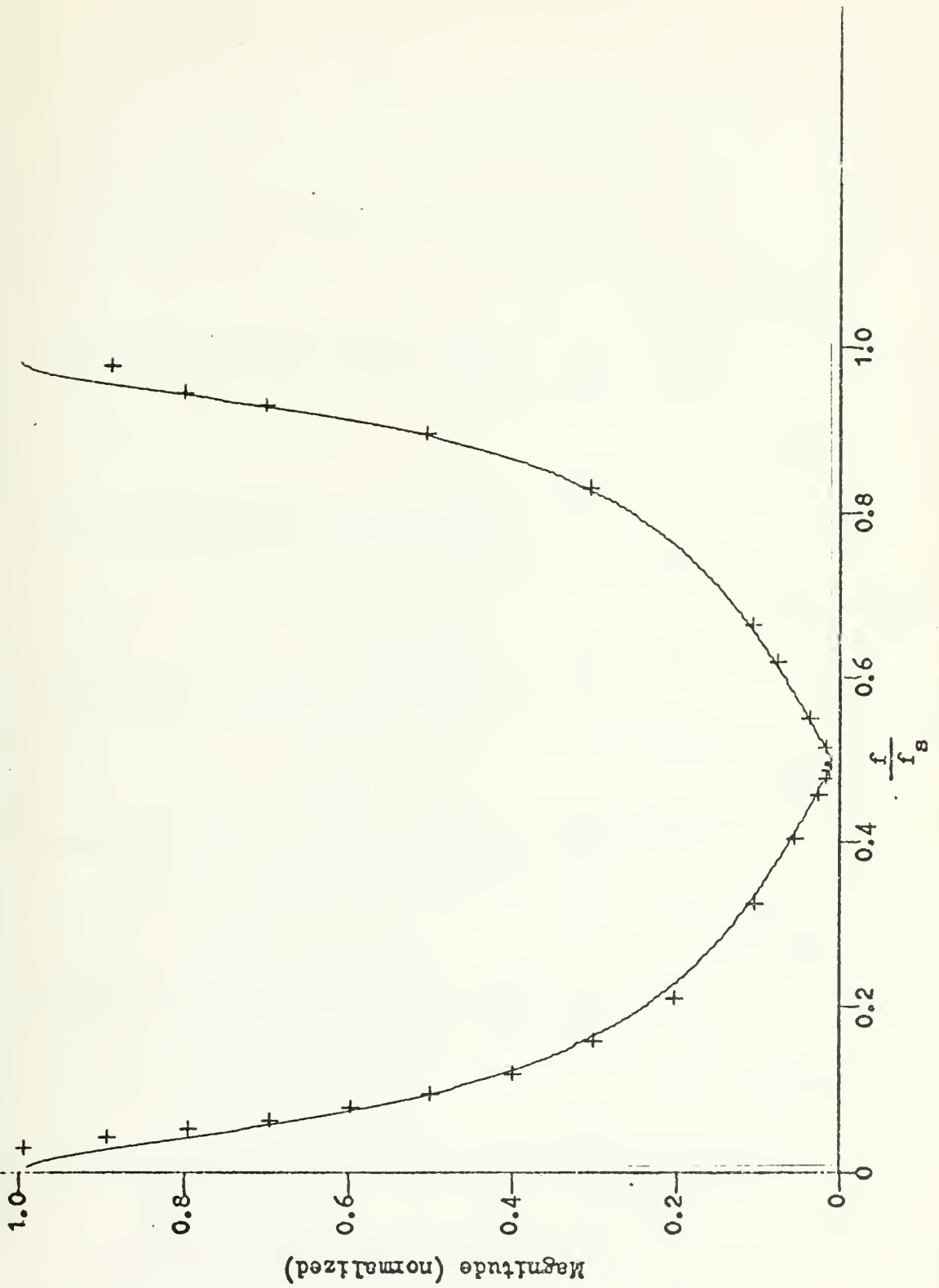


FIGURE 2.14a Theoretical and Observed Frequency Response of Bilinear Z Low Pass Filter; $b_1 = -0.7$

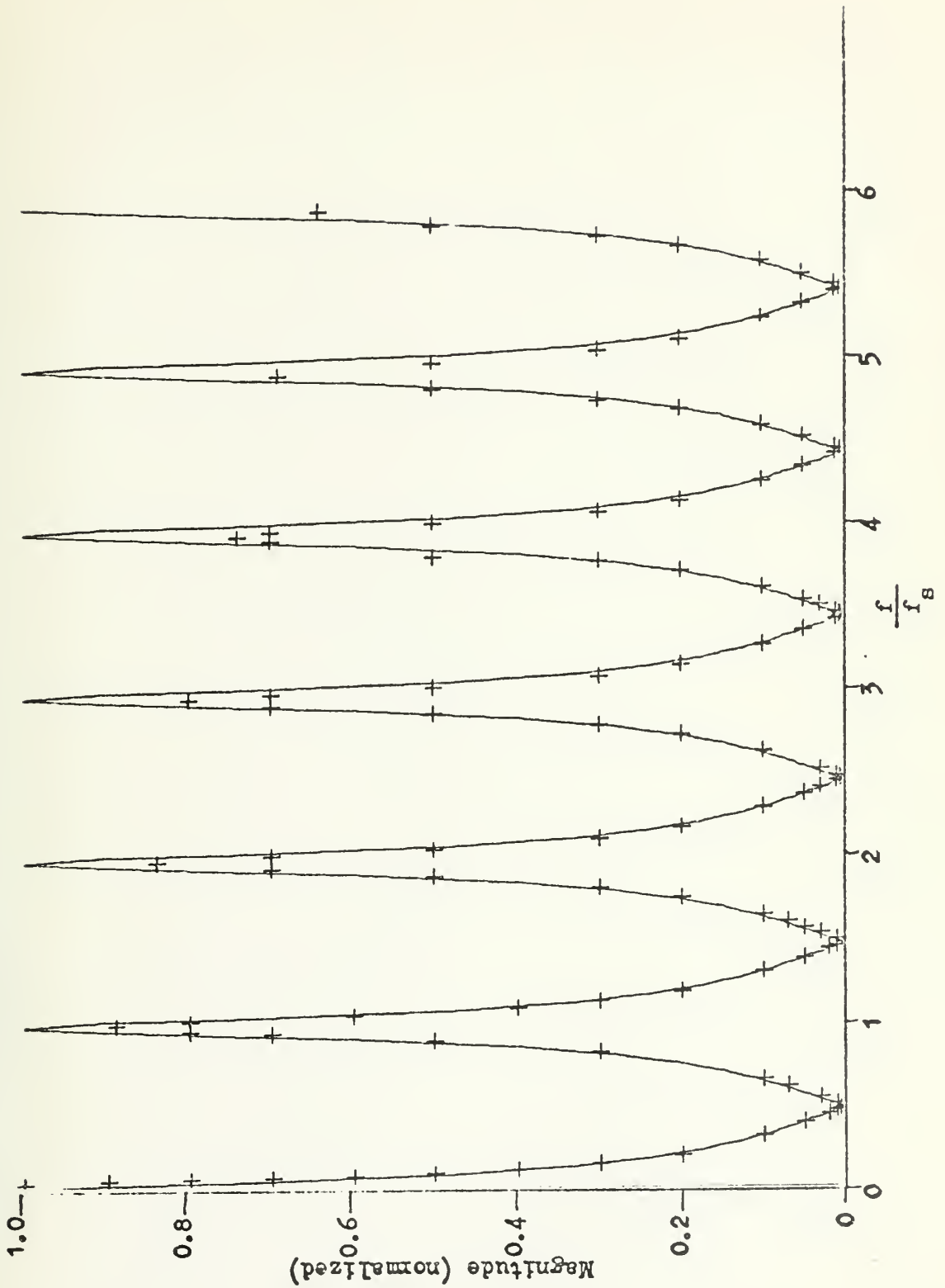


FIGURE 2.14b Theoretical and Observed Frequency Response of Bilinear Z Low Pass Filter; $b_1 = -0.7$

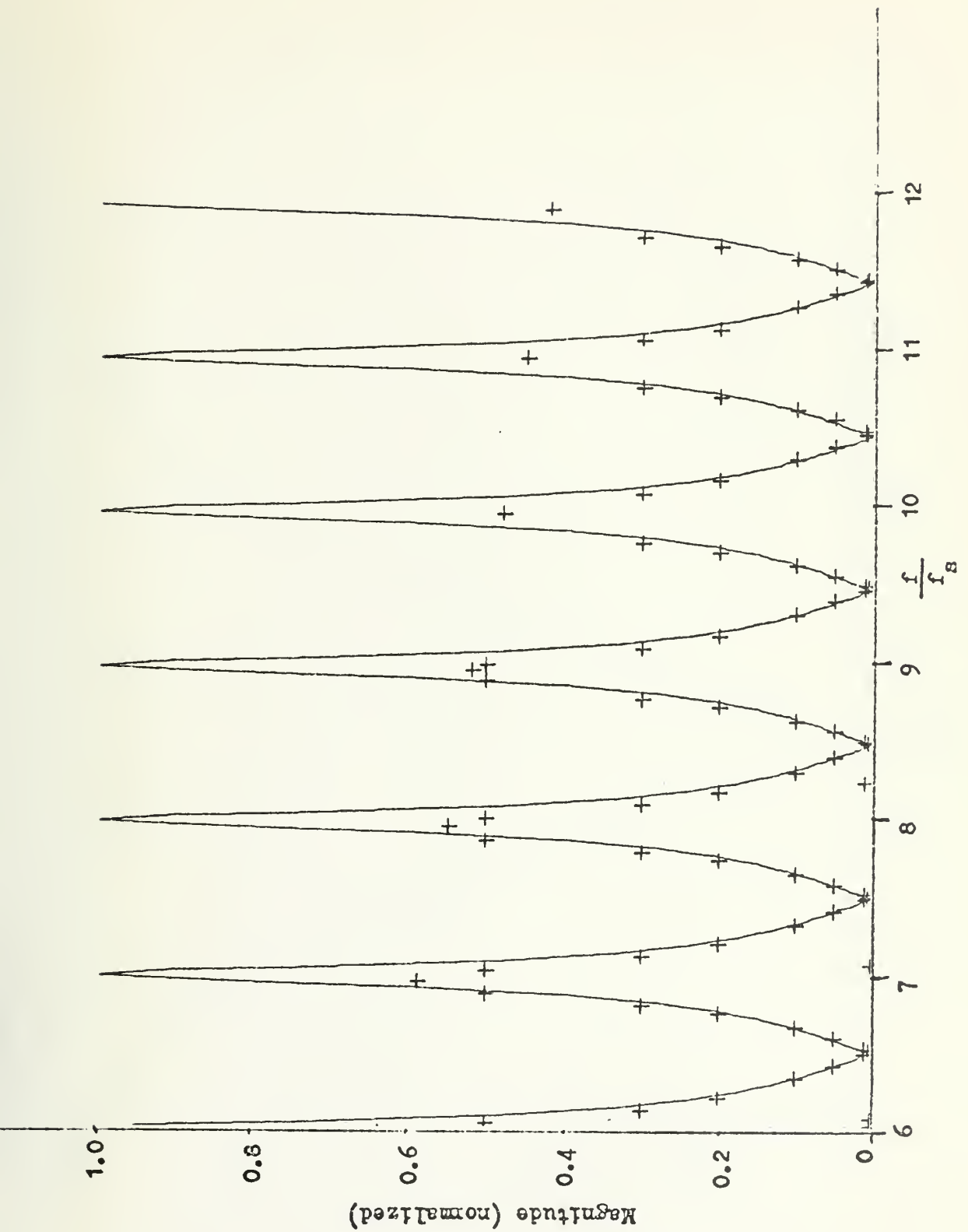


FIGURE 2.14c Theoretical and Observed Frequency Response of Bilinear Z Low Pass Filter; $b_1 = -0.7$

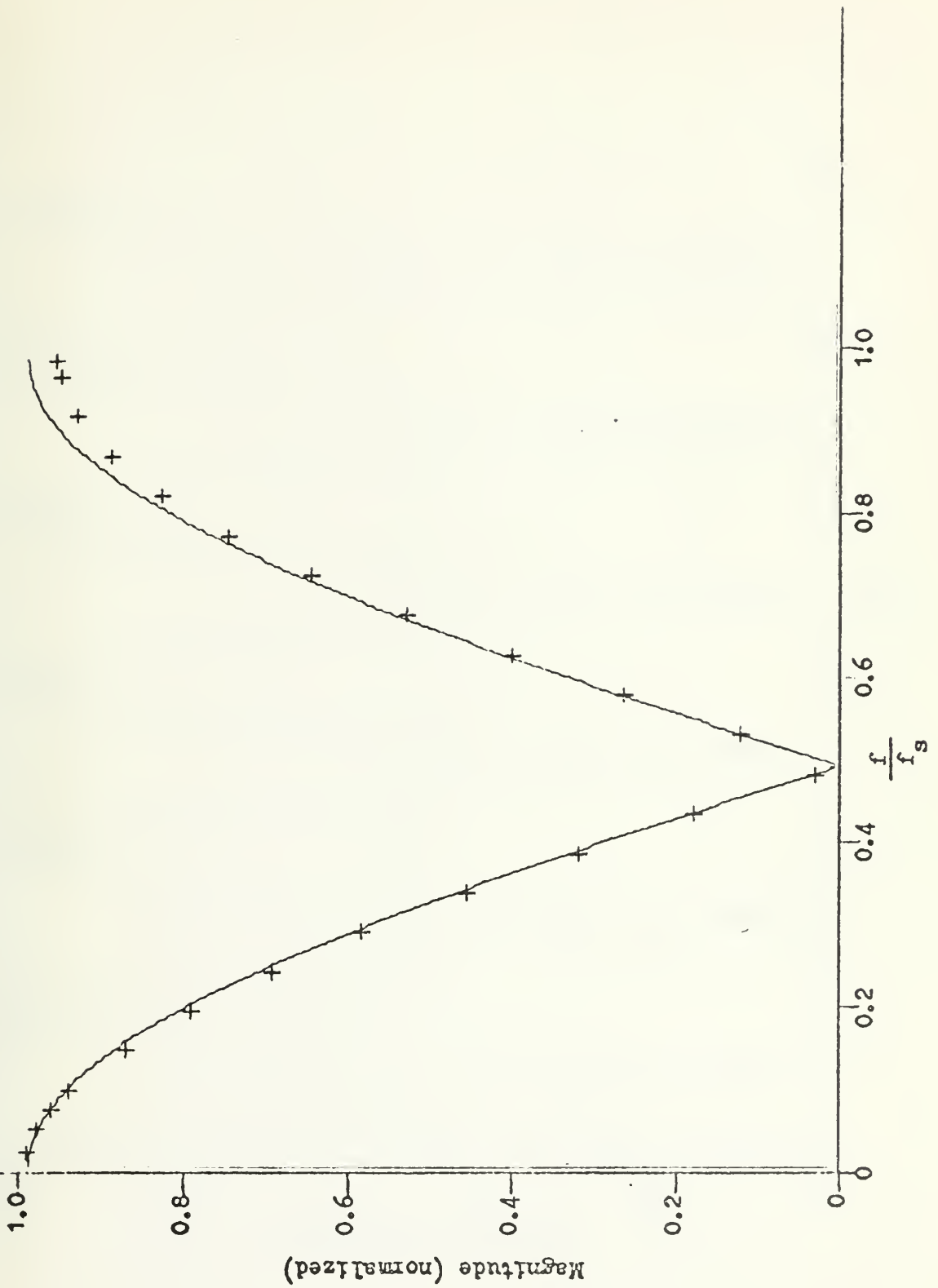


FIGURE 2.15a Theoretical and Observed Frequency Response of Bilinear Low Pass Filter; $b_1 = 0.0$

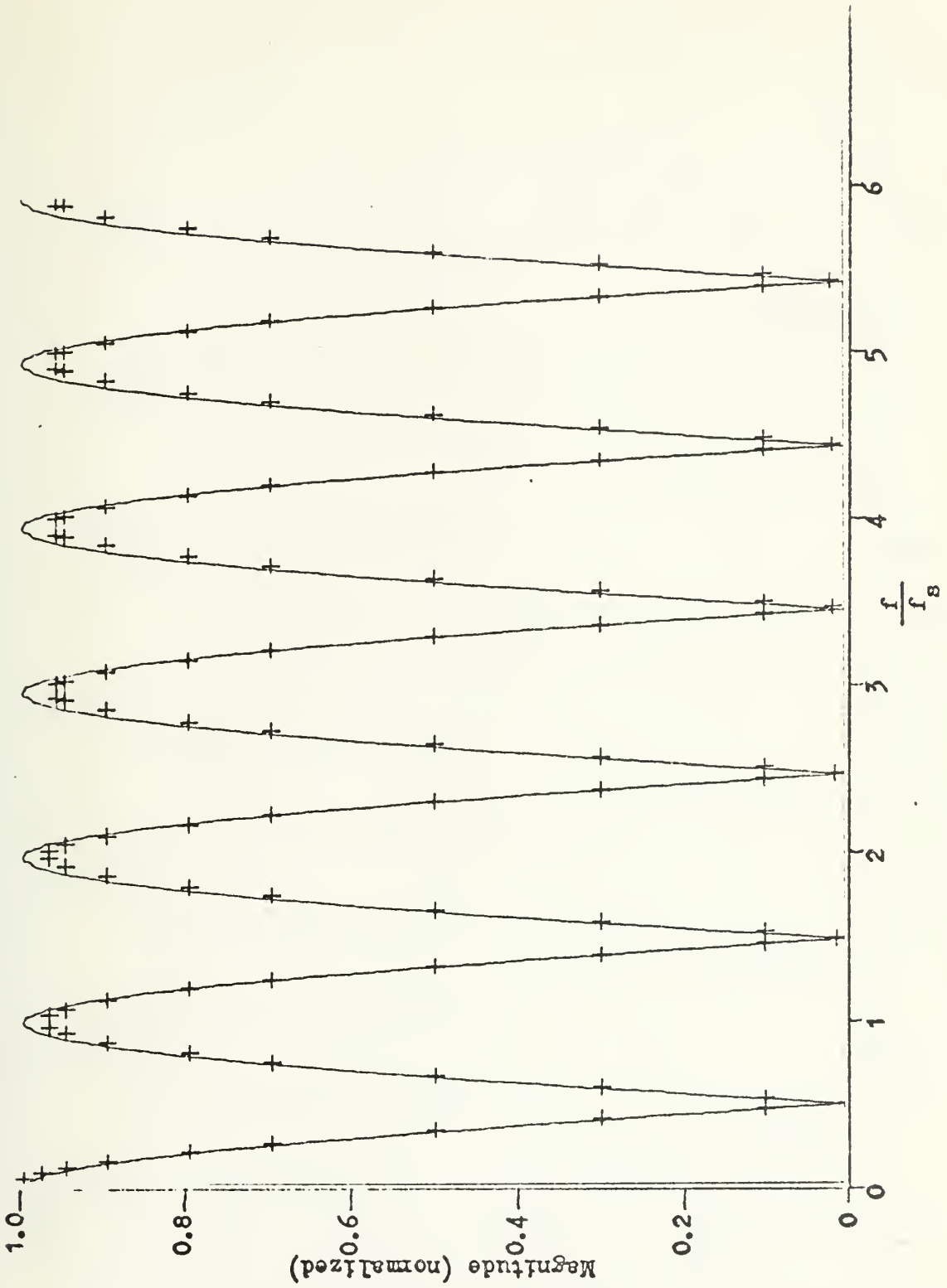


FIGURE 2.15b Theoretical and Observed Frequency Response of Bilinear Low Pass Filter; $b_1 = 0.0$

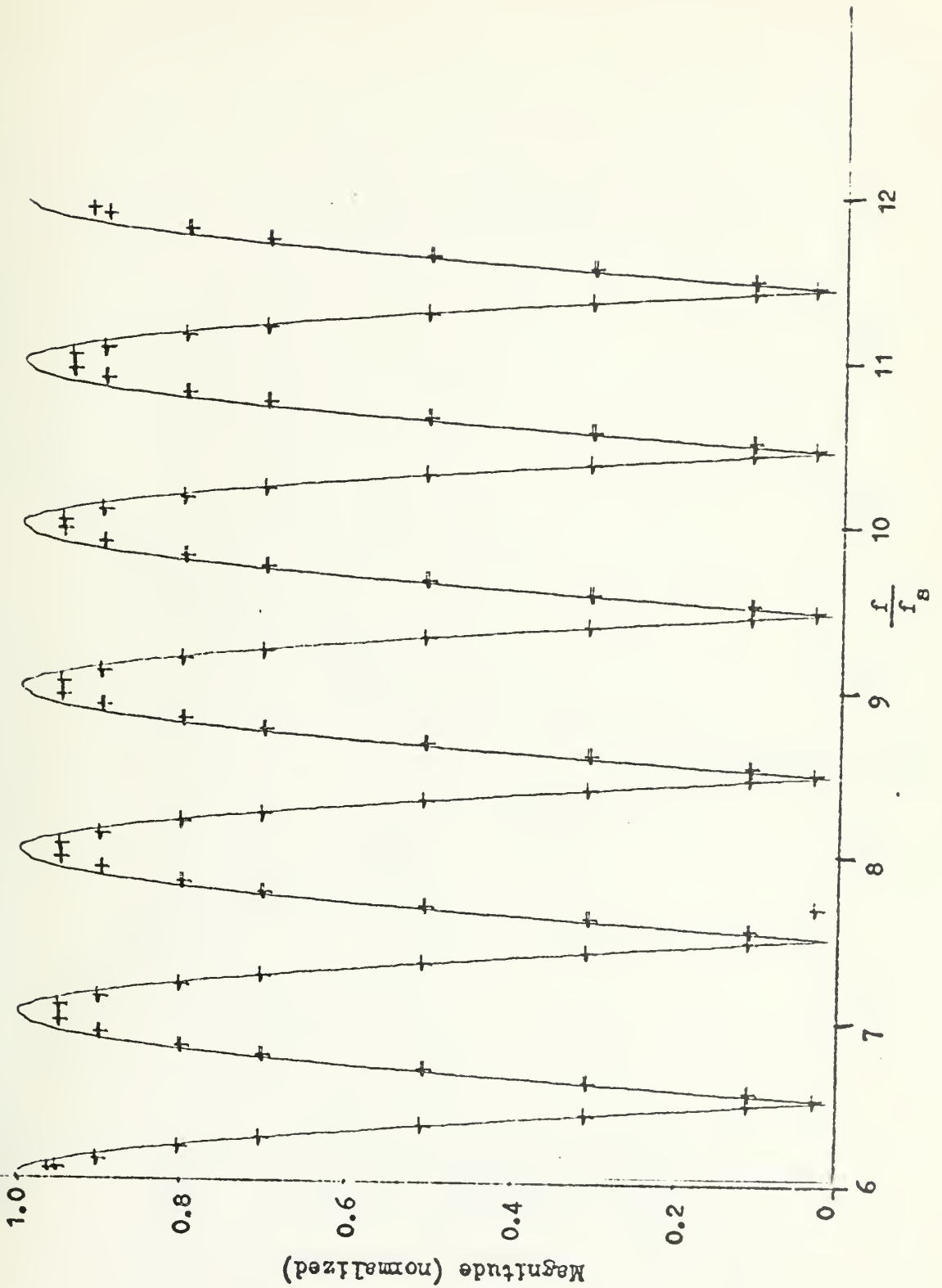


FIGURE 2.15c Theoretical and Observed Frequency Response of Bilinear Low Pass Filter; $b_1 = 0.0$

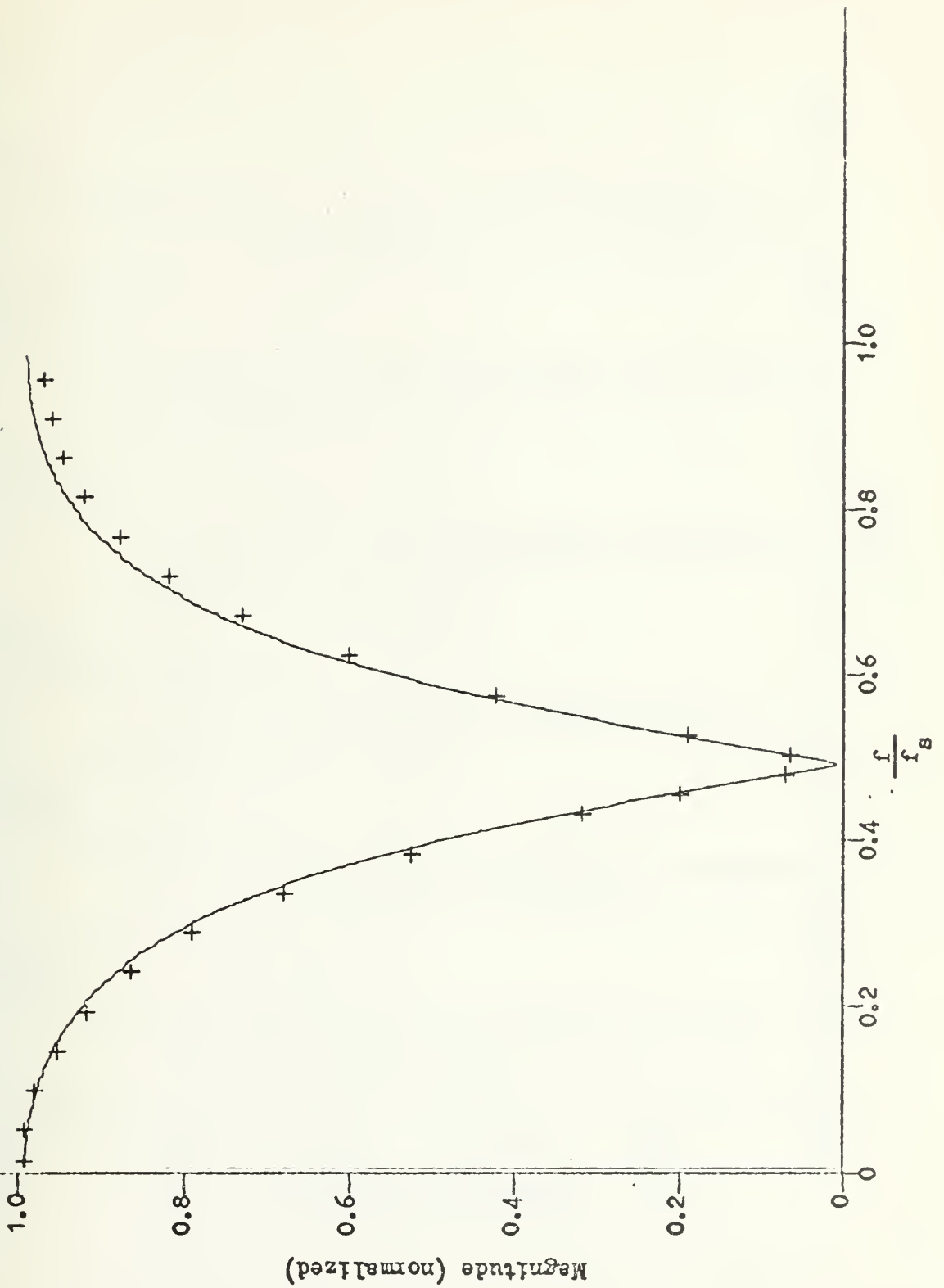


FIGURE 2.16a Theoretical and Observed Frequency Response of Bilinear Low Pass Filter; $b_1 = 0.3$

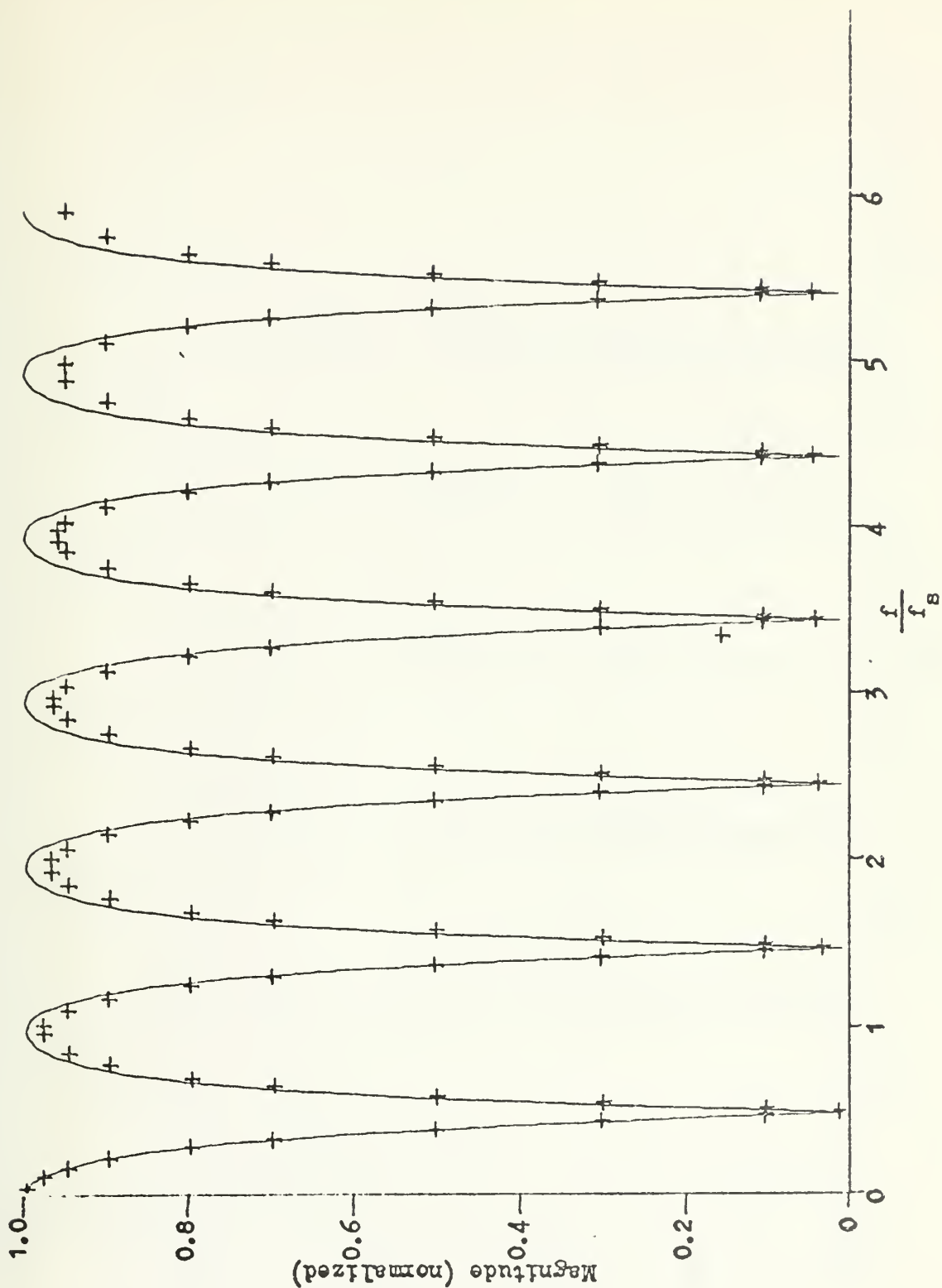


FIGURE 2.16b Theoretical and Observed Frequency Response of Bilinear Low Pass Filter; $b_1 = 0.3$

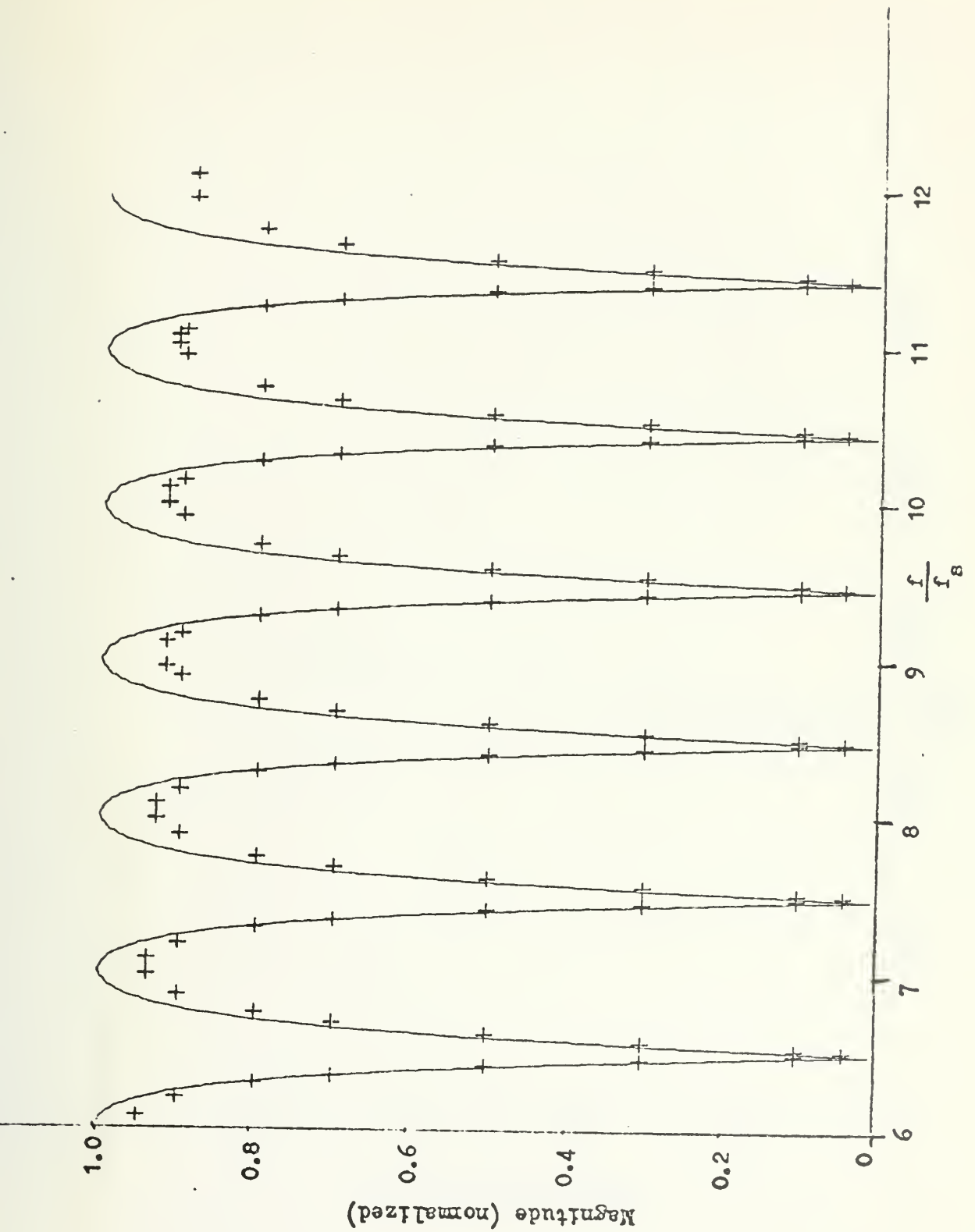


FIGURE 2.16c Theoretical and Observed Frequency Response of Bilinear Low Pass Filter; $b_1 = 0.3$

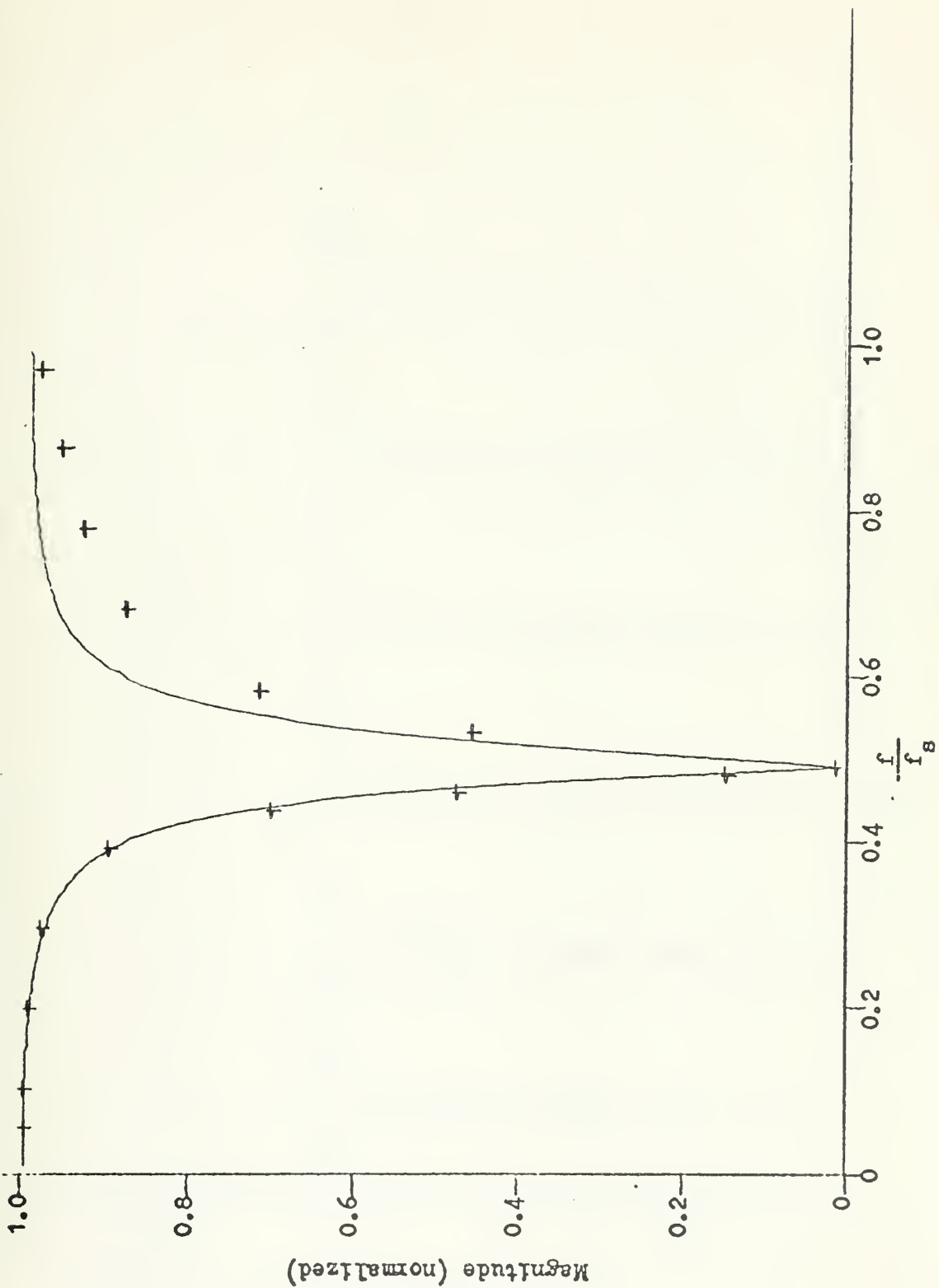


FIGURE 2.17a Theoretical and Observed Frequency Response of Bilinear Low Pass Filter; $b_1 = 0.7$

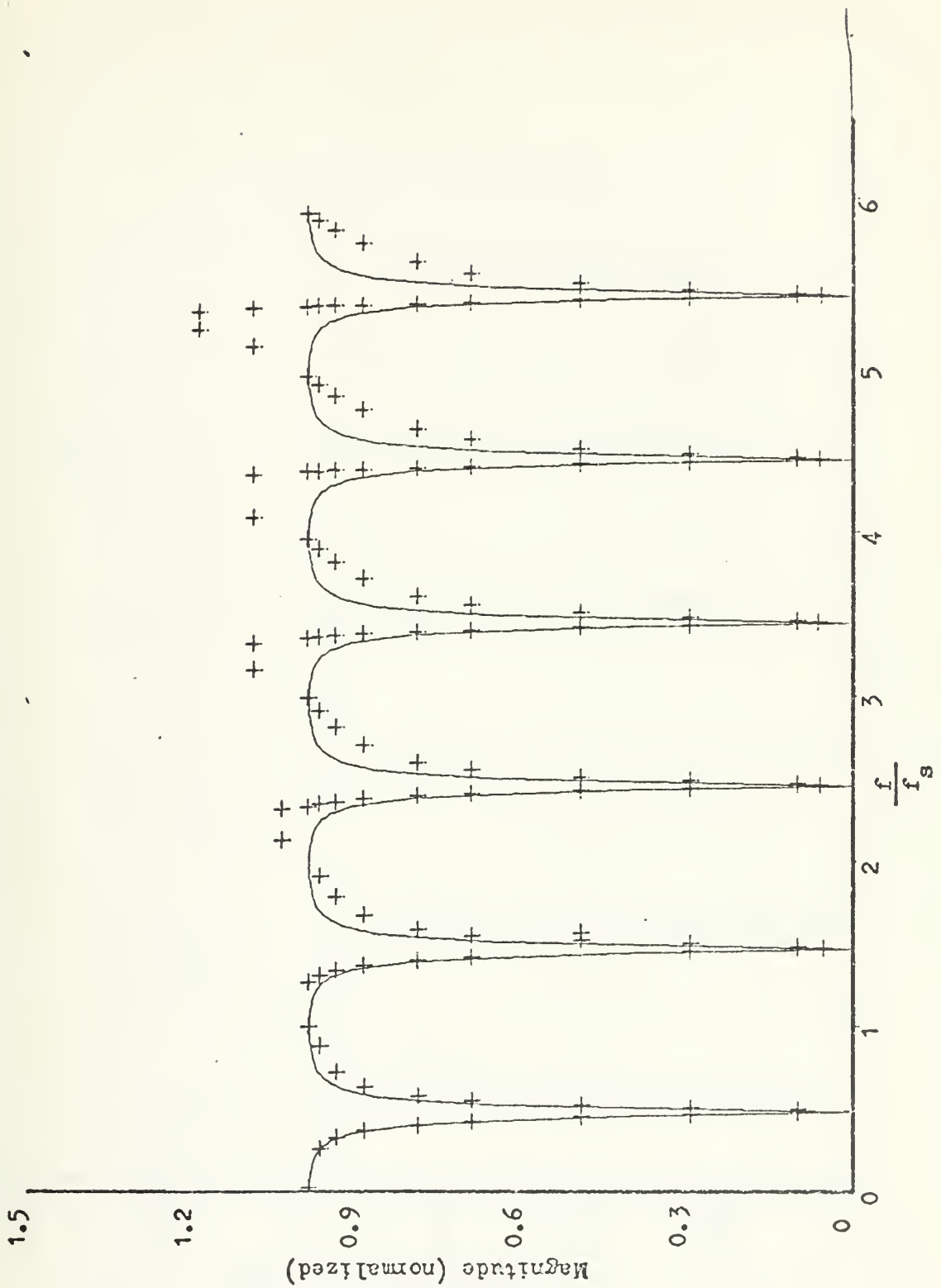


FIGURE 2.17b Theoretical and Observed Frequency Response of Bilinear Low Pass Filter; $b_1 = 0.7$

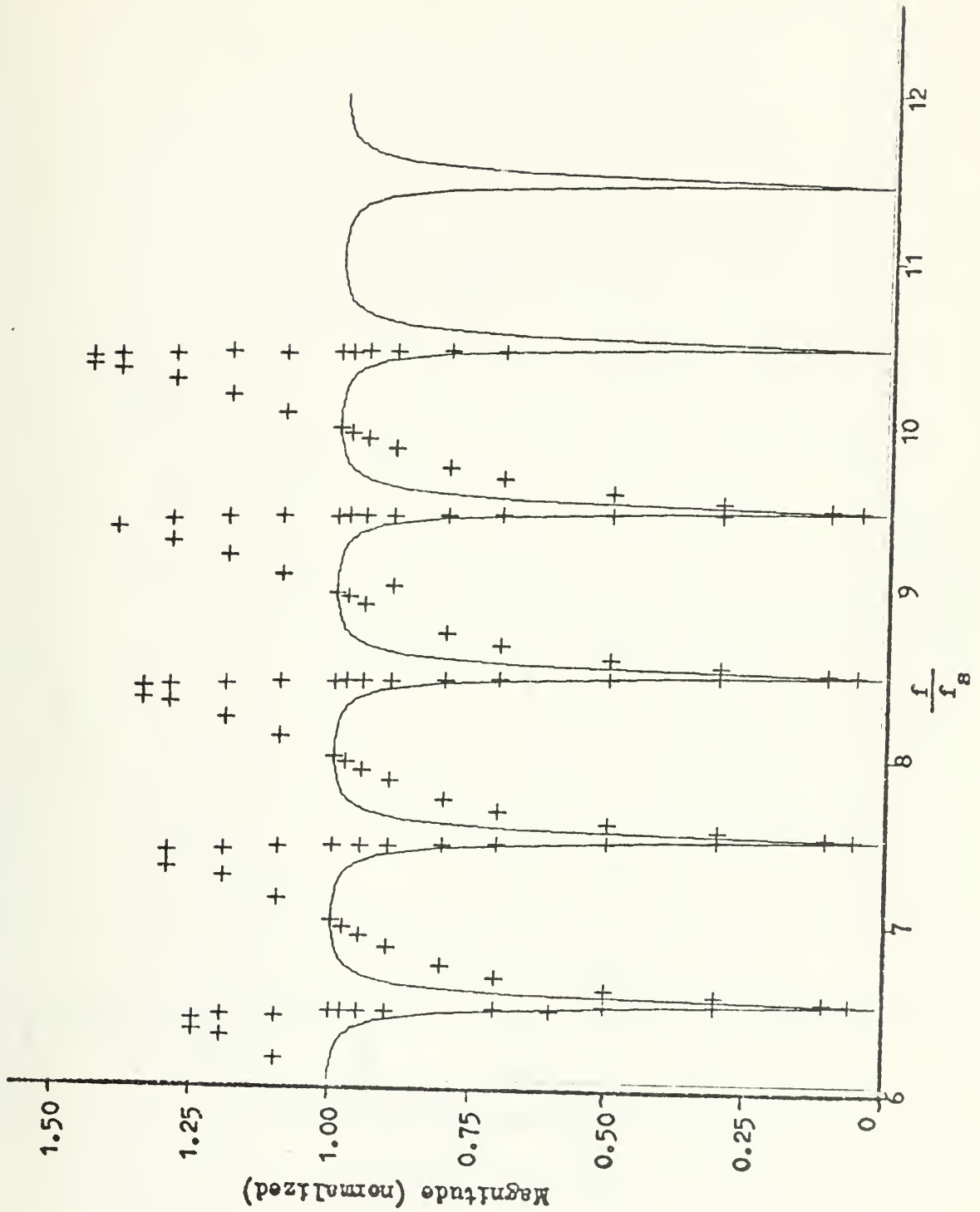


FIGURE 2.17c Theoretical and Observed Frequency Response of Bilinear Low Pass Filter; $b_1 = 0.7$

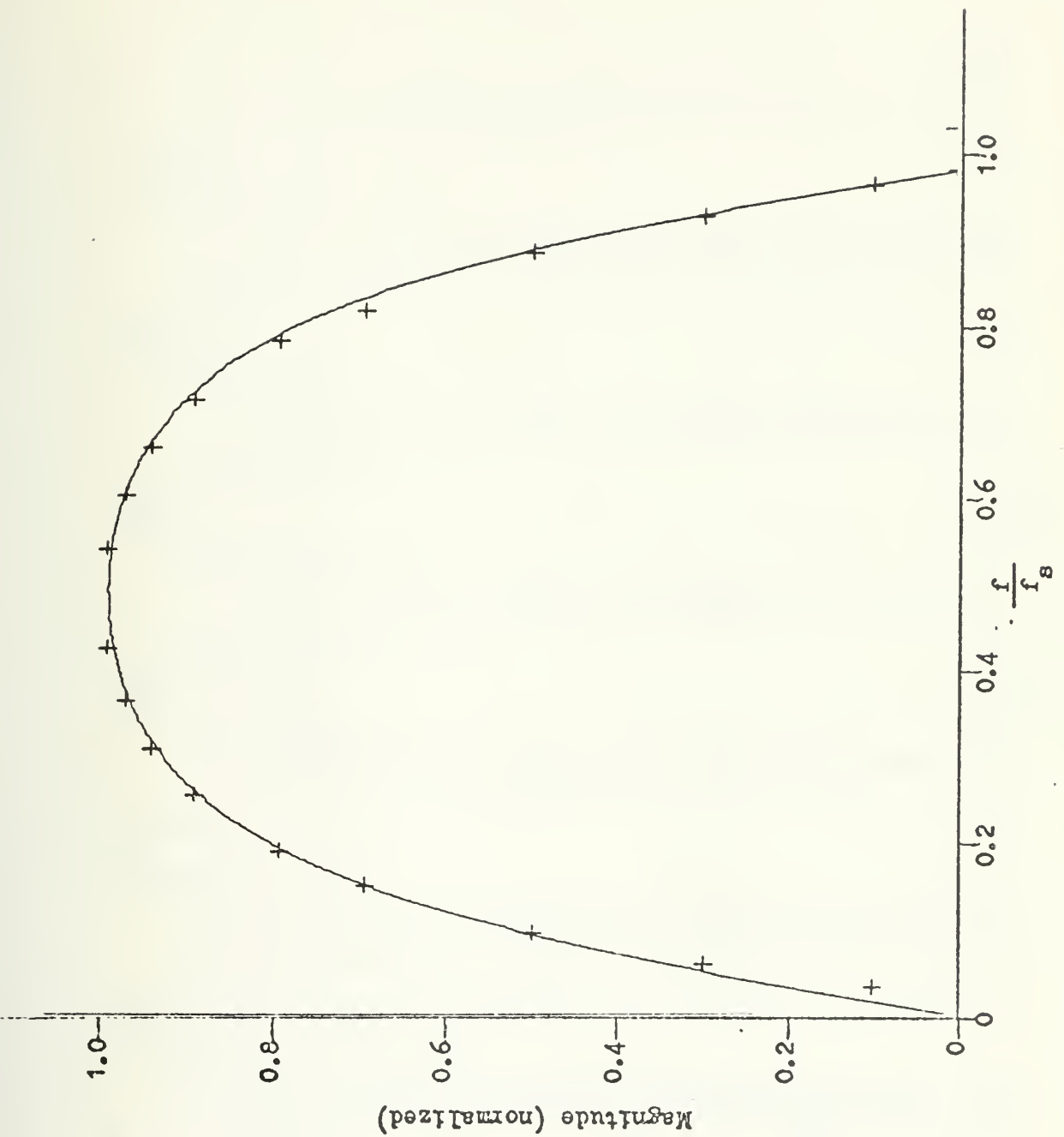


FIGURE 2.18a Theoretical and Observed Frequency Response of Bilinear Z High Pass Filter; $b_1 = -0.3$

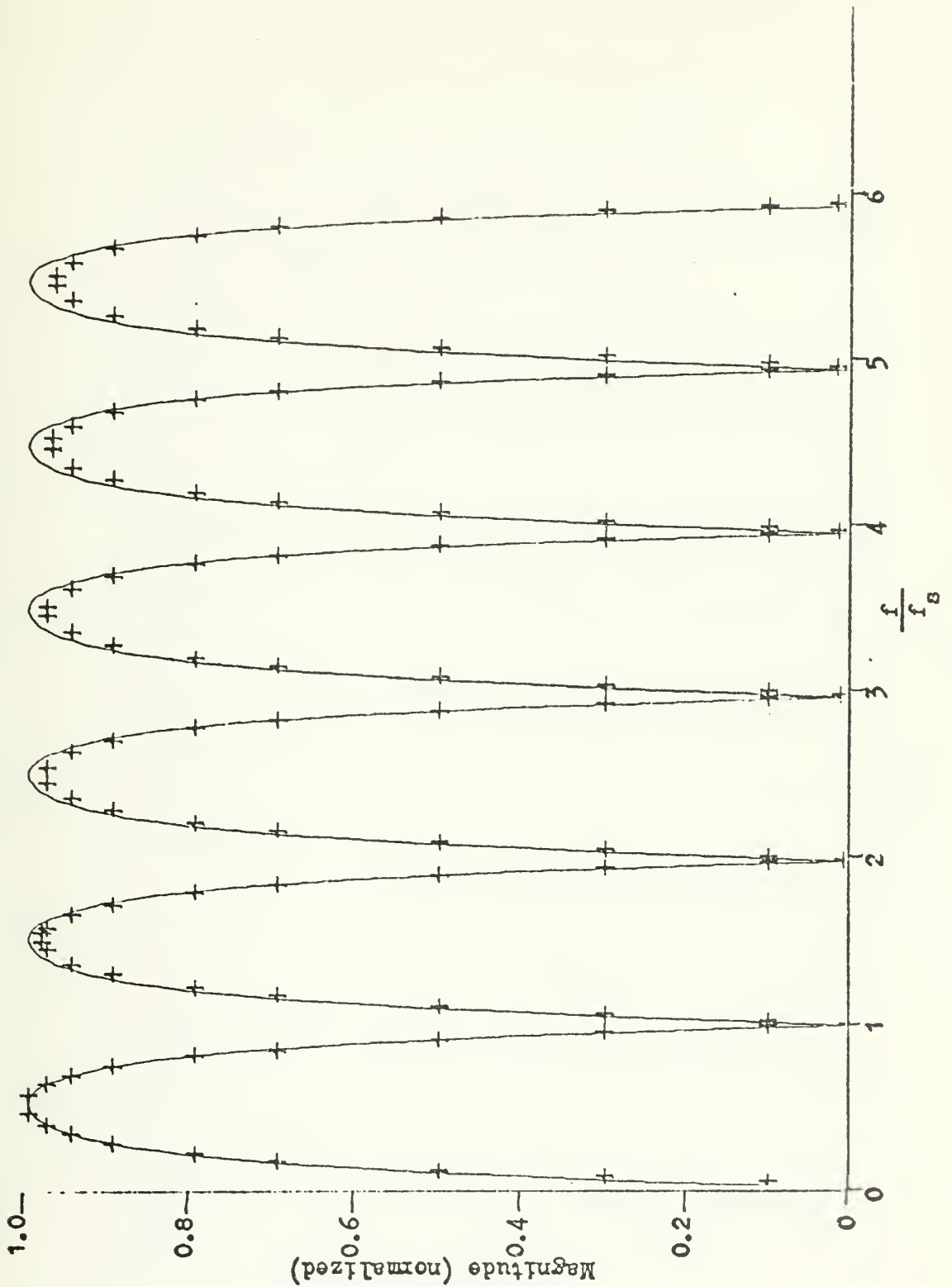


FIGURE 2.18b Theoretical and Observed Frequency Response of Bilinear Z High Pass Filter; $b_1 = -0.3$

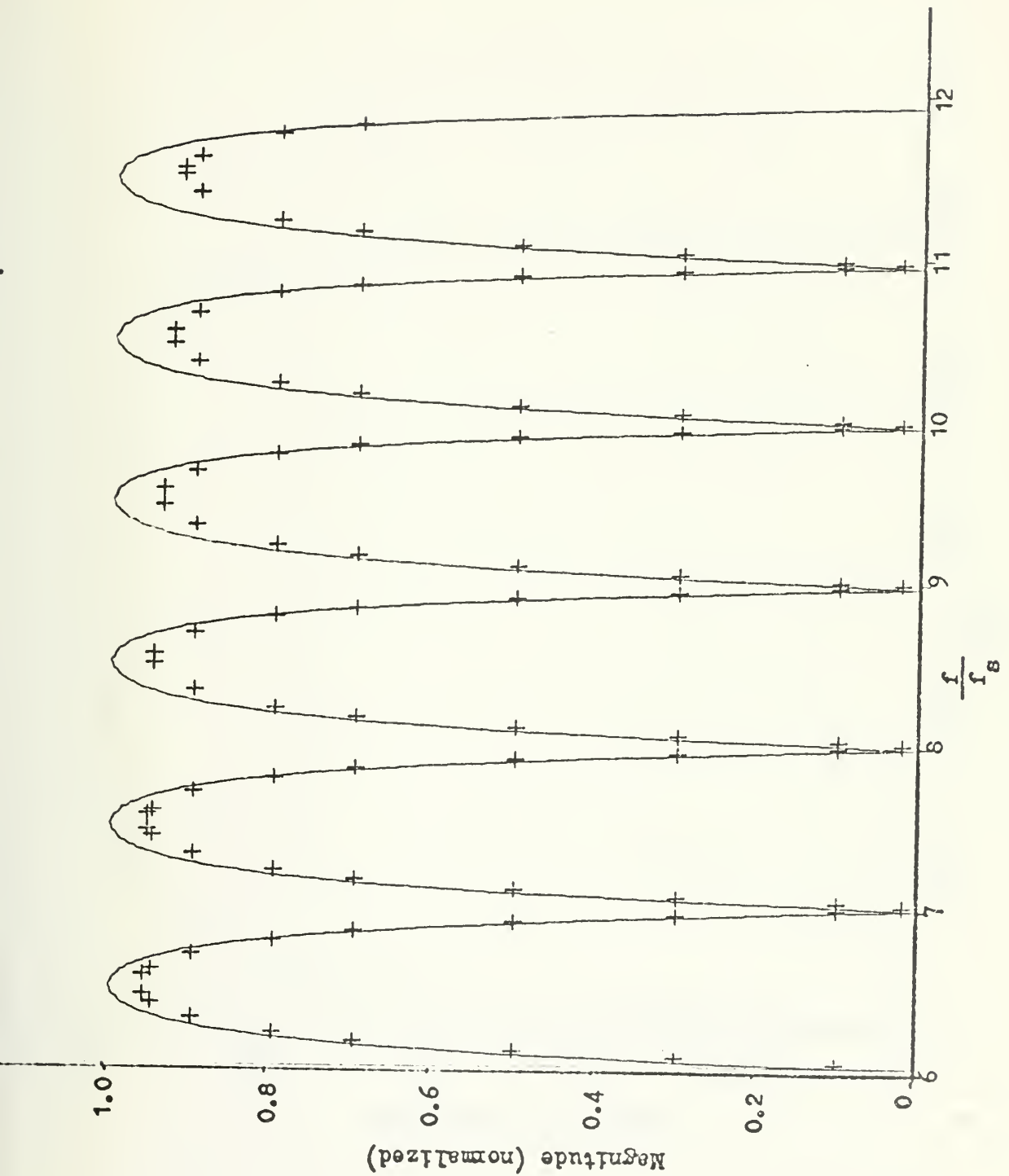


FIGURE 2.18c Theoretical and Observed Frequency Response of Bilinear Z High Pass Filter; $b_1 = -0.3$

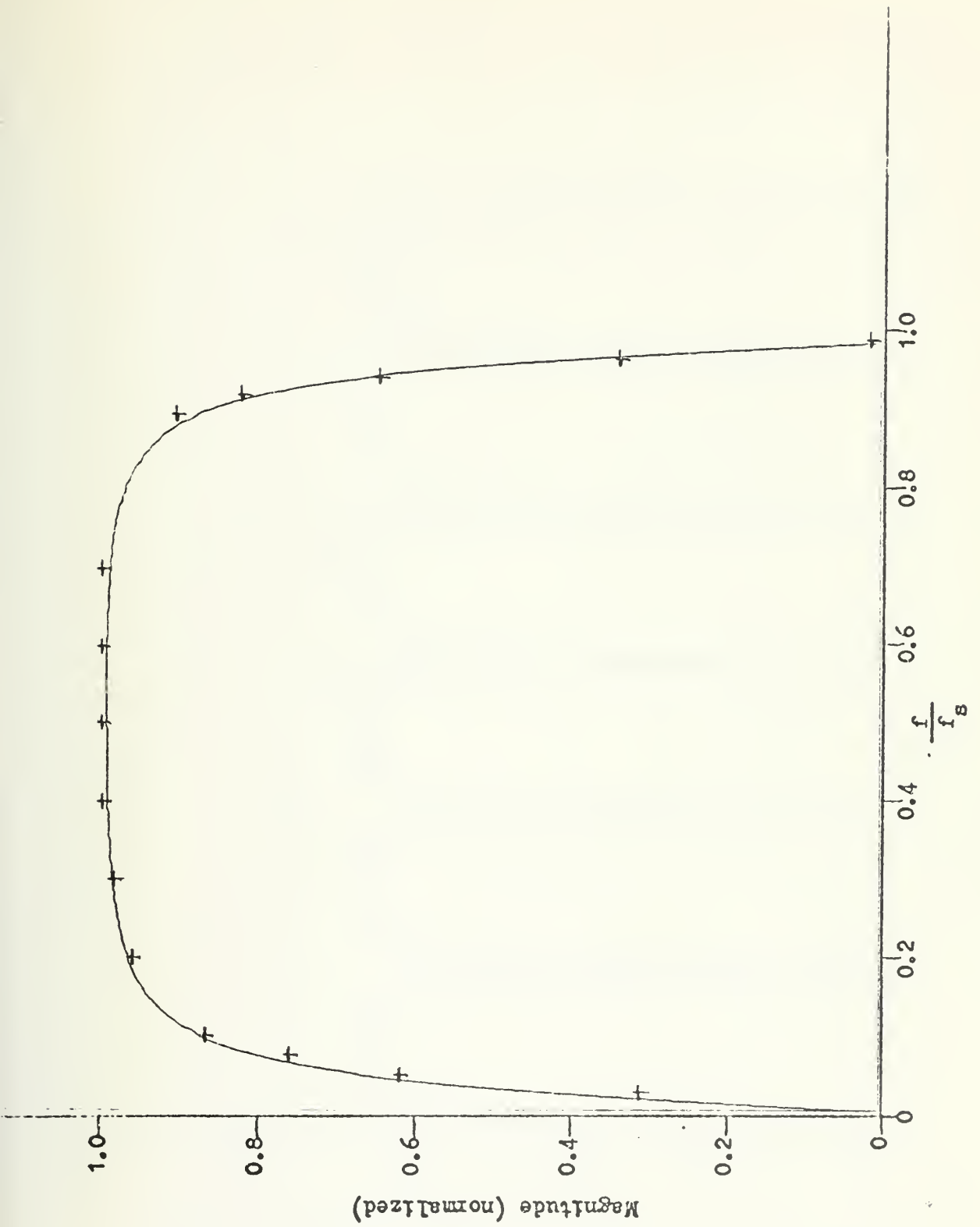


FIGURE 2.19a Theoretical and Observed Frequency Response of Bilinear Z High Pass Filter; $b_1 = -0.7$

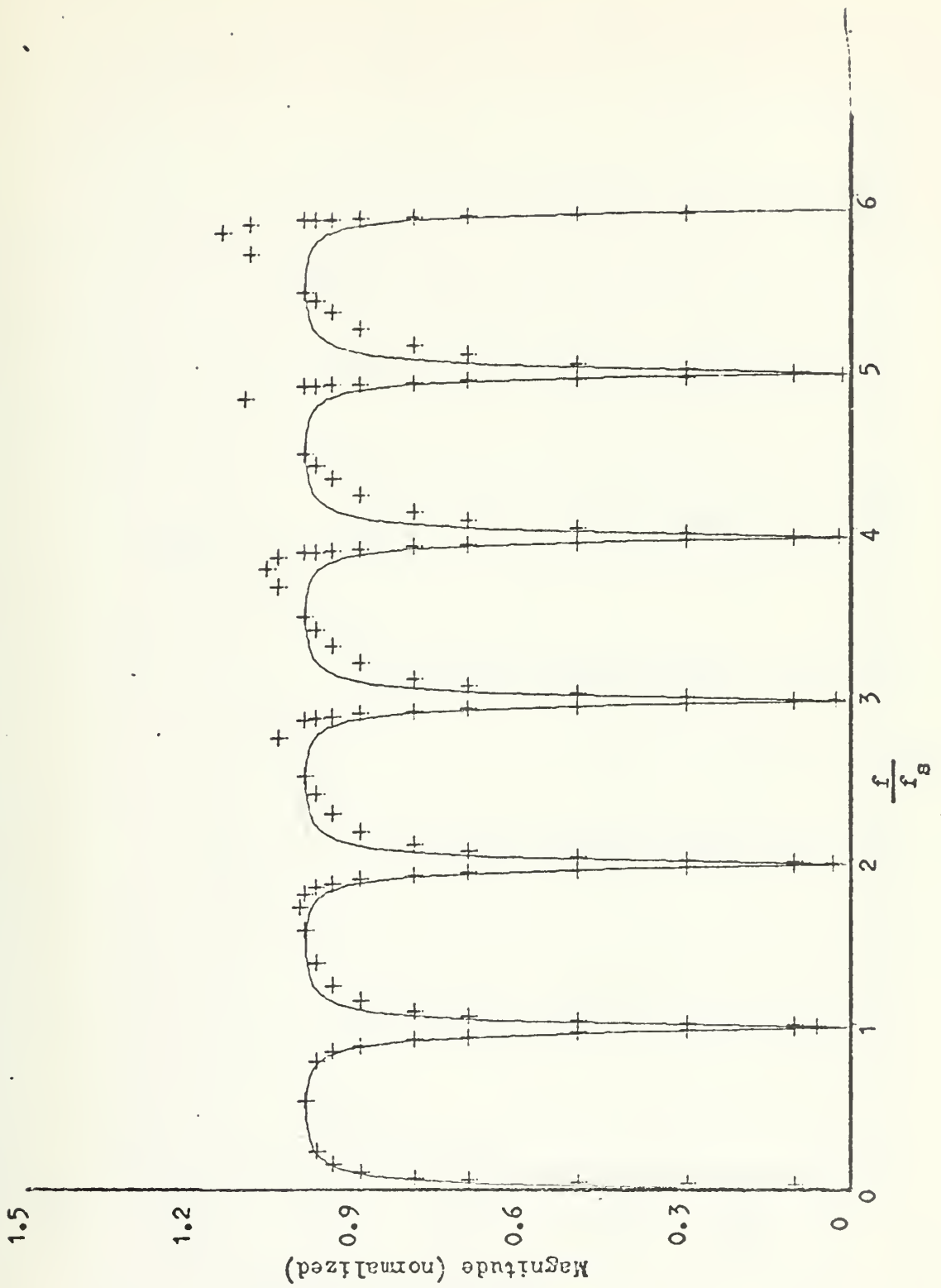


FIGURE 2.19b Theoretical and Observed Frequency Response of Bilinear Z High Pass Filter; $b_1 = -0.7$

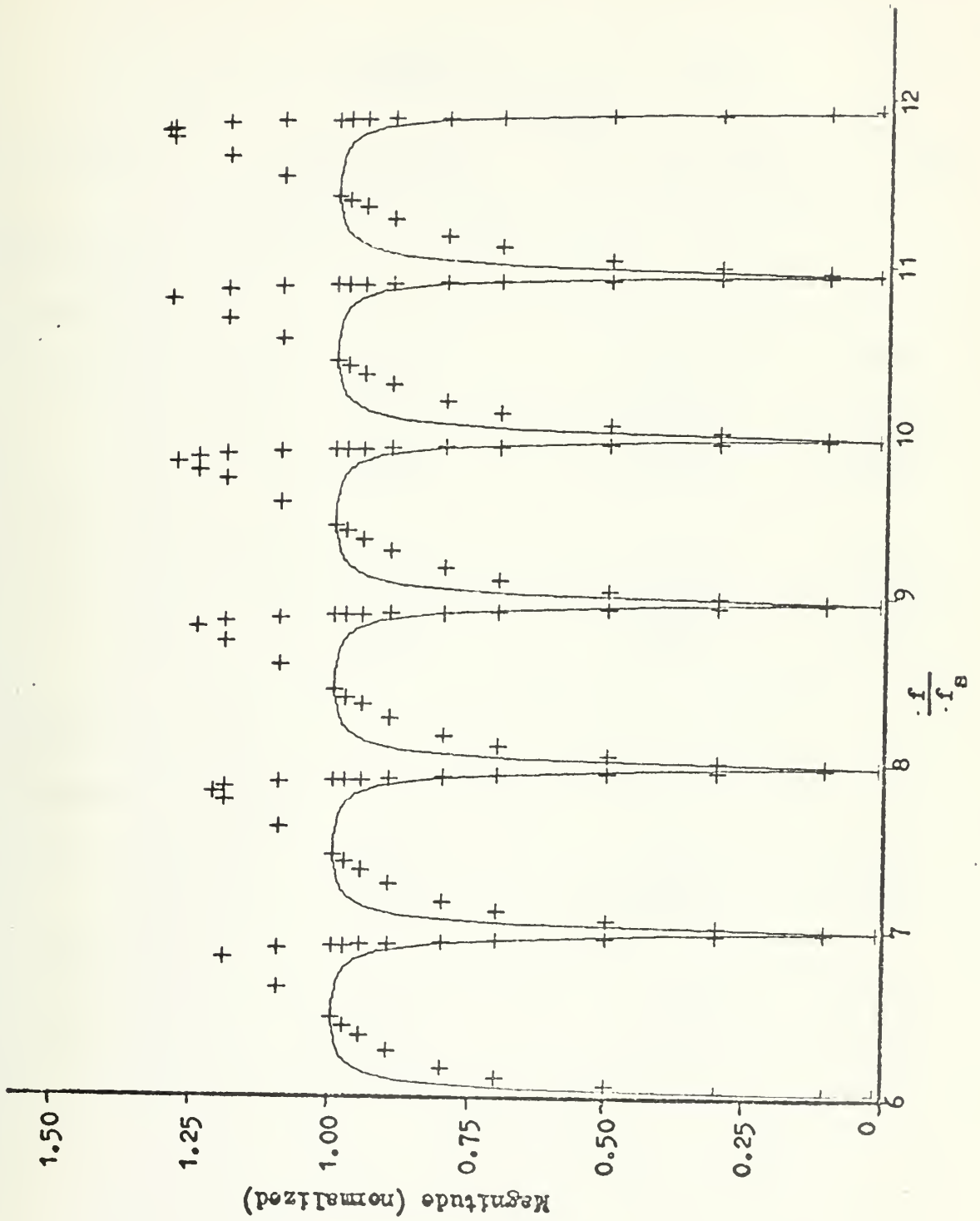


FIGURE 2.19c Theoretical and Observed Frequency Response of Bilinear Z High Pass Filter; $b_1 = -0.7$

TABLE I

| Filter | Theoretical | ω_c / ω_s | |
|--------------|-------------|-------------------------|-----------------------|
| | | $f_c = 400 \text{ kHz}$ | $f_c = 1 \text{ MHz}$ |
| Bilinear Z | | | |
| Low Pass | | | |
| $b_1 = 0.0$ | 0.250 | 0.251 | 0.246 |
| 0.3 | 0.343 | 0.338 | 0.330 |
| 0.7 | 0.444 | 0.438 | 0.431 |
| High Pass | | | |
| $b_1 = -0.3$ | 0.157 | 0.153 | 0.151 |
| -0.7 | 0.056 | 0.061 | 0.065 |
| Standard Z | | | |
| Low Pass | | | |
| $b_1 = -0.3$ | 0.221 | 0.239 | 0.219 |
| -0.7 | 0.057 | 0.072 | 0.063 |
| High Pass | | | |
| $b_1 = 0.3$ | 0.279 | 0.254 | 0.252 |
| 0.7 | 0.443 | 0.429 | 0.428 |

III. SAMPLED ANALOG NON-RECURSIVE FILTER

A. THEORY

Since the frequency response of a sampled filter is periodic, it may be described by a Fourier series [1],

$$H(j\omega) = \sum_{k=-\infty}^{\infty} D_k e^{j\omega T k} ,$$

where

$$D_k = \frac{T}{2\pi} \int_{-\pi/T}^{\pi/T} H(j\omega) e^{-jk\omega T} d\omega .$$

This expression for D_k is mathematically equivalent to an inverse Laplace transform of the transfer function, $H(s)$, which is $h(t)$, evaluated at $t = kT$,

$$D_k = h(kT) ,$$

where $h(t)$ is the impulse response of the filter. By using the definition of z ,

$$H(z) = \sum_{k=-\infty}^{\infty} h(kT) z^k ,$$

where $h(t)$ is assumed to be an even function in time, therefore it is not a true impulse response.

For a delay device with $2N$ taps available, $H(z)$ can be approximated by the series,

$$H(z) = \sum_{k=-N}^N h(kT) z^k .$$

Figure 3.1 illustrates the implementation of this series. The approximation can be made closer to the designed response by truncating the series at larger values of N . At least $2N$ storage elements are required.

For a rectangular bandpass filter response, such as that shown in Figure 3.2, repeated with a period of $\omega_s = \frac{2\pi}{T}$, the coefficients of the Fourier series are calculated in Appendix G by the following expression,

$$D_k = D_{-k} = \frac{2}{k\pi} \sin(2k\pi BT) \cos\left(2k \frac{\omega_0}{\omega_s}\right) .$$

Since truncating the series is like multiplying the infinite series by a window which is unity for $-NT \leq t \leq NT$ and zero elsewhere, the result of the truncation is to convolve the frequency response with the Fourier transform of the window function. A rectangular window transforms to a $\frac{\sin x}{x}$ function which adds sidelobes to the response as a result of the convolution. By choosing a different window function, such as a Hamming window, these sidelobes can be minimized at the expense of greater passband width [8]. To use a Hamming window, each coefficient, D_k , is multiplied by a weighting factor, W_k , where,

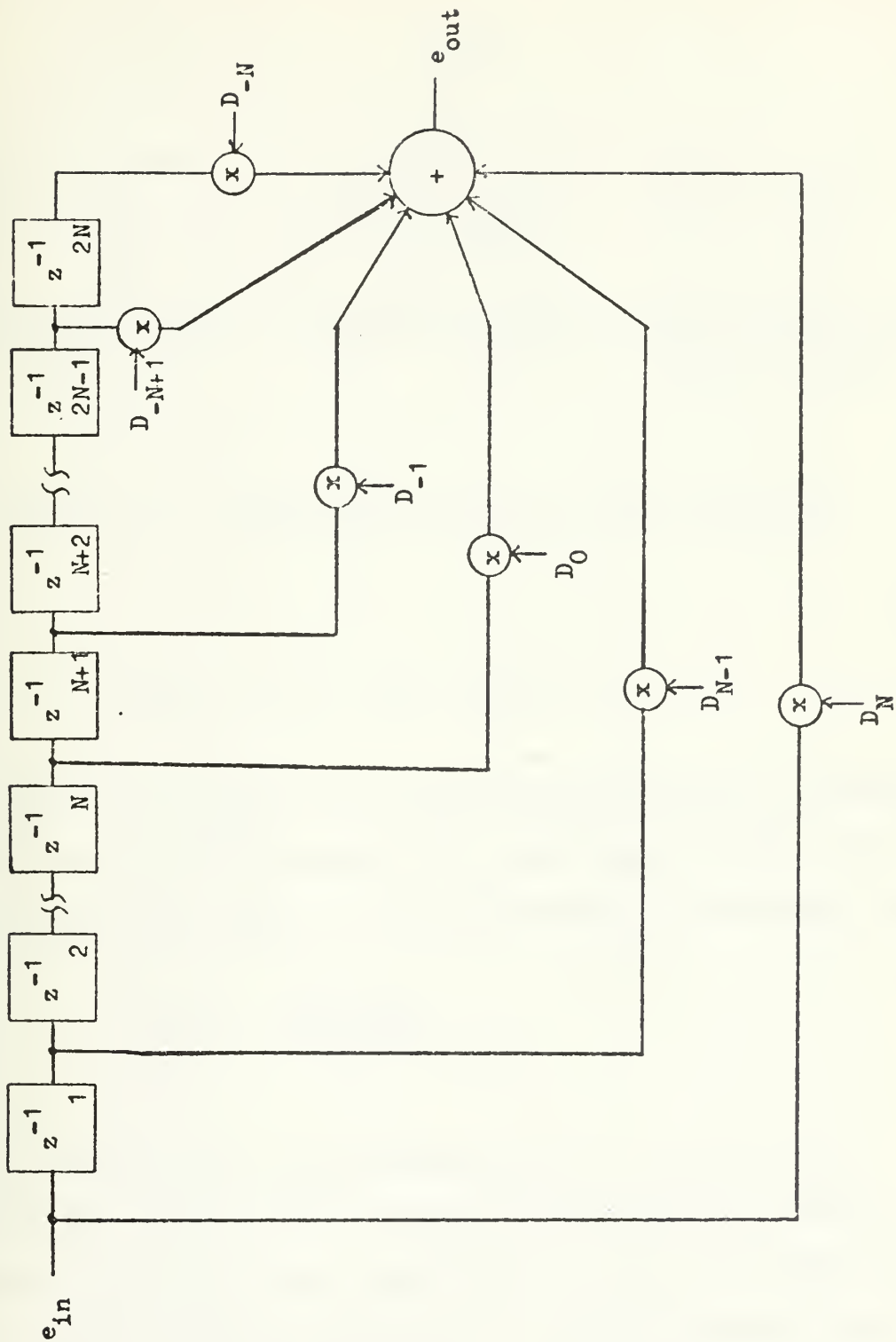


FIGURE 3.1 Implementation of a Non-Recursive Filter

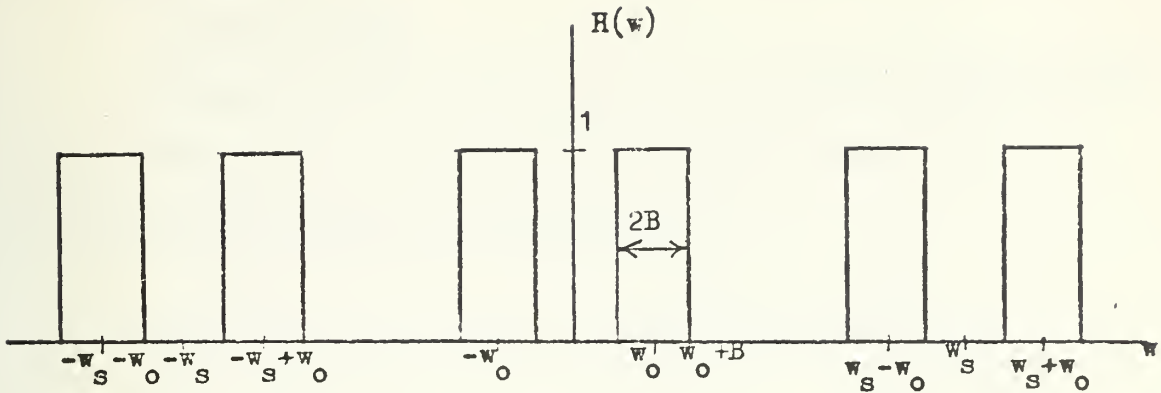


FIGURE 3.2 Rectangular Bandpass Filter Response

$$W_k = 0.54 + 0.46 \cos\left(\pi \frac{k}{N}\right) .$$

Since the input to the non-recursive filter is sampled with a finite width pulse of T_c , the clock period, the spectrum of the input is enclosed within an envelope, $E(f)$,

$$E(f) = \frac{\sin(\pi f T_c)}{\pi f T_c} .$$

This envelope has its first null at $f = f_c$, the clock frequency. Though this envelope is imposed by sampling rather than the filter algorithm, it can be included within the filter response function as a multiplicative factor.

B. EXPERIMENT

1. Configuration

Reticon Corporation markets a 12-term Tapped Analog Device (TAD-12) which provides 12 output taps with the following time delay configuration.

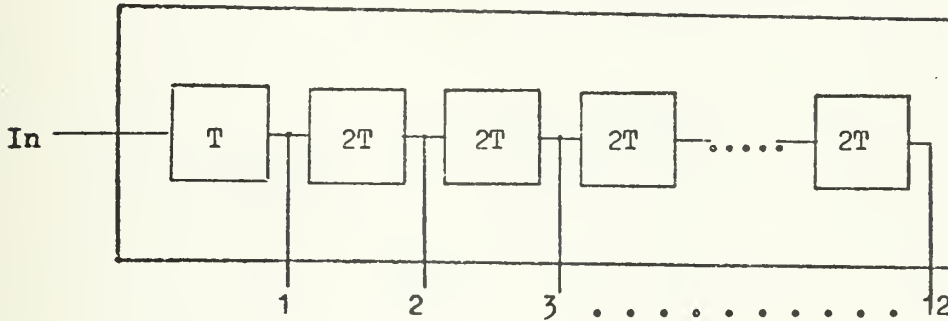


FIGURE 3.3 TAD-12 Delay Configuration

Since the first tap is only T_c delayed from the input and the remainder of the taps are spaced with $2T_c$, the undelayed input can not be used for the A_N term, therefore, only 11 terms of a given tapped delay device can be utilized.

The filter is implemented by weighting the tap outputs proportional to the Fourier series coefficients. Analysis performed in Appendix G and the computer program described in Appendix H provide design values for the tapping resistances, R_k . Figure 3.4 describes the filter set-up. The lower ends of R_k are connected either to the inverting or non-inverting input of the summer depending upon the relative coefficient polarity. Since $D_k = D_{-k}$,

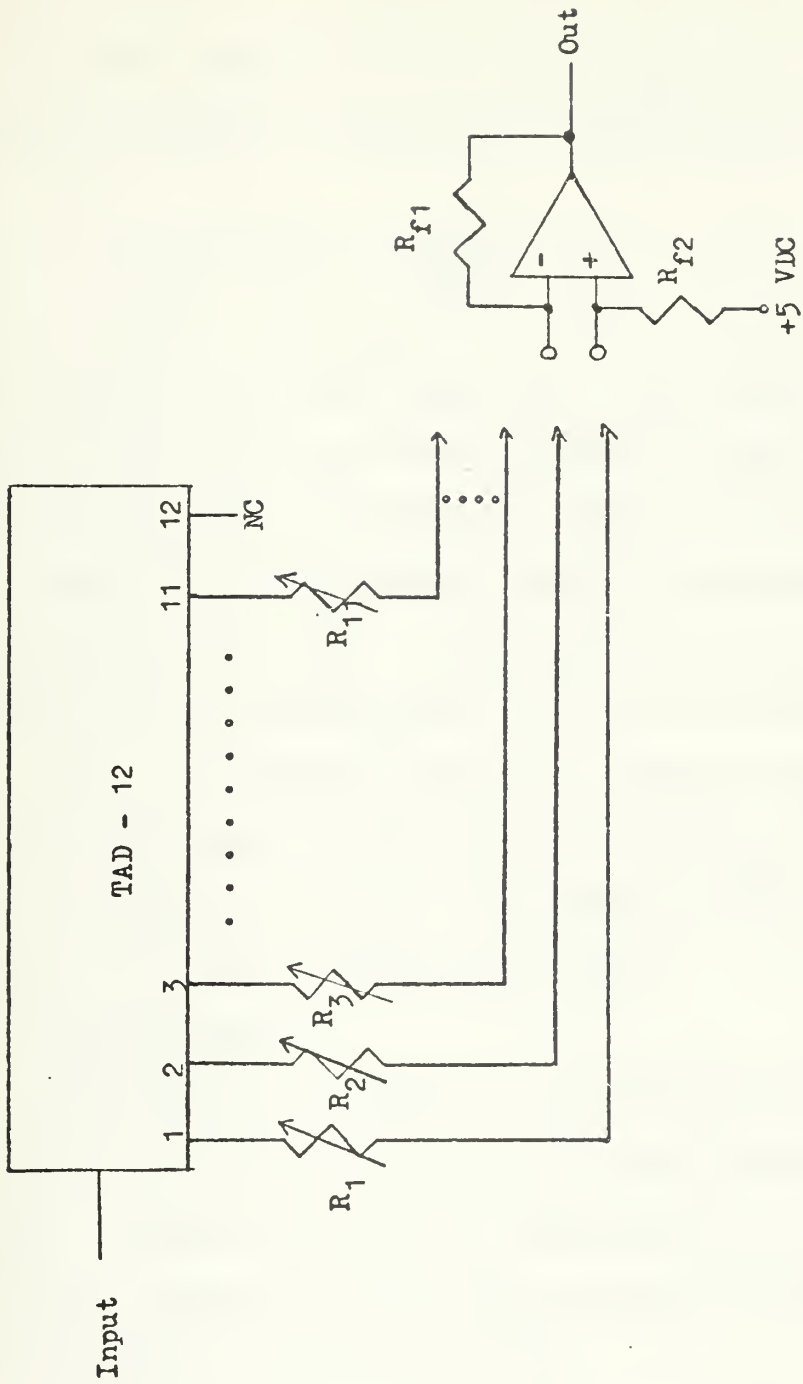


FIGURE 3.4 Non-Recursive Filter Set-Up

$R_k = R_{-k}$. In order to not load down the taps, a minimum value of 10,000 ohms is set for the tapping resistances. Appendix H indicates the following expression for R_k ,

$$R_k = (10K + r) \left(\frac{D_{\max}}{|D_k|} \right) - r ,$$

where r is the tap output impedance. For the TAD-12, r is about 5K. Since the resistances depend on the relative values of the series coefficients rather than the absolute values, gain scaling is accomplished by adjustment of the feedback resistance, R_{f_1} . For consistent scaling for opposite polarity coefficients, R_{f_2} must be equal to R_f .

Due to the TAD-12 circuitry, the tap outputs are at a +5 volt bias level, so the lower end of R_{f_2} returns to +5 volts rather than ground. The output of the summer, therefore, rides on a 5 volt bias level.

2. Observations

Two sets of coefficients were designed for a Q of 15. The first set are for $f_0 = \frac{1}{4}f_s$ and the other for $f_0 = \frac{1}{2}f_s$. Table II lists the coefficients and corresponding resistances. These sets of coefficients were measured at clock frequencies of 50 and 100 kHz.

Figures 3.5 through 3.12 illustrate the experimental frequency response compared to the theoretical calculations. For these data, the measured center frequency, f_0 , passband width, BW, and Q are listed in Table III.

TABLE II

| k | $f_o = \frac{1}{4}f_s$ | | $f_o = \frac{1}{2}f_s$ | |
|---|------------------------|-----------|------------------------|-----------|
| | $D_{ k }$ | $R_{ k }$ | $D_{ k }$ | $R_{ k }$ |
| 0 | 0.03333 | 10 K | 0.03333 | 10 K |
| 1 | 0.0 | open | -0.03084 | 11.2 |
| 2 | -0.02770 | 17.0 | 0.02419 | 15.7 |
| 3 | 0.0 | open | -0.01556 | 27.1 |
| 4 | 0.00555 | 85.0 | 0.00773 | 59.7 |
| 5 | 0.0 | open | -0.00314 | 154.3 |

TABLE III

| f_c | FFS | f_o | BW | Q |
|---------|------|----------|-----------|------|
| 50 kHz | 0.25 | 6.25 kHz | 3.213 kHz | 1.95 |
| | 0.5 | 12.5 | 3.033 | 4.12 |
| 100 kHz | 0.25 | 12.5 | 6.402 | 1.95 |
| | 0.5 | 25.0 | 6.154 | 4.06 |

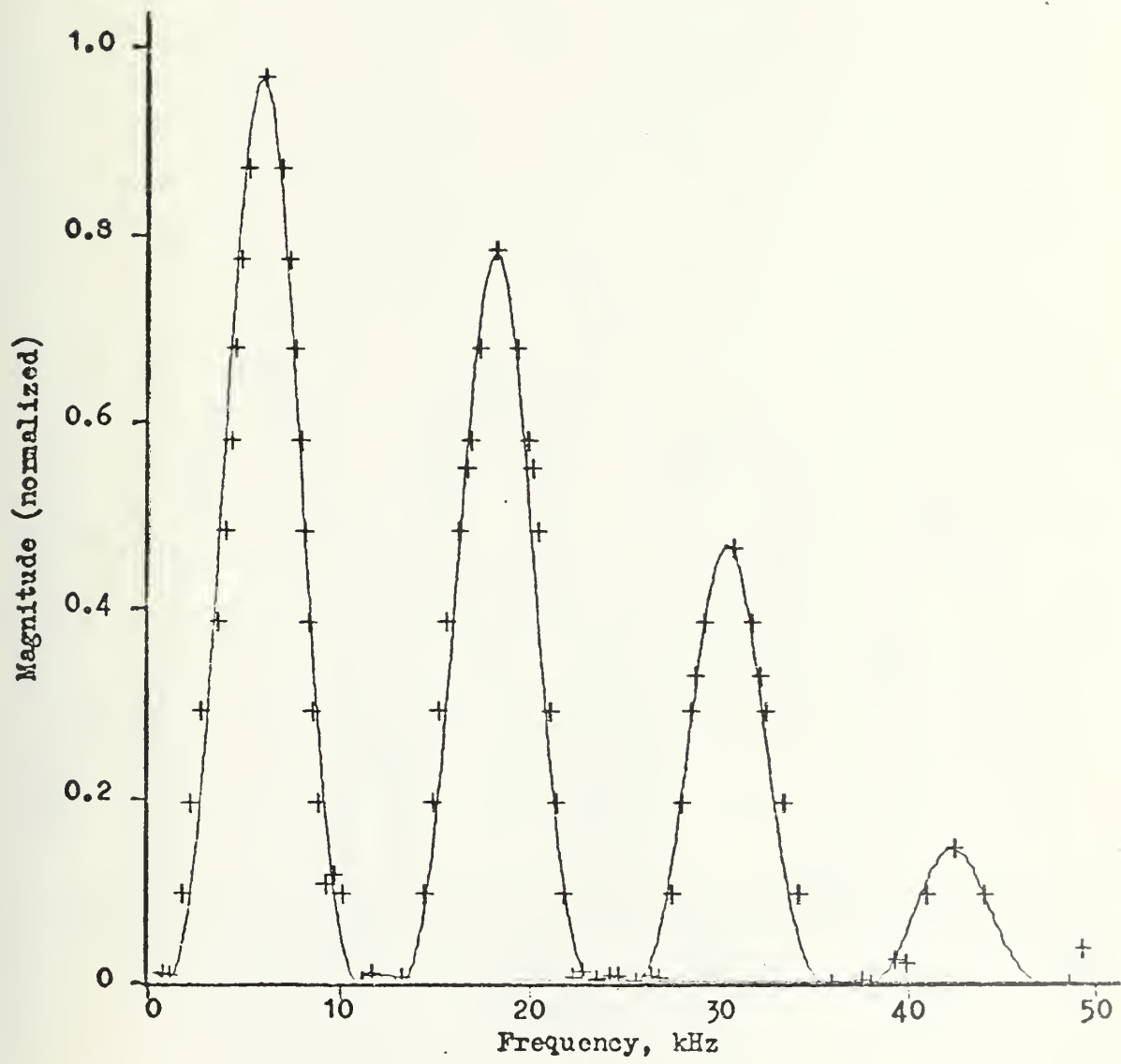


FIGURE 3.5 Theoretical and Observed Frequency Response;
 $f_0 = \frac{1}{4}f_s$, $f_c = 50$ kHz

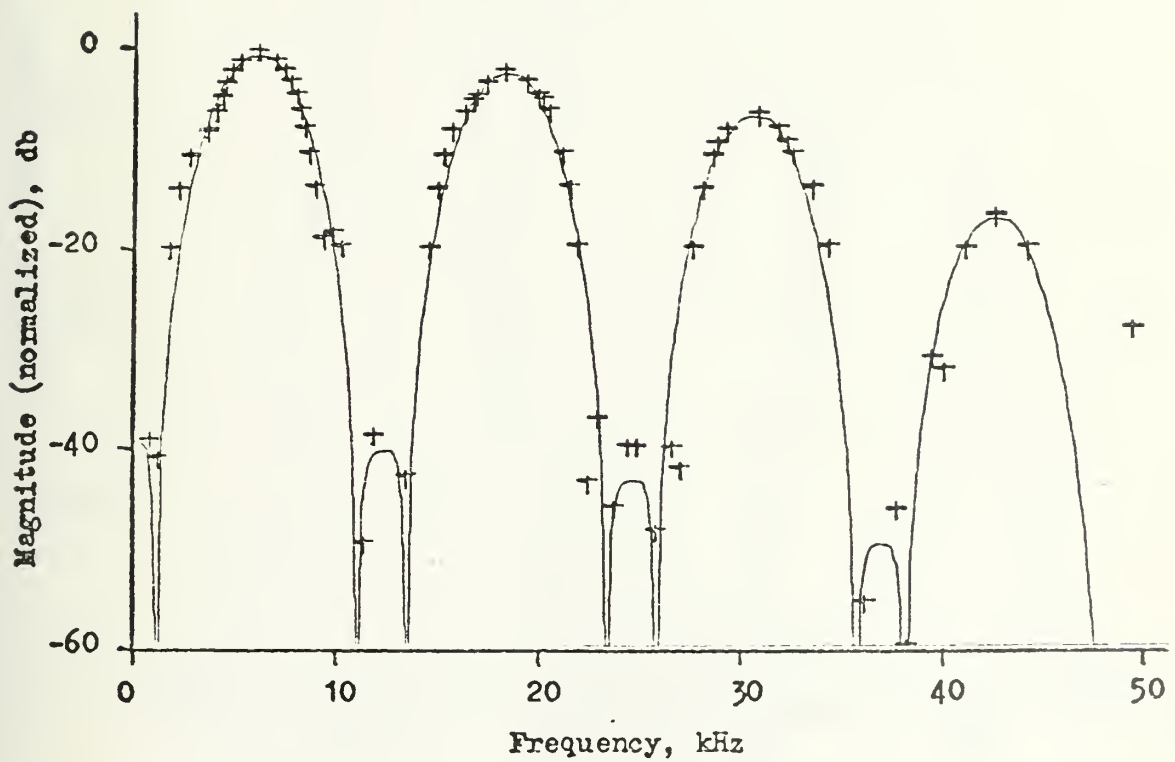


FIGURE 3.6 Theoretical and Observed Frequency Response; $f_o = \frac{1}{4}f_s$, $f_c = 50$ kHz, Magnitude in dB

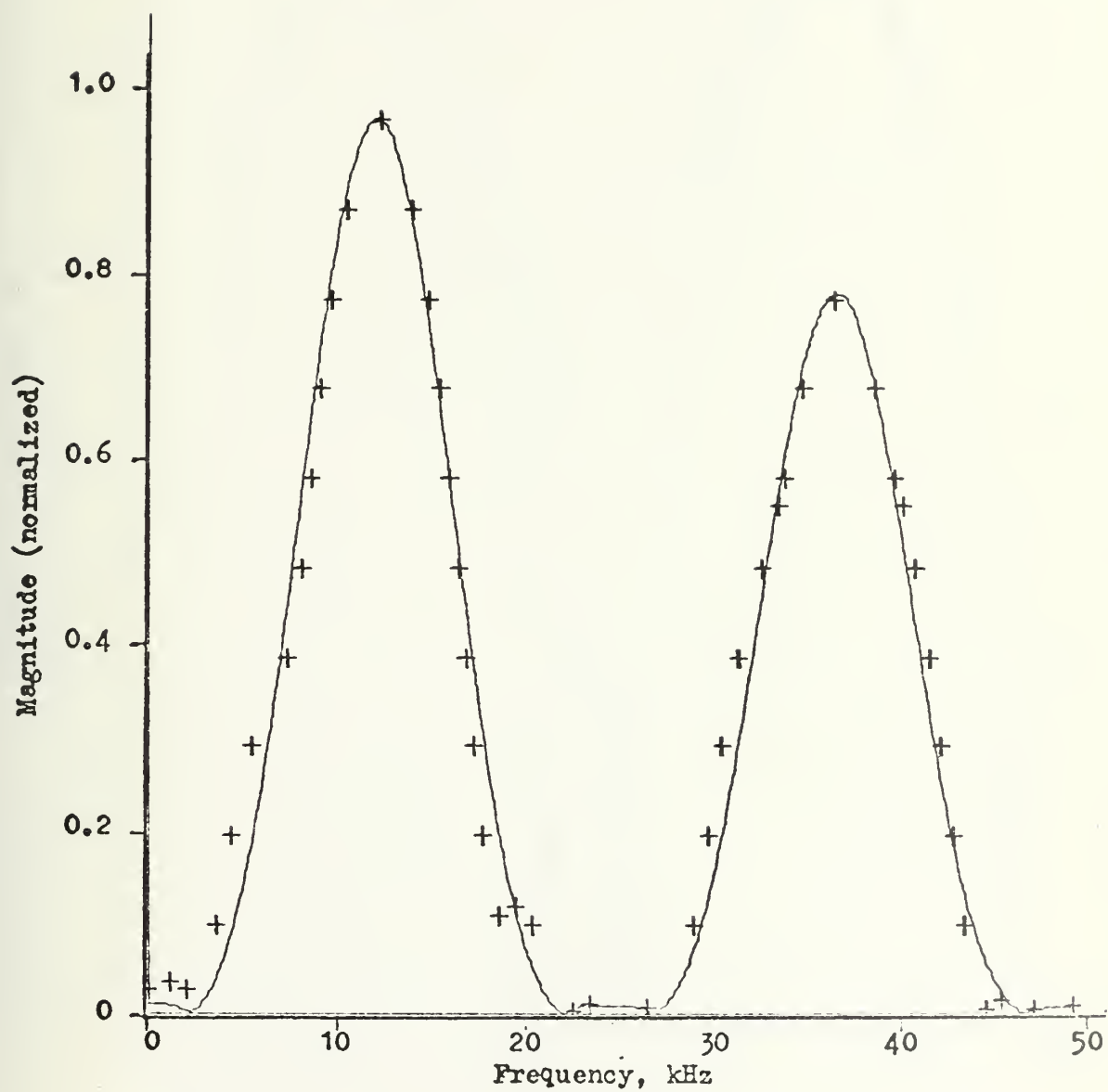


FIGURE 3.7 Theoretical and Observed Frequency Response;
 $f_o = \frac{1}{4}f_s$, $f_c = 100$ kHz

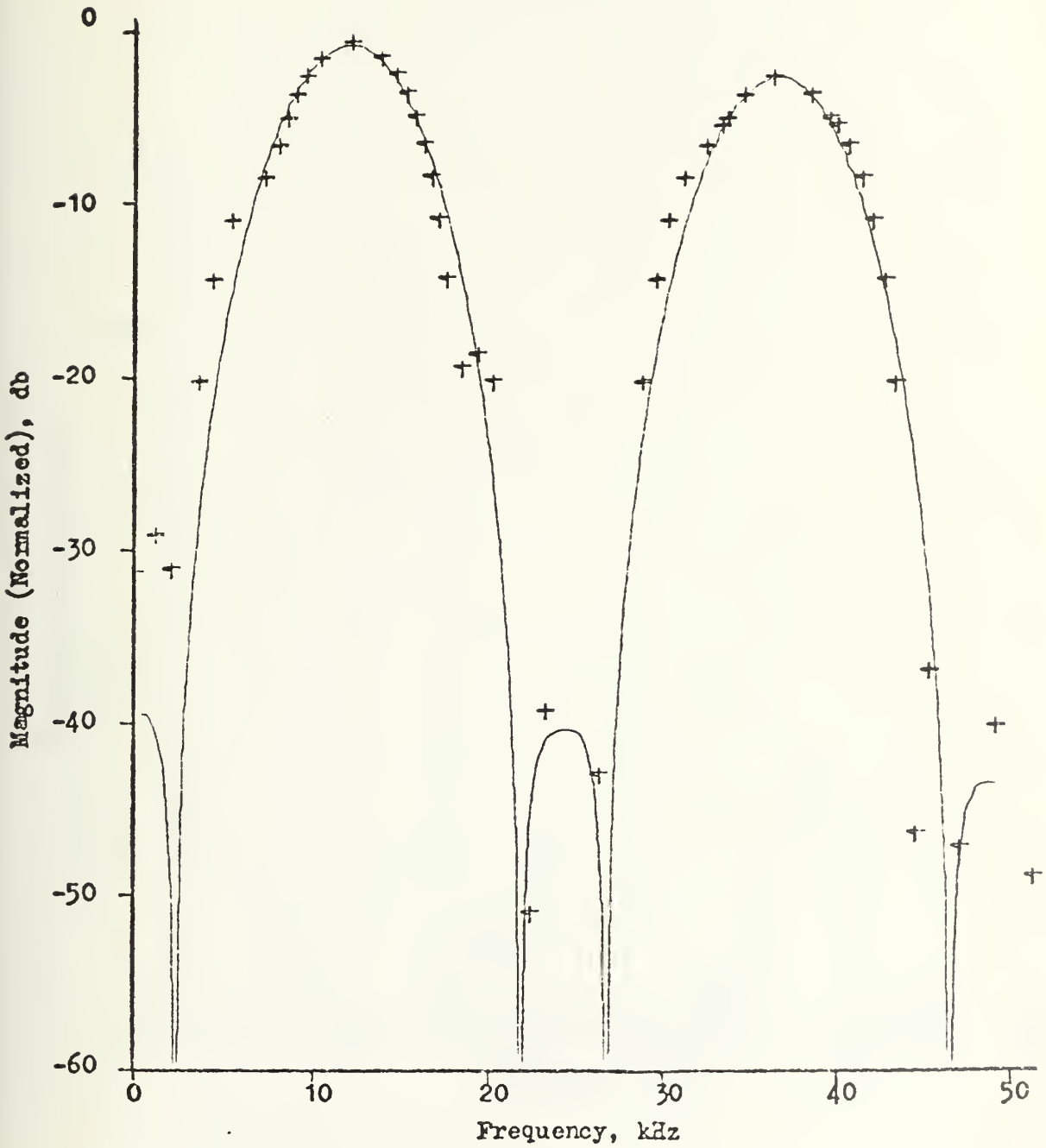


FIGURE 3.8 Theoretical and Observed Frequency Response; $f_o = \frac{1}{4}f_s$, $f_c = 100$ kHz, Magnitude in dB

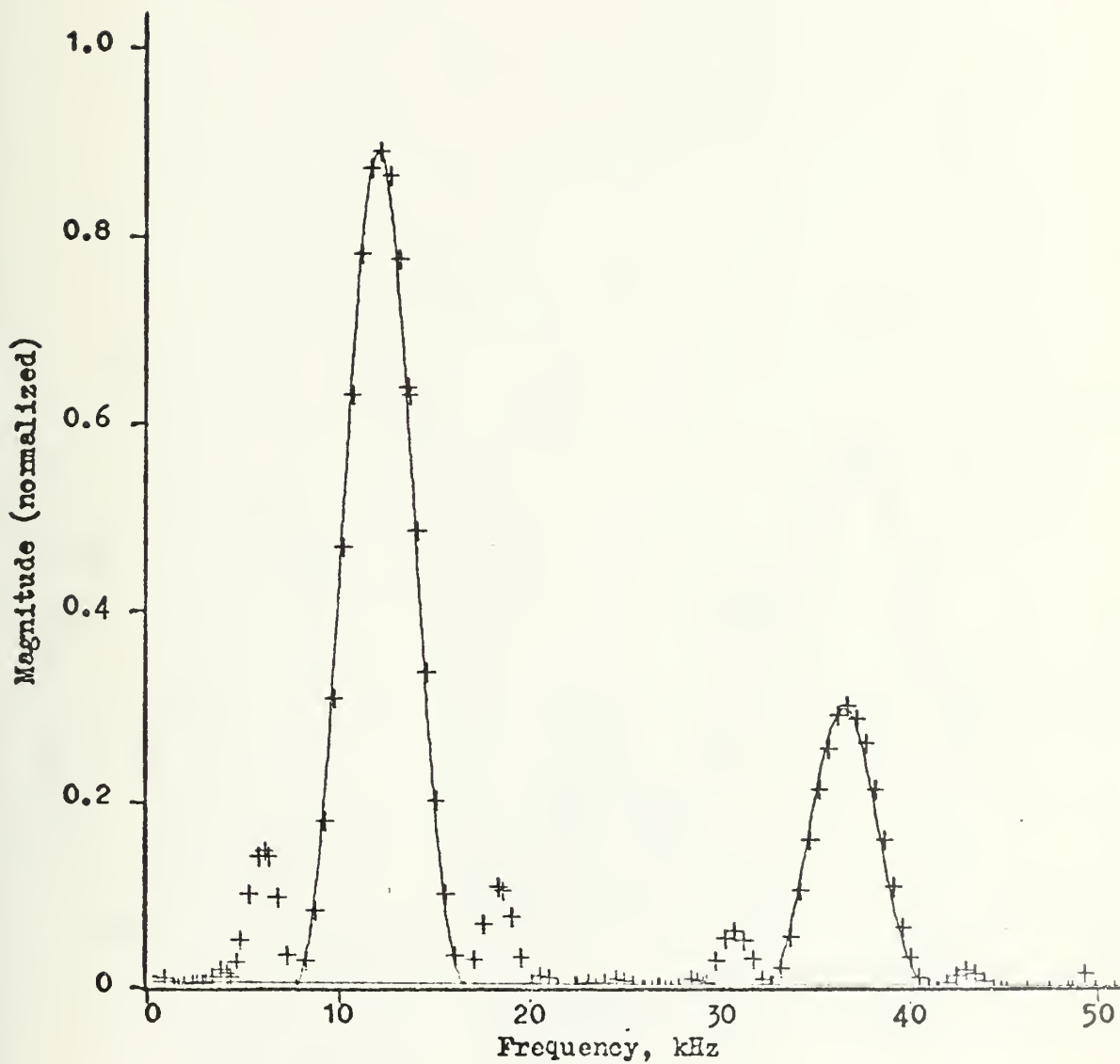


FIGURE 3.9 Theoretical and Observed Frequency Response;
 $f_o = \frac{1}{2}f_s$, $f_c = 50$ kHz

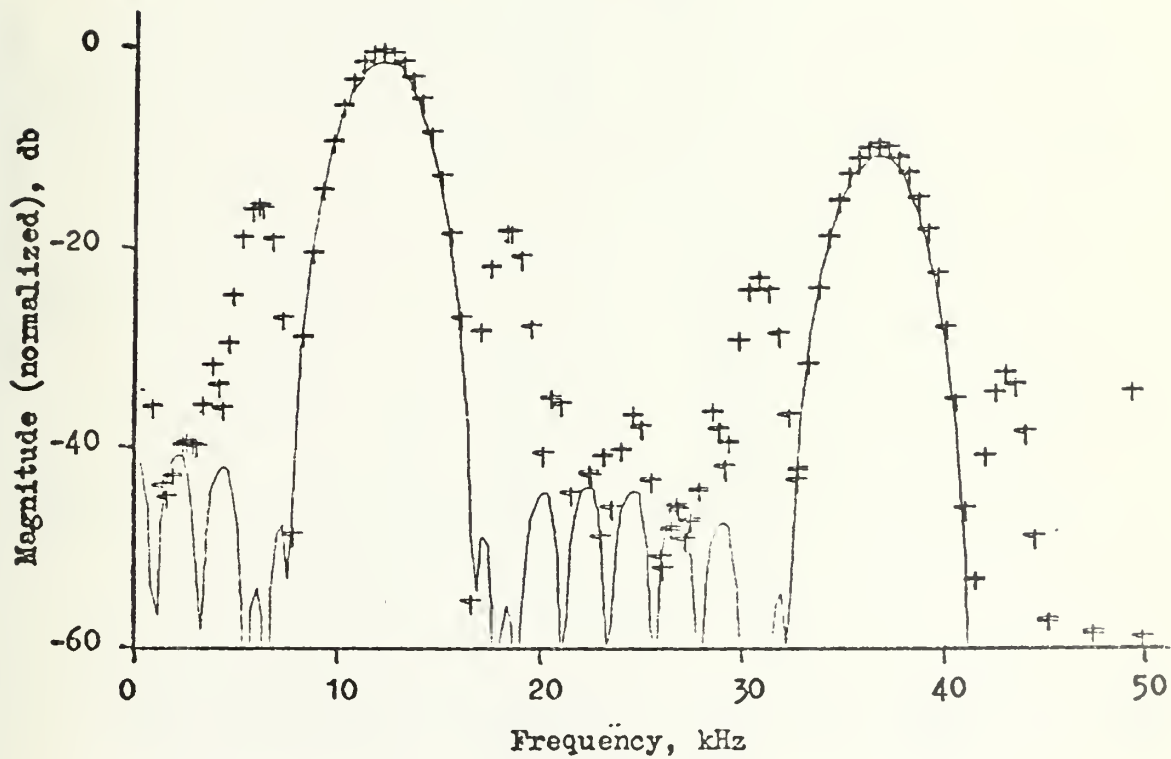


FIGURE 3.10 Theoretical and Observed Frequency Response;
 $f_o = \frac{1}{2}f_s$, $f_c = 50$ kHz, Magnitude in dB

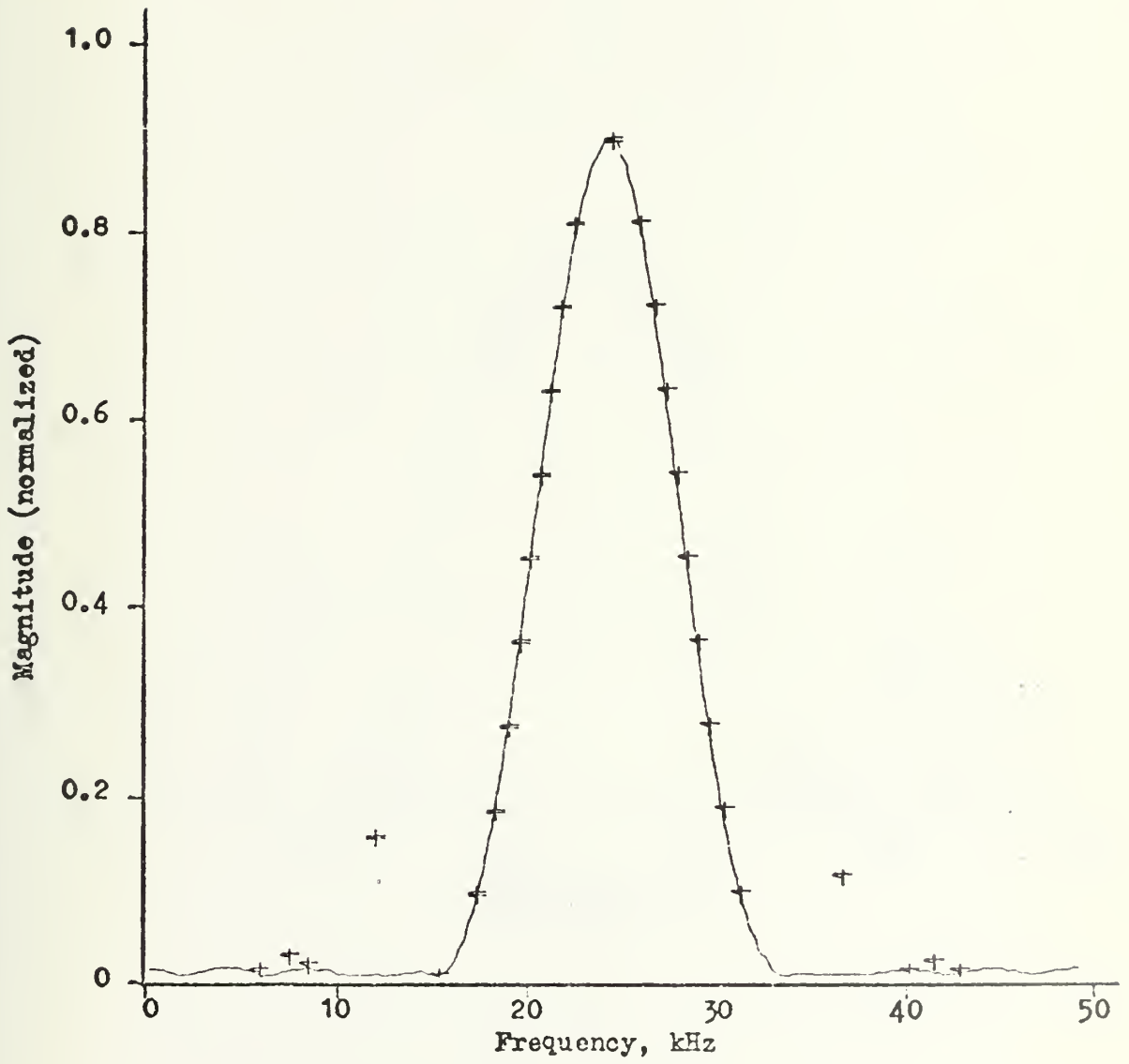


FIGURE 3.11 Theoretical and Observed Frequency Response;
 $f_o = \frac{1}{2}f_s$, $f_c = 100$ kHz

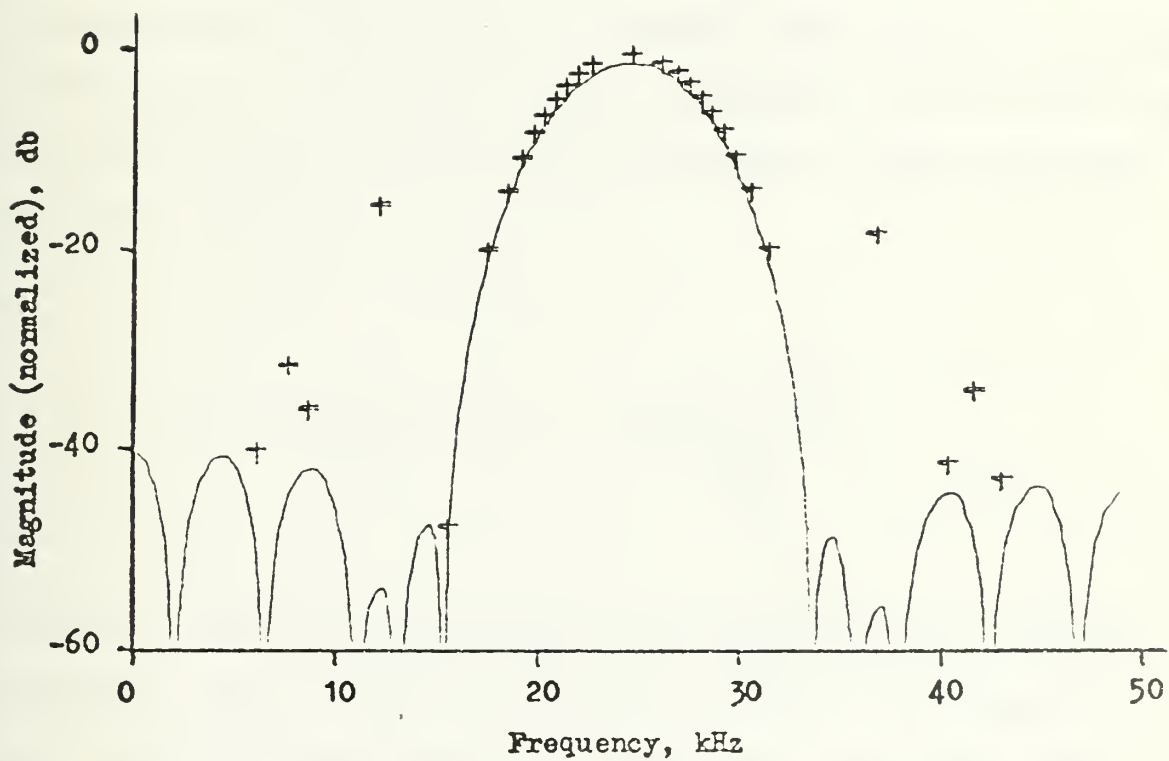


FIGURE 3.12 Theoretical and Observed Frequency Response; $f_o = \frac{1}{2}f_s$, $f_c = 100$ kHz, Magnitude in dB

It is noteworthy that Q did not change significantly when the clock frequency was doubled and that the bandwidth changed by a small amount when the center frequency was doubled by coefficient changes.

The measured Q was significantly below the designed value of 15. Some insight into the reason for this discrepancy may be found by looking at the impulse response of a rectangular bandpass filter. Without rejecting the negative time portion of the impulse response, since the non-recursive filter uses a 'two-sided' impulse response, one has from the inverse Fourier transform of a rectangular window centered at plus and minus ω_0 ,

$$h(t) = \frac{2}{Q} \frac{\omega_0}{\omega_s} \cos(\omega_0 t) \left[\frac{\sin\left(\pi \frac{\omega_0 t}{Q}\right)}{\pi \frac{\omega_0 t}{Q}} \right] .$$

This is a continuous function for a non-repeating frequency response. For a frequency response periodic with period, ω_s , the impulse response is discrete with the above function acting as an envelope. Figure 3.13 illustrates the response. In actuality, the sampled nature of the impulse response causes the repetitious frequency response, but the duality of the Fourier transform ignores the true cause and effect relationship. The spacing of samples is,

$$\Delta t = \frac{2\pi}{\omega_s} .$$

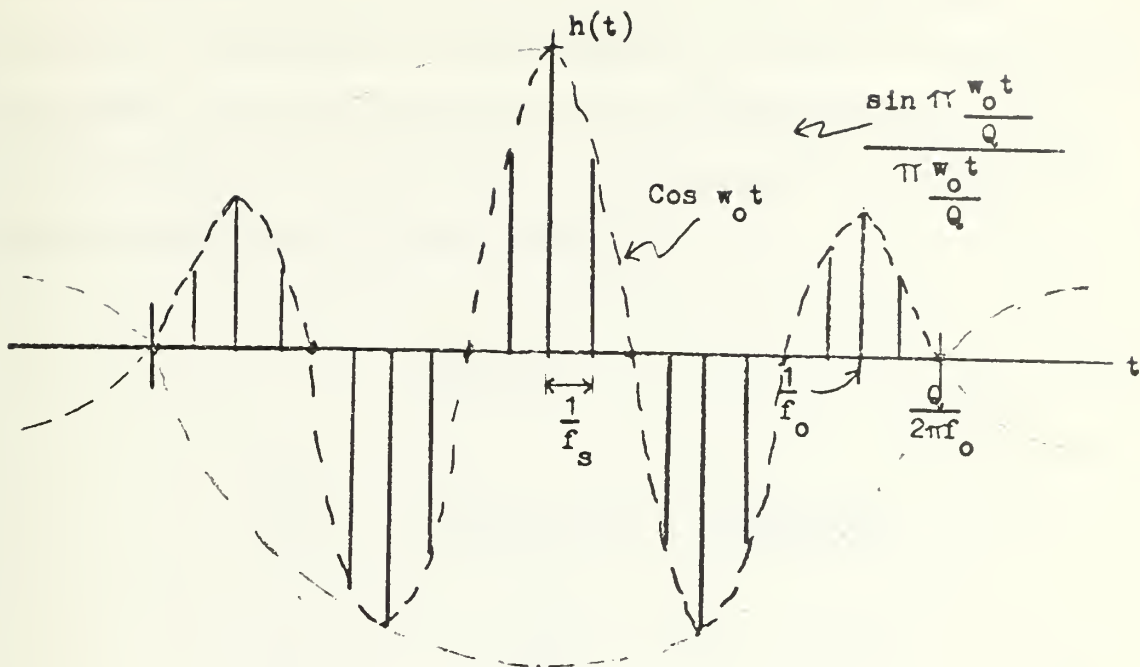


FIGURE 3.13 Two-Sided Impulse Response

For $\frac{\omega_0}{\omega_s} = a$, there will be a^{-1} samples per cosine period. There are Q divided by π cosine periods under the main lobe of the envelope. Therefore, the number of samples within the main lobe is,

$$M = \frac{Q}{a\pi} .$$

If one uses the criterion that the main lobe must be represented completely in order to approximate the impulse response, i.e. M samples are required, then some estimate of the number of terms required to give a selected Q at a

center frequency of $a\omega_s$ is available from the above equation. Conversely, if the number of terms is fixed, the realizable Q may be estimated given the ratio of ω_o to ω_s . In this study, $M = 11$ and $a = 0.25$ and 0.5 . Table IV lists the expected and measured Q 's.

TABLE IV

| $\frac{\omega_o}{\omega_s}$ | Q_{expected} | Q_{measured} |
|-----------------------------|-----------------------|-----------------------|
| 0.25 | 8.64 | 1.95 |
| 0.5 | 17.28 | 4.1 |

The observed Q 's did occur in about the expected ratio of two to one, but were significantly less than the expected values. Analysis in Appendix J indicates that this lowering of Q is mostly due to the Hamming weighting used. The expected values for this weighting are 2.17 for the center frequency to repetition period ratio of 0.25 and 4.35 for the 0.5 ratio. These match more closely to the observed values. The remaining difference is probably due to the need for more impulse response terms than those in the main lobe.

A significant amount of clock noise, up to 40 millivolts, was observed at the output. A low pass filter would be desirable at the output to decrease this noise content.

Perhaps this low pass filter could be built in conjunction with a level shifter to remove the output bias. It was further observed that using lead lengths of a few inches to connect the coefficient potentiometers to the TAD added significantly to the clock pick-up, which severely limits the small signal handling capability of the device. Input signals beyond 8 volts peak to peak began causing distortion in the tap outputs. Therefore, without using a low pass filter to suppress the clock noise, the dynamic range of this device is less than 54 dB.

IV. SAMPLED ANALOG FOURIER TRANSFORMS

A. THEORY

As mentioned in Chapter I, a possible application of sampled analog signal processing is to use the combination of a recursive comb filter and a non-recursive bandpass filter as a sampled analog Fourier transformer. The teeth of the comb filter breaks a signal into its Fourier components, while the bandpass filter selects one of the components. Figure 4.1 illustrates such a system.

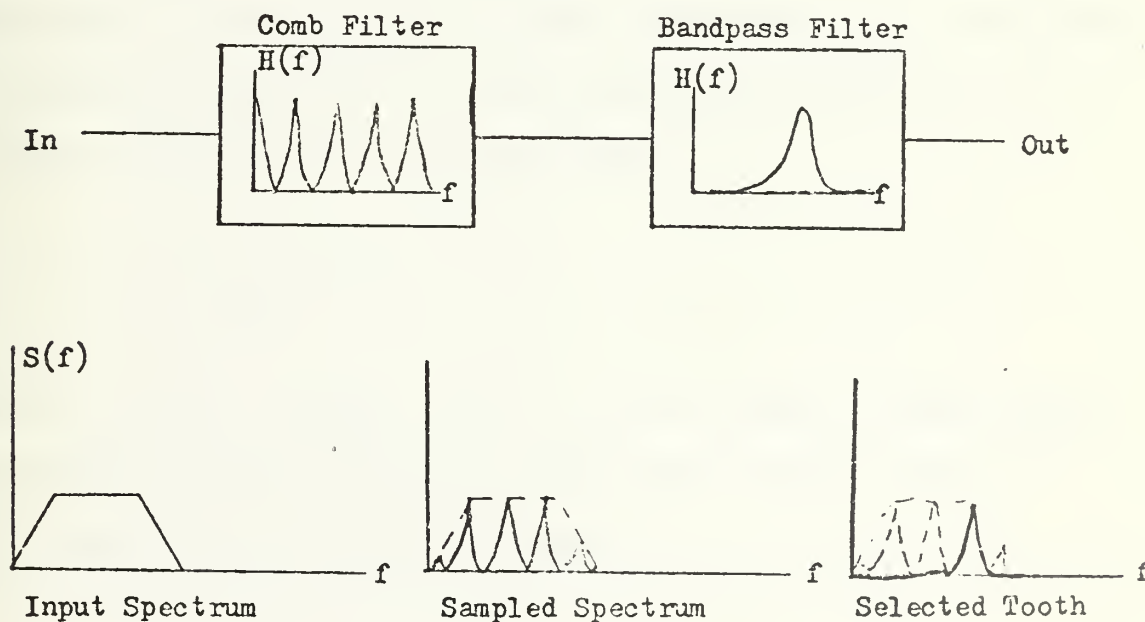


FIGURE 4.1 Sampled Analog Fourier Transformer

B. EXPERIMENT

For the purpose of demonstration, a bilinear Z-transform low pass filter with a narrow tooth width and a non-recursive bandpass filter are implemented and cascaded. For this example, the comb filter coefficients are chosen as,

$$\begin{aligned} a_0 &= 1 , \\ a_1 &= 1 , \\ b_1 &= -0.7 . \end{aligned}$$

The design of a generalized analog Fourier transformer can be made based on the number of frequency components desired, i.e. the number of comb teeth selected. The number of desired components, K , determines the frequency of the highest order tooth to be selected,

$$f_{\max} = K f_s .$$

Since $f_s = \frac{1}{T}$, where $T = LT_c$ for L equal to the number of delays in the recursive filter delay device and T_c is the recursive filter clock period ,

$$f_{\max} = \frac{K}{L} f_c , \quad \text{where } f_c = \frac{1}{T_c} .$$

Since f_c is the sampling rate, the Nyquist criteria states that,

$$f_{\max} \leq \frac{1}{2} f_c ,$$

so

$$L \geq 2K .$$

For a bandpass filter designed for a center frequency to repetition period ratio,

$$\frac{\omega_0}{\omega_s} = \alpha ,$$

the next highest passband is located at $(1 - \alpha)\omega_s$. Since the first K teeth should be distinct, the first repeated passband should occur at least at a frequency,

$$(1 - \alpha)\omega_s \geq \frac{(K + 1) 2\pi}{T} ,$$

while,

$$\alpha\omega_s = \frac{2\pi}{T} .$$

These restrictions on α can be summarized,

$$\alpha \leq \frac{1}{K + 2} .$$

If the bandpass is tuned by changing its clock frequency, its Q will remain constant, so its bandwidth will increase

as it is tuned to higher ordered teeth. At the maximum value, i.e. $K f_s$, the bandwidth will be,

$$BW_{\max} = \frac{K f_s}{Q} = \beta f_s .$$

The term, β , is a design choice that should be some fraction less than unity. The required Q is, therefore,

$$Q \geq \frac{K}{\beta} .$$

From the equation relating Q , α , and M , the number of taps, a guess at the required device length is made,

$$M \geq \frac{Q}{\alpha\pi} \geq \frac{K(K+2)}{\beta\alpha} .$$

Thus, for a possible design to find 100 frequency components, and a maximum bandwidth of one tooth repetition period, i.e. $\beta = 1$,

$$M \geq \frac{100(100+2)}{\pi} = 3247 .$$

This means that the Fourier series is from the -1623^{rd} term to the 1623^{rd} term.

The non-recursive filter coefficients are selected for a center passband frequency of $\frac{1}{2}f_s$. Figure 4.2 shows the resulting transfer function for the cascaded filters plotted against the comb response. The comb filter clock was run at

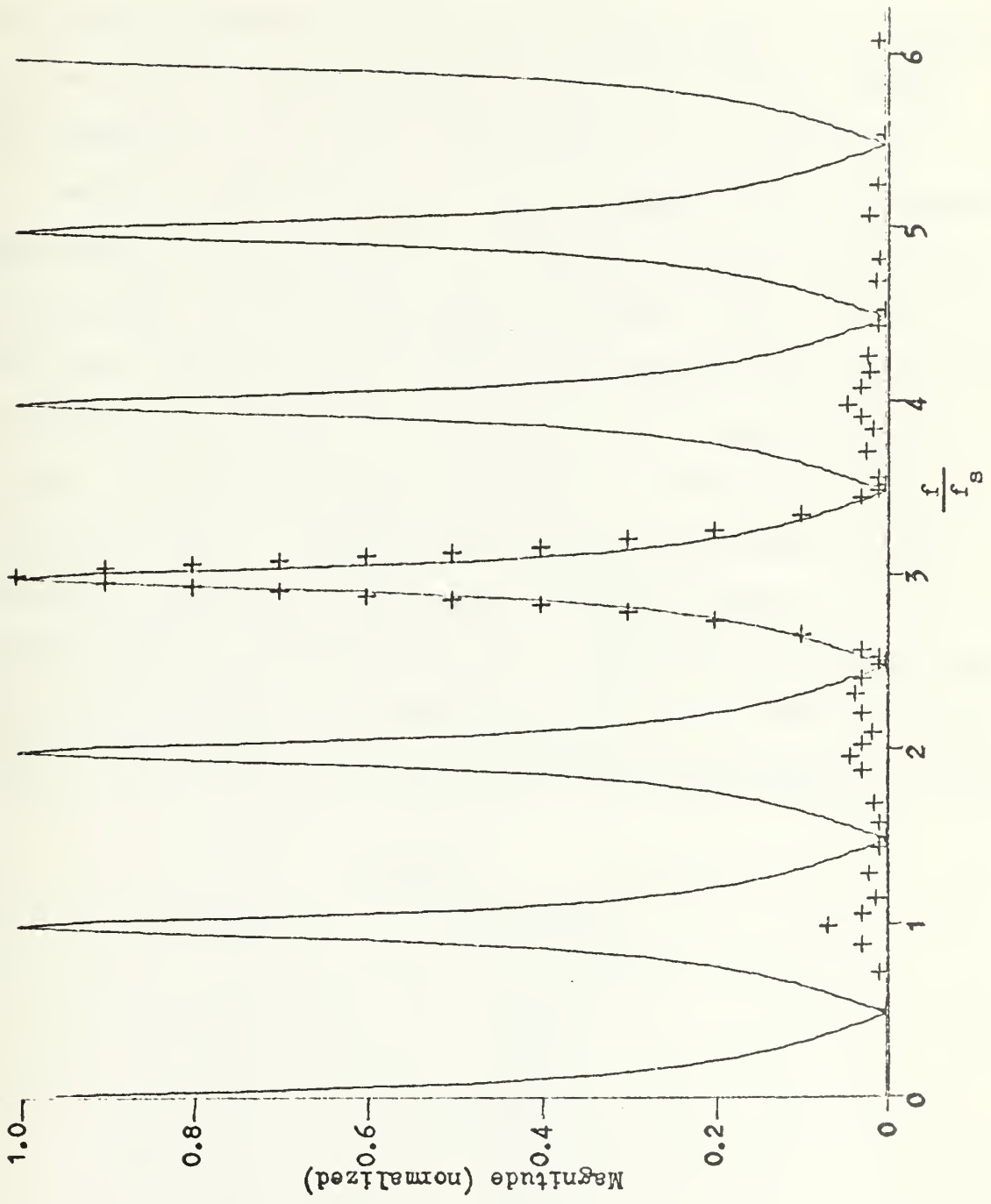


FIGURE 4.2 Observed Frequency Response

at 400 kHz, which placed comb teeth at approximately 4.1 kHz increments. The bandpass filter clock was adjusted so that the passband selected the third tooth. The frequency of the third tooth maximum was measured to be 12.452 kHz. The bandpass filter clock was measured to be 49.555 kHz.

Several aspects of the cascaded response are noteworthy. The shape of the passband is determined by the comb filter tooth shape, which should remain constant from one tooth to the next, whereas the non-recursive bandpass filter bandwidth, as shown in Chapter III, changes as it is tuned with its clock. This use of the comb filter to maintain a constant spectrum 'sample' window allows one to keep higher order harmonics separated. The other important aspect of the system which is noteworthy is the isolation achieved between the selected tooth and the unselected teeth. The following table lists the first several teeth and the isolation of each.

TABLE V

| Tooth | Isolation |
|-------|-----------|
| 1 | -23.1 dB |
| 2 | -27.1 |
| 3 | 0.0 |
| 4 | -26.7 |
| 5 | -34.2 |
| 6 | -44.0 |
| 7 | -37.1 |
| 8 | -34.9 |
| 9 | -13.4 |
| 10 | -44.0 |

The low isolation figure for the ninth tooth resulted from the repeated response at $\frac{3}{2} f_s$.

V. CONCLUSIONS

The Z-transform design methods developed for digital filter theory are useful for sampled analog recursive filter design. High and low pass cut-off frequencies were predictably determined by the filter feedback coefficient values. These values were adjusted by means of a generalized calibration curve or by measurement of the unit step response of the filter. Some deviations from theoretical frequency responses were observed. These deviations are apparently caused by instrumentation limitations.

Non-recursive filters were implemented by truncation of a Fourier series expression for the desired repetitive frequency response. The center frequency of the bandpass filter response passband was tuned at nearly constant Q by varying the clock frequency. The pass band was also shifted at nearly constant bandwidth by changes made to the coefficients of the filter. The $\sin X$ over X envelope caused by the finite sampling pulse-width multiplies the desired frequency response. This result decreases the signals passing through the repeated passbands.

Several particular frequency components of an input signal spectrum were examined in real time by cascading a recursive 'comb' filter and a non-recursive bandpass filter to form a sampled analog Fourier transformer. An estimate of the required delay device lengths for implementation of a sampled Fourier transformer by the above method was found for a general number of desired components.

APPENDIX A

Derivation of Filter Transfer Function

For the system diagram illustrated below,

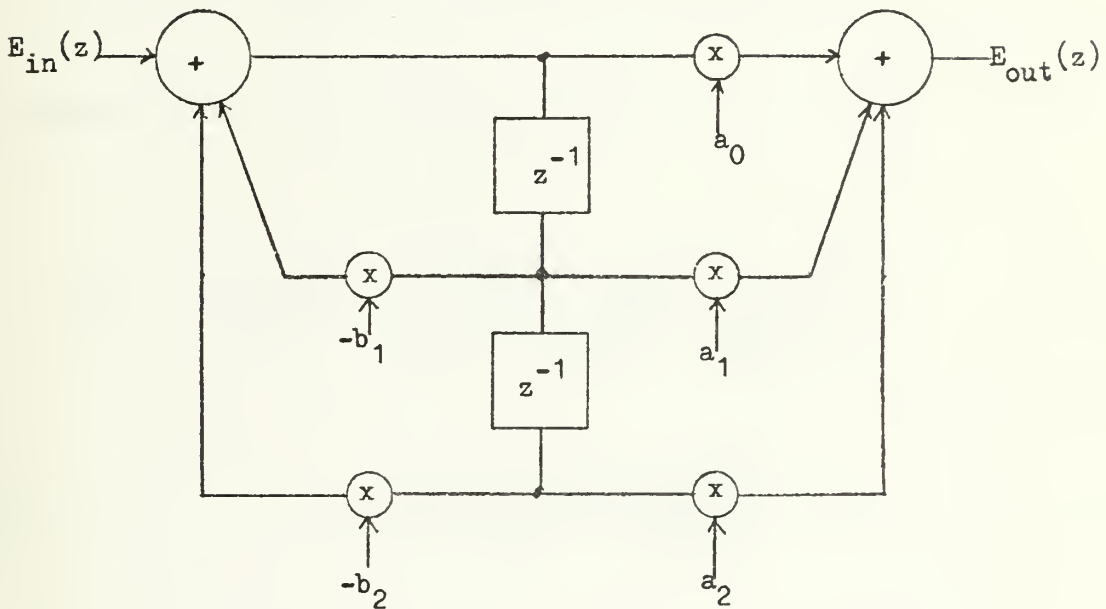


FIGURE A-1

the transfer function, $H(z)$, is defined as,

$$H(z) = \frac{E_{out}(z)}{E_{in}(z)} .$$

From the system diagram it follows that,

$$X(z) = E_{in}(z) + (-b_1)(X(z)z^{-1}) + (-b_2)(X(z)z^{-2}) ,$$

so,

$$E_{in}(z) = X(z) + b_1X(z)z^{-1} + b_2X(z)z^{-2} .$$

The output of the system is,

$$E_{out}(z) = a_0X(z) + a_1X(z)z^{-1} + a_2X(z)z^{-2} ,$$

therefore,

$$\begin{aligned} H(z) &= \frac{E_{out}(z)}{E_{in}(z)} = \frac{X(z)(a_0 + a_1z^{-1} + a_2z^{-2})}{X(z)(1 + b_1z^{-1} + b_2z^{-2})} \\ &= \frac{a_0 + a_1z^{-1} + a_2z^{-2}}{1 + b_1z^{-1} + b_2z^{-2}} . \end{aligned}$$

APPENDIX B

Recursive Filter Design

The transfer function of a given second-order sampled recursive filter is given by the following expression,

$$H(z) = \frac{a_0 + a_1 z^{-1} + a_2 z^{-2}}{1 + b_1 z^{-1} + b_2 z^{-2}} .$$

By using the definition of z ,

$$z = e^{sT} = e^{j\omega T} , \text{ where } T \text{ is the time delay,}$$

the frequency response, $H(j\omega)$, can be determined:

$$\begin{aligned} H(j\omega) &= \frac{a_0 + a_1 e^{-j\omega T} + a_2 e^{-j2\omega T}}{1 + b_1 e^{-j\omega T} + b_2 e^{j2\omega T}} , \\ &= \frac{a_0 + a_1 (\cos \omega T - j \sin \omega T) + a_2 (\cos 2\omega T - j \sin 2\omega T)}{1 + b_1 (\cos \omega T - j \sin \omega T) + b_2 (\cos 2\omega T - j \sin 2\omega T)} . \end{aligned}$$

Since the only variation of $H(j\omega)$ with frequency is due to the sine and cosine functions, and since they are periodic in ω for a fixed T , $H(j\omega)$ is periodic in frequency. In fact, the period of the response is $(k) \frac{2\pi}{T} \leq \omega \leq (k+1) \frac{2\pi}{T} ,$

for $k = \dots, -2, -1, 0, 1, 2, \dots$. Since the sine and cosine terms repeat themselves exactly, the entire frequency response of the filter can be described by looking at a single period, say $0 \leq \omega \leq \frac{2\pi}{T}$. The frequency, $\frac{2\pi}{T}$, is called the repetition period, ω_s , which is related to the time delay, T . As illustrated in Figure 2.6, the frequency response from $0 \leq \omega \leq \frac{1}{2}\omega_s$ is mirrored for $\frac{1}{2}\omega_s \leq \omega \leq \omega_s$. This periodic nature of the filter frequency response, which arises from the use of delays, can be used to implement comb filters as described above.

There are several methods for designing the coefficients of the transfer function, $H(z)$. Two methods are frequently used if the Laplace transfer function, $H(s)$, or the impulse response, $h(t)$, of the desired continuous response is known. One is the standard Z-transform procedure. The other is the bilinear Z-transform method.

For the standard Z-transform approach, $h(t)$ is determined for the desired response and then sampled at intervals, T , the time delay,

$$h_{\text{sampled}}(t) = \sum_{k=0}^{\infty} h(kT) \delta(t - kT) \quad .$$

Its Laplace transform is,

$$\mathcal{L}[h_{\text{sampled}}(t)] = \sum_{k=0}^{\infty} h(kT) e^{-skT} \quad .$$

From the definition of $z = e^{sT}$,

$$H(z) = \sum_{k=0}^{\infty} h(kT) z^{-k}.$$

Z-transform tables are available for those impulse functions of interest where a closed form of the series is known.

The second technique, the bilinear Z-transform, involves the use of an approximation for s in terms of z . The transfer function, $H(s)$, is converted directly to $H(z)$ by the substitution of,

$$s = \frac{2}{T} \frac{z-1}{z+1}.$$

The use of this approximation for s leads to a non-linear relationship between the frequencies of $s = j\omega$ and $z = e^{j\omega'T}$:

$$s = j\omega = \frac{2}{T} \frac{z-1}{z+1},$$

so

$$\frac{j\omega T}{2} = \frac{z(z^{\frac{1}{2}} - z^{-\frac{1}{2}})}{z^{\frac{1}{2}}(z^{\frac{1}{2}} + z^{-\frac{1}{2}})} = \frac{e^{j\frac{1}{2}\omega'T} - e^{-j\frac{1}{2}\omega'T}}{e^{j\frac{1}{2}\omega'T} + e^{-j\frac{1}{2}\omega'T}},$$

therefore,

$$\frac{\omega T}{2} = \tan \frac{1}{2}\omega'T,$$

or,

$$\omega = \frac{2}{T} \tan(\frac{1}{2}\omega'T) \quad \text{and} \quad \omega' = \frac{2}{T} \tan^{-1}(\frac{1}{2}\omega T).$$

Since $\omega_s = \frac{2\pi}{T}$,

$$\omega' = \frac{\omega_s}{\pi} \tan^{-1}(\frac{1}{2}\omega T) .$$

This non-linearity is defined as frequency warping.

A. STANDARD Z-TRANSFORM DESIGN PROCEDURE

1. First-Order

a. Low Pass Filter

A first order RC low pass filter has the impulse response,

$$h(t) = \omega_c e^{-\omega_c t} , \quad \text{where } \omega_c = \frac{1}{RC} .$$

The standard Z-transform is,

$$\begin{aligned} H(z) &= \omega_c \sum_{n=0}^{\infty} e^{-\omega_c nT} z^{-n} \\ &= \frac{\omega_c}{1 - e^{-\omega_c T} z^{-1}} . \end{aligned}$$

For a first order low pass filter,

$$\begin{aligned} a_0 &= \omega_c , \\ a_1 &= 0 , \\ b_1 &= -e^{-\omega_c T} . \end{aligned}$$

Since the value of a_0 is a constant factor which sets the filter gain, normalizing the response is equivalent to making a normalized transfer function with $a_0 = 1$. Since the coefficient b_1 is the only term which acts on the frequency dependent z , the cut-off frequency, ω_c , is determined solely by b_1 . From the definition of cut-off frequency,

$$\begin{aligned}
 |H(j\omega_c)|^2 &= \frac{1}{2} |H(j\omega)|_{\max}^2 \\
 &= \frac{1}{1 + b_1(\cos \omega_c T - j \sin \omega_c T)}^2 \\
 &= \frac{1}{1 + 2b_1 \cos \omega_c T + b_1^2} .
 \end{aligned}$$

The maximum value of $H(j\omega)$ occurs when $2b_1 \cos \omega_c T$ is most negative, i.e. that factor is equal to $-2|b_1|$.

Therefore,

$$\frac{1}{1 + 2b_1 \cos \omega_c T + b_1^2} = \frac{\frac{1}{2}}{1 - 2|b_1| + b_1^2}$$

or

$$\begin{aligned}
 1 + 2b_1 \cos \omega_c T + b_1^2 &= 2 - 4|b_1| + 2b_1^2 \\
 \cos \omega_c T &= \frac{1 - 4|b_1| + b_1^2}{2b_1}
 \end{aligned}$$

$$\omega_c T = \omega_c \left(\frac{2\pi}{\omega_s} \right) = \cos^{-1} \left(\frac{1 - 4|b_1| + b_1^2}{2b_1} \right)$$

$$\frac{\omega_c}{\omega_s} = \frac{1}{2\pi} \cos^{-1} \left(\frac{1 - 4|b_1| + b_1^2}{2b_1} \right)$$

TABLE VI

| b_1 | $\frac{\omega_c}{\omega_s}$ |
|---------|-----------------------------|
| -0.1716 | 0.5000 |
| -0.2 | 0.3524 |
| -0.3 | 0.2207 |
| -0.4 | 0.1573 |
| -0.5 | 0.1150 |
| -0.6 | 0.0831 |
| -0.7 | 0.0574 |
| -0.8 | 0.0357 |
| -0.9 | 0.0168 |
| -1.0 | 0.0000 |

For the first order low pass filter, $b_1 < 0$, therefore maximum values will occur whenever $2b_1 \cos \omega T = 2b_1$, or when $\cos \omega T = 1$, or

$$\begin{aligned} \omega &= k \left(\frac{2\pi}{T} \right) , \quad k = \dots -2, -1, 0, 1, 2, \dots , \\ &= k\omega_s . \end{aligned}$$

Likewise, the minimum value of the response occurs when

$$\omega T = -1, \text{ or,}$$

$$\begin{aligned}\omega &= (2k+1) \left(\frac{\pi}{T}\right) \\ &= (k+\frac{1}{2}) \omega_s .\end{aligned}$$

The ratio of the maximum response to minimum response yields an interesting result,

$$\begin{aligned}\mu^2 &= \frac{|H(j\omega)|_{\min}^2}{|H(j\omega)|_{\max}^2} = \frac{\frac{1}{1 + 2|b_1| + b_1^2}}{\frac{1}{1 - 2|b_1| + b_1^2}} \\ &= \frac{(1 - |b_1|)^2}{(1 + |b_1|)^2} , \\ \mu &= \frac{1 - |b_1|}{1 + |b_1|} .\end{aligned}$$

Solving this equation for b_1 yields,

$$b_1 = \frac{1 - \mu}{1 + \mu}$$

TABLE VII

| μ | $ b_1 $ |
|-------|---------|
| 0.0 | 1.0000 |
| 0.01 | 0.9802 |
| 0.025 | 0.9512 |
| 0.05 | 0.9048 |
| 0.1 | 0.8182 |
| 0.2 | 0.6667 |
| 0.3 | 0.5385 |
| 0.4 | 0.4286 |
| 0.5 | 0.3333 |
| 0.6 | 0.2500 |
| 0.7 | 0.1765 |
| 0.8 | 0.1111 |
| 0.9 | 0.0526 |
| 1.0 | 0.0000 |

This result can be of use in experimental determination of the effective value of b_1 .

b. High Pass Filter

The low pass filter just described above can be transformed into a high pass filter by shifting the response by $\frac{1}{2}\omega_s$ so that the maximum values occur at $(k + \frac{1}{2})\omega_s$ and the minimum values at $k\omega_s$. Changing the polarity of b_1 would accomplish this result since the maximum response occurs when $2b_1 \cos \omega T = -2|b_1|$, which would make $\cos \omega T = -1$ and $\omega = (k + \frac{1}{2})\omega_s$ for $b_1 > 0$.

The minimum response would occur when $\cos \omega T = 1$, or $\omega = k\omega_s$. The cut-off frequency, ω_c , is found by the same procedure as for the low pass case:

$$\begin{aligned}
 |H(j\omega_c)|^2 &= \frac{1}{2}|H(j\omega)|_{\max}^2 \\
 &= \left| \frac{1}{1 + b_1 e^{-j\omega_c T}} \right|^2 \\
 &= \frac{1}{1 + 2b_1 \cos \omega_c T + b_1^2} .
 \end{aligned}$$

From the previous case, since the expressions for the cut-off magnitudes are identical,

$$\frac{\omega_c}{\omega_s} = \frac{1}{2\pi} \cos^{-1} \left(\frac{1 - 4b_1 + b_1^2}{2b_1} \right)$$

TABLE VIII

| b_1 | $\frac{\omega_c}{\omega_s}$ |
|--------|-----------------------------|
| 0.1716 | 0.0000 |
| 0.2 | 0.1476 |
| 0.3 | 0.2793 |
| 0.4 | 0.3427 |
| 0.5 | 0.3850 |
| 0.6 | 0.4169 |
| 0.7 | 0.4426 |
| 0.8 | 0.4643 |
| 0.9 | 0.4832 |
| 1.0 | 0.5000 |

For this form of the first order high pass filter, the other coefficients are the same as for the low pass case, i.e.

$a_0 = 1, a_1 = 0$ for a normalized transfer function.

Another type of high pass filter may be implemented by the standard Z-transform technique. For a first order RC high pass filter the impulse response is,

$$\begin{aligned} h(t) &= \mathcal{L}^{-1}[H(s)] = \mathcal{L}^{-1}\left[\frac{s}{s + \omega_c}\right] \\ &= \delta(t) - \omega_c e^{-\omega_c T} \quad , \quad \text{where } \omega_c = \frac{1}{RC} \quad . \end{aligned}$$

The Z-transform of this impulse response is,

$$\begin{aligned} H(z) &= \sum_{n=0}^{\infty} (\delta(nT) - \omega_c e^{-\omega_c nT}) z^{-n} \\ &= \frac{1 - \omega_c - e^{-\omega_c T} z^{-1}}{1 - e^{-\omega_c T} z^{-1}} \quad . \end{aligned}$$

The transfer coefficients are,

$$\begin{aligned} a_0 &= 1 - \omega_c \quad , \\ a_1 &= -e^{-\omega_c T} \quad , \\ b_1 &= -e^{-\omega_c T} \quad . \end{aligned}$$

The corner frequency is a function of both a_1 and b_1 .

2. Second-Order

a. Low Pass Filter

For a second-order LC low pass filter, the impulse response is

$$h(t) = \mathcal{L}^{-1} \left[\frac{\omega_c^2}{s^2 + \omega_c^2} \right] = \omega_c \sin \omega_c t, \quad \text{where } \omega_c = (LC)^{\frac{1}{2}}.$$

The resulting Z-transform is,

$$\begin{aligned} H(z) &= \sum_{n=0}^{\infty} \omega_c \sin \omega_c nT z^{-n} \\ &= \frac{\omega_c \sin \omega_c T z^{-1}}{1 - 2 \cos \omega_c T z^{-1} + z^{-2}}. \end{aligned}$$

For a normalized transfer function, $a_0 = a_2 = 0$, $b_1 = 1$, and,

$$a_1 = 1,$$

$$b_1 = -2 \cos \omega_c T.$$

From the expression above, the relationship between b_1 and the corner frequency, ω_c , can be stated,

$$\frac{\omega_c}{\omega_s} = \frac{1}{2\pi} \cos^{-1}(-\frac{1}{2}b_1).$$

TABLE IX

| b_1 | $\frac{\omega_c}{\omega_s}$ |
|-------|-----------------------------|
| -2.0 | 0.0000 |
| -1.8 | 0.0718 |
| -1.6 | 0.1024 |
| -1.4 | 0.1266 |
| -1.2 | 0.1476 |
| -1.0 | 0.1667 |
| -0.8 | 0.1845 |
| -0.6 | 0.2015 |
| -0.4 | 0.2180 |
| -0.2 | 0.2341 |
| 0.0 | 0.2500 |
| 0.2 | 0.2659 |
| 0.4 | 0.2820 |
| 0.6 | 0.2985 |
| 0.8 | 0.3155 |
| 1.0 | 0.3333 |
| 1.2 | 0.3524 |
| 1.4 | 0.4734 |
| 1.6 | 0.3976 |
| 1.8 | 0.4282 |
| 2.0 | 0.5000 |

b. High Pass Filter

The impulse response for a second order LC high pass filter is,

$$h(t) = \mathcal{L}^{-1} \left[\frac{s^2}{s^2 + \omega_c^2} \right] = \delta(t) - \omega_c \sin \omega_c t .$$

This transforms into,

$$\begin{aligned} H(z) &= \sum_{n=0}^{\infty} (\delta(nT) - \omega_c \sin n\omega_c T) z^{-n} \\ &= \frac{1 - (2 \cos \omega_c T + \omega_c \sin \omega_c T) z^{-1} + z^{-2}}{1 - 2 \cos \omega_c T z^{-1} + z^{-2}} \end{aligned}$$

where,

$$a_0 = 1 ,$$

$$a_1 = -2 \cos \omega_c T + \omega_c \sin \omega_c T ,$$

$$a_2 = 1 ,$$

$$b_1 = -2 \cos \omega_c T ,$$

$$b_2 = 1 .$$

The cut-off frequency for this filter will be dependent on both a_1 and b_1 .

B. BILINEAR Z-TRANSFORM DESIGN PROCEDURE

1. First-Order

a. Low Pass Filter

The transfer function of a first-order RC low pass filter is,

$$H(s) = \frac{\omega_c}{s + \omega_c} .$$

By substitution of the bilinear approximation, $s = \frac{2}{T} \frac{z-1}{z+1}$,

$$\begin{aligned}
H(z) &= \frac{\omega_c}{\frac{2}{T} \frac{z-1}{z+1} + \omega_c} \\
&= \frac{\omega_c T (z+1)}{2z - 2 + \omega_c (z+1)} \\
&= \frac{\omega_c T + \omega_c T z^{-1}}{2 + \omega_c + (\omega_c - 2) z^{-1}} \\
&= \frac{\frac{\omega_c T}{2 + \omega_c} + \frac{\omega_c T}{2 + \omega_c} z^{-1}}{1 + \frac{\omega_c T - 2}{\omega_c T + 2} z^{-1}} .
\end{aligned}$$

Normalizing the transfer function by $\frac{\omega_c T}{2 + \omega_c}$ yields,

$$H(z) = \frac{1 + z^{-1}}{1 + \frac{\omega_c T - 2}{\omega_c T + 2} z^{-1}} ,$$

where,

$$a_0 = 1 ,$$

$$a_1 = 1 ,$$

$$b_1 = \frac{\omega_c T - 2}{\omega_c T + 2} .$$

The bilinear Z-transform warps the frequency response, so the actual cut-off frequency, $\omega_{c'}$, is ,

$$\omega_{c'} = \frac{2}{T} \tan^{-1}(\frac{1}{2}\omega_c T) .$$

From the expression for b_1 in terms of $\omega_{c'}$,

$$\omega_{c'} = \frac{-2}{T} \left(\frac{b_1 + 1}{b_1 - 1} \right) ,$$

so,

$$\omega_{c'} = \frac{-2}{T} \tan^{-1} \left(\frac{b_1 + 1}{b_1 - 1} \right) ,$$

or,

$$\frac{\omega_{c'}}{\omega_s} = \frac{-1}{\pi} \tan^{-1} \left(\frac{b_1 + 1}{b_1 - 1} \right) .$$

TABLE X

| b_1 | $\frac{\omega_{c'}}{\omega_s}$ |
|-------|--------------------------------|
| -1.0 | 0.0000 |
| -0.9 | 0.0167 |
| -0.8 | 0.0352 |
| -0.7 | 0.0556 |
| -0.6 | 0.0780 |
| -0.5 | 0.1024 |
| -0.4 | 0.1289 |
| -0.3 | 0.1572 |
| -0.2 | 0.1872 |
| -0.1 | 0.2183 |
| 0.0 | 0.2500 |
| 0.1 | 0.2817 |
| 0.2 | 0.3128 |
| 0.3 | 0.3428 |
| 0.4 | 0.3711 |
| 0.5 | 0.3976 |
| 0.6 | 0.4220 |
| 0.7 | 0.4444 |
| 0.8 | 0.4648 |
| 0.9 | 0.4833 |
| 1.0 | 0.5000 |

b. High Pass Filter

For a first-order RC high pass filter the transfer function is,

$$H(s) = \frac{s}{s + \omega_c} ,$$

which transforms to,

$$\begin{aligned} H(z) &= \frac{\frac{2}{T} \frac{z-1}{z+1}}{\frac{2}{T} \frac{z-1}{z+1} + \omega_c} \\ &= \frac{z-1}{z-1 + \frac{\omega_c T}{2} (z+1)} \\ &= \frac{\frac{2}{\omega_c T + 2} - \frac{2}{\omega_c T + 2} z^{-1}}{1 + \frac{\omega_c T - 2}{\omega_c T + 2} z^{-1}} . \end{aligned}$$

For the normalized transfer function,

$$a_0 = 1 ,$$

$$a_1 = -1 ,$$

$$b_1 = \frac{\omega_c T - 2}{\omega_c T + 2} .$$

It is noteworthy that the only change from a high pass filter to a low pass filter, other than the gain normalization factor, is the polarity of a_1 . Since the expression for b_1 in terms of the design cut-off frequency, ω_c , is the same as for the low pass filter, the same relationship between b_1 and the actual cut-off frequency, ω_c , as found for the low pass case exists.

2. Second-Order

a. Low Pass Filter

The transfer function for a second-order LC low pass filter is,

$$H(s) = \frac{\omega_c^2}{s^2 + \omega_c^2}, \quad \text{where } \omega_c = (LC)^{\frac{1}{2}}.$$

The bilinear Z-transform for this function is,

$$\begin{aligned} H(z) &= \frac{\omega_c^2}{\left[\frac{2}{T} \frac{z-1}{z+1}\right]^2 + \omega_c^2} \\ &= \frac{\omega_c^2 T^2 (z^2 + z + 1)}{4z^2 - 8z + 4 + \omega_c^2 T^2 (z^2 + 2z + 1)} \\ &= \frac{\frac{\omega_c^2 T^2}{\omega_c^2 T^2 + 4} + \frac{2\omega_c^2 T^2}{\omega_c^2 T^2 + 4} z^{-1} + \frac{\omega_c^2 T^2}{\omega_c^2 T^2 + 4} z^{-2}}{1 + \frac{2\omega_c^2 T^2 - 8}{\omega_c^2 T^2 + 4} z^{-1} + z^{-2}}, \end{aligned}$$

where, for a normalized transfer function,

$$a_0 = 1 ,$$

$$a_1 = 2 ,$$

$$a_2 = 1 ,$$

$$b_1 = \frac{2 \frac{c}{c} 2T^2 - 8}{\frac{c}{c} 2T^2 + 4}$$

$$b_2 = 1 .$$

By using the expression for b_1 to solve for c in terms of b_1 , one finds,

$$\omega_c = \frac{2}{T} \left(\frac{2 + b_1}{2 - b_1} \right)^{\frac{1}{2}}$$

Because of the frequency warping,

$$\omega_{c'} = \frac{2}{T} \tan^{-1} \left(\frac{2 + b_1}{2 - b_1} \right)^{\frac{1}{2}} ,$$

or

$$\frac{\omega_{c'}}{\omega_s} = \frac{1}{\pi} \tan^{-1} \left[\frac{2 + b_1}{2 - b_1} \right]^{\frac{1}{2}} .$$

It is interesting that this design table is the same as Table IX, the standard Z-transform second-order low pass filter.

TABLE XI

| b_1 | $\frac{\omega_c'}{\omega_s}$ |
|-------|------------------------------|
| -2.0 | 0.0000 |
| -1.8 | 0.0718 |
| -1.6 | 0.1024 |
| -1.4 | 0.1266 |
| -1.2 | 0.1476 |
| -1.0 | 0.1667 |
| -0.8 | 0.1845 |
| -0.6 | 0.2015 |
| -0.4 | 0.2180 |
| -0.2 | 0.2341 |
| 0.0 | 0.2500 |
| 0.2 | 0.2659 |
| 0.4 | 0.2820 |
| 0.6 | 0.2985 |
| 0.8 | 0.3155 |
| 1.0 | 0.3333 |
| 1.2 | 0.3524 |
| 1.4 | 0.3734 |
| 1.6 | 0.3976 |
| 1.8 | 0.4282 |
| 2.0 | 0.5000 |

b. High Pass Filter

A second-order LC high pass filter has the following transfer function,

$$H(s) = \frac{s^2}{s^2 + \omega_c^2} ,$$

which is transformed to,

$$\begin{aligned}
H(z) &= \frac{\left[\frac{2}{T} \frac{z-1}{z+1}\right]^2}{\left[\frac{2}{T} \frac{z-1}{z+1}\right]^2 + \omega_c^2} \\
&= \frac{4(z^2 - 2z + 1)}{4z^2 - 8z + 4 + \omega_c^2 T^2 (z^2 + 2z + 1)} \\
&= \frac{\frac{4}{c^2 T^2 + 4} - \frac{8z^{-1}}{c^2 T^2 + 4} + \frac{4z^{-2}}{c^2 T^2 + 4}}{1 + \frac{2}{c} \frac{c^2 T^2 - 8}{c^2 T^2 + 4} z^{-1} + z^{-2}}
\end{aligned}$$

For a normalized transfer function,

$$a_0 = 1 ,$$

$$a_1 = -2 ,$$

$$a_2 = 1 ,$$

$$b_1 = \frac{2\omega_c^2 T^2 - 8}{\omega_c^2 T^2 + 4} ,$$

$$b_2 = 1 .$$


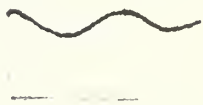


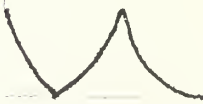



It is noteworthy that this transfer function has the same coefficients as the low pass filter with the exception of the sign of a_1 . The corner frequency is dependent on b_1 in the same manner as for the low pass case. It is now apparent that the polarity of a_1 is the means for converting

high pass bilinear Z-transforms to low pass and vice versa. In addition, the a_0 , a_1 , and a_2 values are always integral multiples of one another.

C. SUMMARY

The following table summarizes the design procedures for the standard Z-transform and the bilinear Z-transform for first order filters.

TABLE XII

| Design Method | Filter Type | Coefficients | | | Response Period |
|---------------|---|-------------------------------------|-------------------------------------|---|---|
| | | a_0 | a_1 | b_1 | |
| Standard Z | Low Pass | | | | |
| | $\frac{\omega_c}{\omega_s} < \frac{1}{4}$ | ω_c | 0 | $-e^{-\omega_c T}$ |  |
| | Low Pass | | | | |
| | $\frac{\omega_c}{\omega_s} > \frac{1}{4}$ | $1 - \omega_c$ | $-e^{-\omega_c T}$ | $e^{-\omega_c T}$ |  |
| Standard Z | High Pass | | | | |
| | $\frac{\omega_c}{\omega_s} < \frac{1}{4}$ | $1 - \omega_c$ | $-e^{-\omega_c T}$ | $-e^{-\omega_c T}$ |  |
| | High Pass | | | | |
| | $\frac{\omega_c}{\omega_s} > \frac{1}{4}$ | ω_c | 0 | $e^{-\omega_c T}$ |  |
| Bilinear Z | Low Pass | | | | |
| | $\frac{\omega_c}{\omega_s} < \frac{1}{4}$ | $\frac{\omega_c T}{\omega_c T + 2}$ | $\frac{\omega_c T}{\omega_c T + 2}$ | $-\left \frac{\omega_c T - 2}{\omega_c T + 2} \right $ |  |
| | Low Pass | | | | |
| | $\frac{\omega_c}{\omega_s} > \frac{1}{4}$ | $\frac{\omega_c T}{\omega_c T + 2}$ | $\frac{\omega_c T}{\omega_c T + 2}$ | $\left \frac{\omega_c T - 2}{\omega_c T + 2} \right $ |  |
| Bilinear Z | High Pass | | | | |
| | $\frac{\omega_c}{\omega_s} < \frac{1}{4}$ | $\frac{2}{\omega_c T + 2}$ | $\frac{-2}{\omega_c T + 2}$ | $-\left \frac{\omega_c T - 2}{\omega_c T + 2} \right $ |  |
| | High Pass | | | | |
| | $\frac{\omega_c}{\omega_s} > \frac{1}{4}$ | $\frac{2}{\omega_c T + 2}$ | $\frac{-2}{\omega_c T + 2}$ | $\left \frac{\omega_c T - 2}{\omega_c T + 2} \right $ |  |

APPENDIX C

Derivation of Calibration Curve For Recursive Filter Coefficients

The coefficients of the recursive filter transfer function are produced by potentiometers. These potentiometers are loaded by the input impedance of the summing circuit and are driven by the output of the SAD-100 driving board as illustrated below.

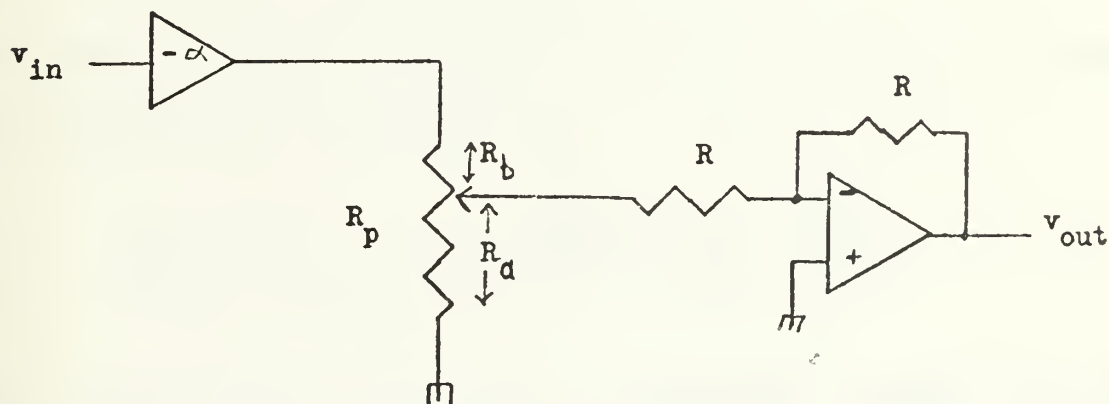


FIGURE C-1 Coefficient Circuit

It is assumed that the summer op amp is operated as a unity gain, inverting device. Therefore, the voltage on the tap of the pot is $-v_{out}$. The voltage on the top of the potentiometer is $-\alpha v_{in}$. The coefficient, b , is defined as the ratio of v_{out} to v_{in} . From the voltage divider equation,

$$-v_{\text{out}} = -\alpha v_{\text{in}} \left[\frac{R_a || R}{R_b + R_a || R} \right],$$

therefore,

$$b = \frac{-v_{\text{out}}}{-v_{\text{in}}} = \frac{\frac{\alpha R_a R}{R_a + R}}{R_b + \frac{R_a R}{R_a + R}}$$

$$= \alpha \frac{R_a R}{R_a (R_p - R_a) + R_p R}.$$

The limit of the coefficient, b , as R , the loading resistance, gets arbitrarily large is,

$$\lim_{R \rightarrow \infty} b = \lim_{R \rightarrow \infty} \alpha \frac{R_a R}{R_a (R_p - R_a) + R_p R} = \alpha \frac{R_a}{R_p}.$$

This is the expected value for a non-loaded voltage divider. Since R is finite in this study, its effect must be considered. For the actual hardware used, $R_p = 10\text{K}$, $R = 30.9\text{K}$, and $\alpha = 1$. The following calibration curve was calculated,

TABLE XIII

| R_a | b | b_{observed} |
|-------|-------|-----------------------|
| 0 | 0.000 | 0.000 |
| 1K | 0.097 | 0.095 |
| 2 | 0.190 | 0.180 |
| 3 | 0.281 | 0.286 |
| 4 | 0.371 | 0.369 |
| 5 | 0.463 | 0.454 |
| 6 | 0.557 | 0.546 |
| 7 | 0.655 | 0.639 |
| 8 | 0.761 | 0.734 |
| 9 | 0.875 | 0.858 |
| 10 | 1.000 | 1.000 |

APPENDIX D

DETERMINATION OF TRANSFER FUNCTION COEFFICIENTS FROM UNIT STEP RESPONSE

A particular filter configuration can be characterized by a transfer function, $H(z)$, where

$$H(z) = \frac{a_0 + a_1 z^{-1} + a_2 z^{-2}}{1 + b_1 z^{-1} + b_2 z^{-2}},$$

for z defined as e^{sT} and T a time delay. Since a transfer function relates the output of a system to its input,

$$H(z) = \frac{E_{\text{out}}(z)}{E_{\text{in}}(z)},$$

or,

$$\begin{aligned} E_{\text{out}}(z) &= E_{\text{in}}(z) H(z) \\ &= E_{\text{in}}(z) \cdot \frac{a_0 + a_1 z^{-1} + a_2 z^{-2}}{1 + b_1 z^{-1} + b_2 z^{-2}}. \end{aligned}$$

Multiplying the above equation by the denominator of $H(z)$ yields,

$$\begin{aligned} E_{\text{out}}(z) + b_1 E_{\text{out}}(z) z^{-1} + b_2 E_{\text{out}}(z) z^{-2} &= \\ a_0 E_{\text{in}}(z) + a_1 E_{\text{in}}(z) z^{-1} + a_2 E_{\text{in}}(z) z^{-2}, \end{aligned}$$

so,

$$E_{\text{out}}(z) = a_0 E_{\text{in}} + a_1 E_{\text{in}} z^{-1} + a_2 E_{\text{in}} z^{-2} - b_1 E_{\text{out}} z^{-1} - b_2 E_{\text{out}} z^{-2} .$$

Taking the inverse Z-transform yields the following time expression,

$$e_{\text{out}}(n) = a_0 e_{\text{in}}(n) + a_1 e_{\text{in}}(n-1) + a_2 e_{\text{in}}(n-2) - b_1 e_{\text{out}}(n-1) - b_2 e_{\text{out}}(n-2) ,$$

where,

$$e_{\text{out}}(i) = e_{\text{out}}(iT) .$$

Assuming zero inputs and outputs for $n \leq 0$ and a unit step input, i.e. $e_{\text{in}}(n) = 1$ for all positive n , the output of the filter will be the following sequence for the first five values of n ,

Table XIV

| n | $e_{in}(n)$ | $e_{out}(n)$ |
|---|-------------|---|
| 0 | 0 | 0 |
| 1 | 1 | a_0 |
| 2 | 1 | $a_0 + a_1 - b_1 a_0$ |
| 3 | 1 | $a_0 + a_1 + a_2 - b_1(a_0 + a_1 - b_1 a_0) - b_2 a_0$ |
| 4 | 1 | $a_0 + a_1 + a_2 - b_1(a_0 + a_1 + a_2 - b_1(a_0 + a_1 - b_1 a_0) - b_2 a_0) - b_2(a_0 + a_1 - b_1 a_0)$ |
| 5 | 1 | $a_0 + a_1 + a_2 - b_1(a_0 + a_1 + a_2 - b_1(a_0 + a_1 + a_2 - b_1(a_0 + a_1 - b_1 a_0) - b_2 a_0) - b_2(a_0 + a_1 - b_1 a_0)) - b_2(a_0 + a_1 + a_2 - b_1(a_0 + a_1 - b_1 a_0) - b_2 a_0)$. |

Defining the difference between successive steps in the output wavefore as $d_i = e_{out}(i) - e_{out}(i-1)$, the following relations are found,

$$d_1 = a_0 - 0 = a_0 ,$$

$$d_2 = a_0 + a_1 - b_1 a_0 - a_0 = a_1 - b_1 a_0 ,$$

$$d_3 = a_0 + a_1 + a_2 - b_1(a_0 + a_1 - b_1 a_0) - b_2 a_0 - a_0 + a_1 - b_1 a_0$$

$$= a_2 - b_1(a_1 - b_1 a_0) - b_2 a_0 ,$$

similarly,

$$d_4 = -b_1(a_2 - b_1(a_1 - b_1 a_0) - b_2 a_0) - b_2(a_1 - b_1 a_0) .$$

The relationship for higher differences is,

$$d_k = -b_1 d_{k-1} - b_2 d_{k-2} , \quad k = 4, 5, 6, \dots .$$

It is clear that the term, $a_0 + a_1 + a_2$, is subtracted out in each difference calculation after $k = 4$, thus the higher differences are a function of only b_1 , b_2 , and previous differences. Solving this relation for b_1 yields,

$$b_1 = \frac{-d_k - b_2 d_{k-2}}{d_{k-1}} , \quad \text{for } k \geq 4,$$

so,

$$b_1 = \frac{-d_4 - b_2 d_2}{d_3} .$$

From the higher difference relation,

$$d_5 = -b_1 d_4 - b_2 d_3 .$$

Solving for b_2 and substituting the above relation for b_1 , one finds,

$$b_2 = \frac{d_4^2 - d_3d_5}{d_3^2 - d_2d_4} .$$

Substituting this expression into the relation for b_1 yields,

$$b_1 = \frac{d_2d_5 - d_3d_4}{d_3^2 - d_2d_4} .$$

The a coefficients are now easily determined,

$$a_0 = d_1 ,$$

$$a_1 = d_2 + b_1d_1$$

$$\begin{aligned} &= d_2 + d_1 \cdot \frac{d_2d_5 - d_3d_4}{d_3^2 - d_2d_4} \\ &= \frac{d_1d_2d_5 + d_2d_3^2 - d_1d_3d_4 - d_2^2d_4}{d_3^2 - d_2d_4} , \end{aligned}$$

$$a_2 = d_3 + b_1d_2 + b_2d_1$$

$$= \frac{d_3^3 - 2d_2d_3d_4 + d_2^2d_5 + d_1d_4^2 - d_1d_3d_5}{d_3^2 - d_2d_4} .$$

All coefficients are now determined solely as functions of the differences between successive steps in the output.

Higher order differences could be used to determine b_1

and b_2 , but using d_4 and d_5 minimizes the differences required to determine the five coefficients.

In the case of a first-order transfer function, i.e. $a_2 = b_2 = 0$, a simplified set of equations would result,

$$a_0 = d_1 ,$$

$$a_2 = d_3 + b_1 d_2 + b_2 d_1$$

$$0 = d_3 + b_1 d_2 + 0 \cdot d_1 ,$$

so,

$$b_1 = 1 - \frac{d_3}{d_2} ,$$

$$\begin{aligned} a_1 &= d_2 + b_1 d_1 \\ &= \frac{d_2^2 - d_1 d_3}{d_2} . \end{aligned}$$

Furthermore, since $d_k = -b_1 d_{k-1} - b_2 d_{k-2}$ and $b_2 = 0$,

$$b_1 = -\frac{d_k}{d_{k-1}} .$$

This is a useful result for experimental determination of the transfer function coefficients through measurement of the step response since b_1 may be determined for several values of k and then averaged to reduce error.

APPENDIX E

PROGRAMS TO CALCULATE THE RECURSIVE FILTER COEFFICIENTS FROM THE UNIT STEP RESPONSE

The formulae resulting from the derivation in Appendix D lend themselves to a programmable algorithm for solution. The programmable Tektronix 31 calculator is used to implement the algorithm in the laboratory. The first five step differences from a unit step input are entered in order. The calculator then determines and prints the five second-order coefficients of the transfer function, a_0 , a_1 , a_2 , b_1 , and b_2 .

The basic instructions for using the program are listed below:

1. Turn on calculator and press "clear".
2. Insert tape cartridge containing filter coefficient programs.
3. Press "reset" and transfer the desired program by pressing "from tape" and the number of the track the program is stored on (0 for second-order, 2 for first-order).
4. When "busy" light extinguishes, enter d_1 on keyboard and press "cont". (Note: the calculator should print out d_1 .)
5. Repeat step 4 for d_2 through d_5 . The calculator will finish execution of the program after "cont"

is pressed for d_5 (d_4 for first-order program).

After the coefficients are calculated and printed, the program returns to its beginning and is ready to read a new d_1 .

Two limitations of the second order program are noteworthy. First, the determination of all coefficients except a_0 is dependent on b_2 which is, in turn, dependent on the higher order differences. For the coefficients of interest in this study the differences became steadily smaller, therefore, the higher ordered ones contain larger percentage error. This error then propagates through the other coefficients. Careful measurement of the step response can minimize this problem.

The other limitation of the second-order program concerns the factor $d_3^2 - d_2d_4$. For a first-order filter,

$$b_1 = -\frac{d_3}{d_2} = -\frac{d_4}{d_3},$$

or,

$$d_3^2 = d_4d_2,$$

thus,

$$d_3^2 - d_2d_4 = 0.$$

This factor, however, appears in the denominator of the expressions for all the coefficients except a_0 . Even if experimental error kept the denominator from equaling zero, the answer would be useless. For this reason the first-order program was written. As noted above the first-order program requires four differences to be entered. The coefficient, b_1 , is calculated by the following weighted average,

$$b_1 = -\frac{3}{4} \frac{d_3}{d_2} - \frac{1}{4} \frac{d_4}{d_3} .$$

The average weighting is a crude compensation for the greater percentage error in the d_4 measurement.

APPENDIX F

COMPUTER GENERATION OF THEORETICAL
RECURSIVE FILTER FREQUENCY RESPONSE

For a given recursive filter transfer function, $H(z)$,
where,

$$H(z) = \frac{a_0 + a_1 z^{-1} + a_2 z^{-2}}{1 + b_1 z^{-1} + b_2 z^{-2}} ,$$

the frequency response, $H(j\omega)$, may be calculated by using
the definition,

$$z = e^{sT} = e^{j\omega T} = \cos(\omega T) + j \sin(\omega T) ,$$

where T is the time delay. By substitution,

$$\begin{aligned} H(j\omega) &= \frac{a_0 + a_1(\cos \omega T - j \sin \omega T) + a_2(\cos 2\omega T - j \sin 2\omega T)}{1 + b_1(\cos \omega T - j \sin \omega T) + b_2(\cos 2\omega T - j \sin 2\omega T)} \\ &= \frac{a_0 + a_1 \cos \omega T + a_2 \cos 2\omega T - j(a_1 \sin \omega T + a_2 \sin 2\omega T)}{1 + b_1 \cos \omega T + b_2 \cos 2\omega T - j(b_1 \sin \omega T + b_2 \sin 2\omega T)} . \end{aligned}$$

For a given frequency, the magnitude and phase of the filter
response can be determined,

$$\left\{ H(j\omega) \right\}^2 = [\operatorname{Re}H(j\omega)]^2 + [\operatorname{Im}H(j\omega)]^2 ,$$

$$\angle H(j\omega) = \operatorname{Tan}^{-1} \left[\frac{\operatorname{Im}H(j\omega)}{\operatorname{Re}H(j\omega)} \right] .$$

A computer program was written to calculate, given the transfer function coefficients, the response magnitude and phase over a specified number of steps of a specified interval of frequency. The results were then plotted on the Calcomp plotter. Experimental magnitude versus frequency measurements were read in, frequency normalized, and super-imposed over the theoretical curves.

A sample data deck follows:

1. Line Printer Plot Characters

```

.. * X Y
 1 2 3 4 5

```

2. Transfer Function Coefficients

```

1.0      -1.0      0.      -0.7      0.
1 . . . 10 11 . . . 20 21 . . . 30 31 . . . 40 41 . . 50
All numbers F10.5, in order: a0, a1, a2, b1, b2

```

3. Experimental Data Head Card

```

 9 0    4.125
 1 2 3 4 . . . 13
 I3     F10.5
# Of points  Response Repetition Period (kHz)

```


4. Experimental Data Points

| | |
|-----------------|------------------------|
| 0.387 | 0.001 |
| 1 . . . 10 | 11 . . . 20 |
| F10.5 | F10.5 |
| Frequency (kHz) | Magnitude (normalized) |

The program will print on the line printer the coefficients, the data points, a theoretical magnitude versus frequency plot, a theoretical phase versus frequency plot, and a message stating the status of the Calcomp plot, if requested. A labeling statement is used to title the Calcomp plot with the coefficients of the transfer function. The title declaration cards need to be changed as different coefficients are used for the title to coincide with the response determining coefficients.

APPENDIX G

Non-Recursive Filter Design

The design of a non-recursive filter is based upon the periodic nature of a sampled filter frequency response. The response may be described by a Fourier series,

$$H(j\omega) = \sum_{k=-\infty}^{\infty} D_k e^{jk \left(\frac{2\pi}{T}\right) \omega},$$

where

$$D_k = \frac{1}{2\pi} \int_{-\pi/T}^{\pi/T} H(j\omega) e^{-jk\omega T} d\omega.$$

The particular filter response of interest in this study is a bandpass filter with rectangular passbands,

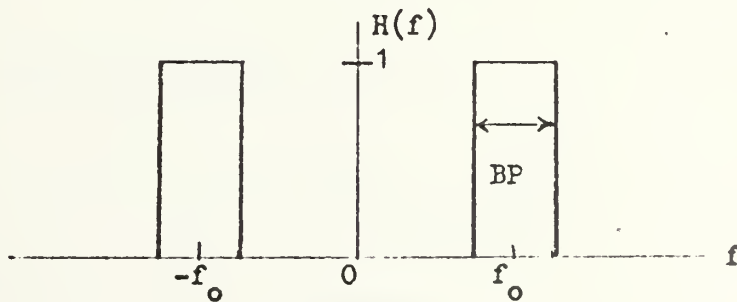


FIGURE G-1 Rectangular Passband Filter

which can be described with the parameters: response repetition period, f_s ; passband center frequency, f_0 ; and pass bandwidth, BP. The filter quality factor, Q , is defined as,

$$Q = \frac{f_0}{BP} ,$$

and the fraction of the response repetition period which corresponds to the center frequency is defined as,

$$FFS = \frac{f_0}{f_s} .$$

The filter description is complete by specifying f_s , Q , and FFS since the center frequency and bandwidth can be calculated from the above three parameters. The repetition period is,

$$f_s = \frac{1}{T} \text{ Hz} \quad \text{or} \quad \omega_s = \frac{2\pi}{T} \text{ radians/second.}$$

For a rectangular bandpass filter,

$$H(j\omega) = \begin{array}{ll} 1 & |f - f_0| \leq \frac{1}{2}BP \\ 0 & \text{elsewhere} \end{array} ,$$

therefore,

$$\begin{aligned}
 D_k &= \frac{2T}{2\pi} \int_{2\pi(f_0 - \frac{1}{2}BP)}^{2\pi(f_0 + \frac{1}{2}BP)} 1 \cdot e^{-jk\omega T} d\omega \\
 &= \frac{2}{k\pi} \sin(k\pi BP T) e^{-jk(2\pi f_0 T)} \\
 &= \frac{2}{k} \sin(k\pi BP T) (\cos 2\pi f_0 T - j \sin 2\pi f_0 T) .
 \end{aligned}$$

Since only real terms may be implemented, the series coefficients are,

$$D_k = \frac{2}{k\pi} \sin(k\pi BP T) \cos(2\pi f_0 T) .$$

The series expansion has infinite terms; however, the non-recursive filter has a finite number of taps available to approximate the series,

$$\begin{aligned}
 H(j\omega) &= \sum_{k=-N}^N D_k e^{jk\omega T} \\
 &= \sum_{k=-N}^N D_k (\cos(k\omega T) - j \sin(k\omega T))
 \end{aligned}$$

By using the definition of,

$$z = e^{sT} = e^{j\omega T} ,$$

$$H(z) = \sum_{k=-N}^N D_k z^k .$$

Since the Z-transform must contain only non-positive powers of z , i.e. no anticipated signal values only delayed values,

$$H(z) \cdot z^{-N} = \sum_{k=-N}^N D_k z^{k-N} .$$

This relation states that the transfer function will contain a constant delay of NT from input to output in addition to the response phase. A possible implementation of this function is illustrated in Figure 3.1. From the expression derived for the bandpass filter,

$$D_k = \frac{2 \text{BP} \cdot T}{1} \frac{\sin(k\pi \text{BP} \cdot T)}{k\pi \text{BP} \cdot T} \cos(2k\pi f_0 T) ,$$

it can be seen that this is an even function of k , so,

$$D_k = D_{-k} .$$

In addition,

$$\lim_{k \rightarrow 0} D_k = 2 \cdot \text{BP} \cdot T \cdot (1) \cdot (1) = 2 \cdot \text{BP} \cdot T ,$$

this can be expressed in terms of the design parameters, Q and FFS,

$$D_0 = 2 \cdot \text{BP} \cdot T = 2 \frac{f_0}{Q} \cdot \frac{1}{f_s} = 2 \cdot \frac{\text{FFS}}{Q} .$$

Window weighting functions are used to modify the coefficients in order to improve the filter characteristics. A Hamming window is frequently used where the weighted coefficient, A_k , is,

$$A_k = D_k \left(0.54 + 0.46 \cos\left(\frac{k}{N} \pi\right) \right) .$$

The expression multiplying D_k is called the window weighting function.

APPENDIX H

Computer Calculation of Coefficients and Tapping Resistances for the Non-Recursive Filter

From the analysis performed in Appendix G for a bandpass filter,

$$D_k = D_{-k} = 2 \frac{FFS}{Q} \frac{\sin(kX)}{kX} \cos(kY) \quad , \quad -N \leq k \leq N \quad ,$$

where,

$$X = \pi \frac{BP}{f_s} \quad , \quad \begin{array}{l} BP = \text{pass bandwidth} \\ f_s = \text{response repetition period,} \end{array}$$

$$Y = 2\pi \frac{f_0}{f_s} \quad , \quad f_0 = \text{passband center frequency,}$$

$$Q = \frac{f_0}{BP} \quad ,$$

$$FFS = \frac{f_0}{f_s} \quad .$$

For a Hamming weighting window,

$$A_k = A_{-k} = D_k (0.54 + 0.46 \cos(\frac{k}{N} \pi)) \quad .$$

For the TAD-12 analog delay device, the coefficients are implemented by input resistances to the operational amplifier summing circuit, as shown in Figure H-1.

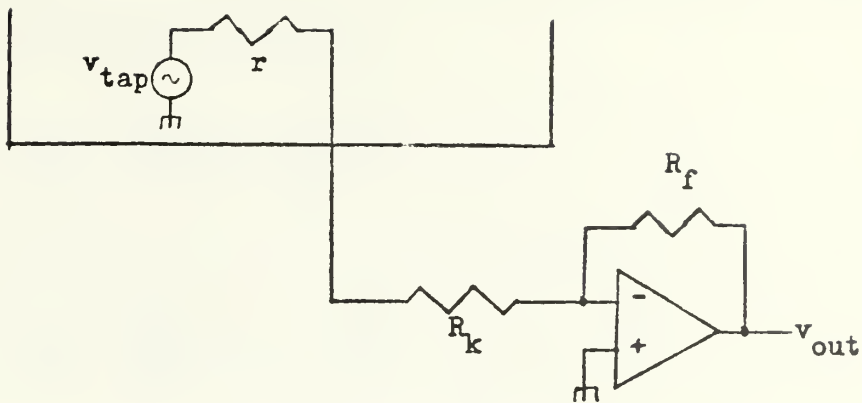


FIGURE H-1 Coefficient Implementation

In order to minimize the loading effect on the tap, the tapping resistors, R_k , are greater than or equal to 10 K ohms. The contribution of a single tap, V_k , to the output, V_{out} , is the product of V_k and the coefficient, A_k , or,

$$|A_k| = \left| \frac{V_{out}}{V_k} \right| = \frac{R_f}{r + R_k} \cdot$$

This expression indicates that R_k is inversely proportional to A_k , therefore the largest coefficient will correspond to the minimum allowable resistance, 10K, so,

$$A_{max} = \frac{R_f}{r + 10K} \cdot$$

Solving this equation for R_f and substituting that result into the A_k expression yields,

$$|A_k| = \frac{A_{\max}(r + 10K)}{r + R_k} ,$$

or,

$$R_k = \frac{A_{\max}}{|A_k|} (r + 10K) - r .$$

For the TAD-12, the output impedance for a tap, r , is about 5K.

A computer program was written to calculate the weighted and unweighted coefficients and their respective tapping resistances for a given $T = f_s^{-1}$, Q , FFS, and a pair of N . These parameters are inserted directly into the program as follows,

1. T

```

      T = 0.001
1 ... 6 7 . . . 13
  
```

2. FFS

```

      FFS = 0.25
1 ... 6 7 . . . 14
  
```


3. Q

```
Q = 15.  
1 ... 6 7 . . . 11
```

4. Truncation points, NM1 and NM2

```
NM1 = 5  
1 ... 6 7 . . .
```

```
NM2 = 11  
1 ... 6 7 . . .
```

Note: The program calculates results for,

$$H(z) = \sum_{k=-NM1}^{NM1} A_k z^{k-NM1} ,$$

and,

$$H(z) = \sum_{k=-NM2}^{NM2} A_k z^{k-NM2} .$$

5. Maximum passband magnitude, CA

```
CA = 1.  
1 ... 6 7 . . .
```

Note: CA was set to one in the derivation in Appendix G, but the program is more general in this respect.

APPENDIX I

Computer Calculation of Non-Recursive Filter Frequency Response

Since the transfer function for a non-recursive filter is,

$$H(z) = \sum_{k=-N}^N A_k z^k \quad , \quad \text{where } z = e^{j\omega T} \quad ,$$

it is possible to calculate the magnitude and phase of $H(j\omega)$, where,

$$\begin{aligned} H(j\omega) &= \sum_{k=-N}^N A_k e^{jk\omega T} \\ &= \sum_{k=-N}^N A_k (\cos(k\omega T) + j \sin(k\omega T)) \\ &= A_0 + \sum_{k=1}^N [(A_k + A_{-k}) \cos k\omega T + j(A_k - A_{-k}) \sin k\omega T] \quad . \end{aligned}$$

The real part of $H(j\omega)$ is clearly the cosine terms,

$$\text{Re } H(j\omega) = A_0 + \sum_{k=1}^N (A_k + A_{-k}) \cos(k\omega T) \quad ,$$

while the imaginary part of $H(j\omega)$ is the sine term portion,

$$\text{Im } H(j\omega) = \sum_{k=1}^N (A_k - A_{-k}) \sin(k\omega T) \quad .$$

The magnitude and phase of $H(j\omega)$ are readily calculated,

$$|H(j\omega)| = \sqrt{[\operatorname{Re} H(j\omega)]^2 + [\operatorname{Im} H(j\omega)]^2} ,$$

$$\angle H(j\omega) = \tan^{-1} \left[\frac{\operatorname{Im} H(j\omega)}{\operatorname{Re} H(j\omega)} \right]$$

A program was written to calculate the magnitude and phase of $H(j\omega)$ from $0 = j\omega = \frac{2\pi}{T}$, plot the result on the line printer and Calcomp lotter for a given set of A_k . In addition, experimental data points may be read and plotted over the theoretical curves.

The above analysis assumes perfect impulse sampling, however, actual devices will have some sampling envelope, usually a $\frac{\sin x}{x}$ function, which will multiply the magnitude of the response. Provision is made in the program to introduce this envelope.

The following sample deck will illustrate the use of the program.

1. Line Printer Plot Characters

```
      . * X Y
1 2 3 4 5
```


2. NMAX, the number of coefficients

$$NMAX = 2N + 1$$

1 1

1 2 3

(I3)

3. Coefficients

-0.0235

1 . . . 10

(F10.5)

4. Data Header Card

NPTS, the number of data points (multiple of 30)

FCK, the clock frequency

XX, the value of sampling envelope at
magnitude maximum frequency

6 0 50. 0.9845

1 2 3 4 . . . 13 14 . . . 23

NPTS FCK XX

(I3) (F10.5) (F10.5)

5. Data Points

FX, observed frequency

HX, normalized magnitude

6.735 0.033

1 ... 10 11 ... 20

| FX | HX |
|---------|---------|
| (F10.5) | (F10.5) |

Note: If dummy cards are required to make NPTS
a multiple of 30, use FX = 999., HX = 1.

When the Calcomp plotter is used the "call draw" cards are included and the title declaration cards are modified to title the plot with the proper number of terms and FFS value. The program will always print the number of coefficients, the coefficients, and the data points so that proper data entry can be checked.

APPENDIX J

Effects of Hamming Weighting

The use of a weighting factor, W_k , in the time domain is equivalent to convolving the frequency response of the desired filter with the Fourier transform of the weighting function. The Hamming weighting function,

$$w_k(t) = (0.54 + 0.46 \cos(\frac{\pi}{NT} kT)) \quad ,$$

which has a Fourier transform, $W_k(j\omega)$,

$$W_k(j\omega) = 0.54 \delta(j\omega) + 0.23(\delta(j\omega + \frac{\omega_s}{2N}) + \delta(j\omega - \frac{\omega_s}{2N})) ,$$

where,

$$\omega_s = \frac{2\pi}{T} \quad .$$

This result can be illustrated as three impulses as in Figure J-1.

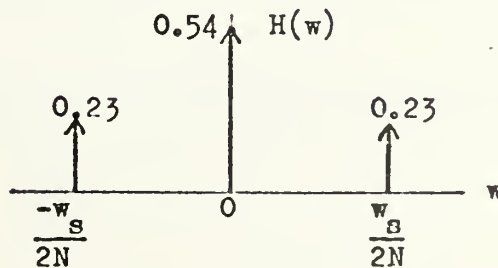


FIGURE J-1 Fourier Transform of Hamming Function

When a bandpass filter is convolved with the impulses, its bandwidth is increased by an amount proportional to the spacing between the impulses. This added bandwidth will be a fraction, γ , of the Hamming function bandwidth,

$$\text{added BW} = \gamma \left(\frac{\omega_s}{2N} - \frac{-\omega_s}{2N} \right) = \gamma \frac{\omega_s}{N} .$$

The value of gamma is estimated by the following procedure. If the values of the impulses were equal, then the -3 dB points of the convolved response would be shifted, roughly, by spacing of the impulses, $\frac{\omega_s}{2N}$, as illustrated below.

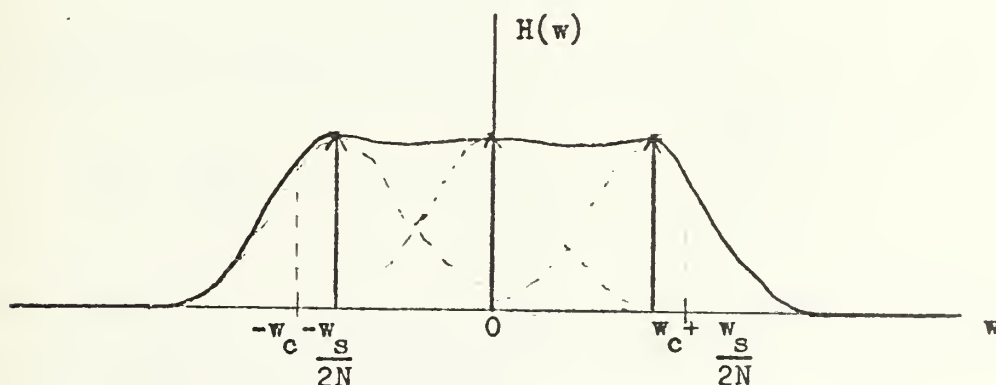


FIGURE J-2 Equal Impulses

The added bandwidth would be equal to the spacing between the impulses, $\frac{\omega_s}{N}$, or ,

$$\gamma = 1 .$$

For the case where the outboard impulses are zero amplitude, the response is just convolved with a single impulse and is exactly reproduced, so zero bandwidth is added. In this case, gamma is zero. A relationship is suggested by this bracketing of gamma,

$$\gamma = \frac{\text{amplitude of outboard impulses}}{\text{amplitude of inboard impulse}} ,$$

thus for a Hamming function,

$$\gamma = \frac{0.23}{0.54} = 0.426 .$$

The expected Q for a bandpass filter is,

$$Q = \frac{\omega_0}{BW} .$$

Since the Hamming weighting adds some to the bandwidth, B, the Q is expected to be less,

$$Q' = \frac{\omega_0}{BW + B} < Q .$$

By dividing the expression for Q' by that for Q yields

$$\begin{aligned}
Q' &= Q \frac{BW}{BW + B} \\
&= Q \frac{BW}{BW + \frac{\gamma \omega_s}{N}} \\
&= Q \frac{aN}{aN + \gamma Q} \quad , \quad \text{where } a = \frac{\omega_0}{\omega_s} \quad .
\end{aligned}$$

It is noteworthy that the expression for Q' indicates that the limit of Q' as N gets larger is Q .

If one uses the main lobe criterion for expressing the impulse response by specifying the responses within the first nulls, one finds that,

$$Q = (2N + 1) a\pi \quad .$$

Substituting this result into the expression for Q' yields,

$$Q' = a \frac{(2N^2 + N) \pi}{(2\pi\gamma + 1)N + \gamma\pi} \quad .$$

For the case of $N = 5$ and $\gamma = 0.43$,

$$Q' = a (8.69) \quad ,$$

so for $a = 0.25$ and 0.5 , Q' will be 2.17 and 4.35, respectively.

LIST OF REFERENCES

1. Gold, B. and Rader, C.M., Digital Processing of Signals, McGraw-Hill, 1969.
2. Busignies and Dishal, "Relations Between Speed of Indication, S/N, Bandwidth in Radio Navigation and DF," Proceedings of The I.R.E., v. 37, no. 5, p. 480-481, May 1949.
3. Skolnik, M.I., Introduction to Radar Systems, McGraw-Hill, 1962.
4. Arndt, G.D., "TV Signal Enhancement in Noisy Channels by Use of Comb Filtering Techniques," IEEE Transactions - Communications, p. 331-336, April 1973.
5. Illetschko, G., "Exact Separation of Luminance and Chrominance Components, PAL to SECAM Conversion," International Elektronische Rundschau, v. 23, no. 8, p. 197-200, August 1969.
6. Mavrodieva, I.K., "Brightness and Chrominance Separation in Color TV Cameras," Tekh. Kino and Telev., v. 11, p. 49-50, November 1970.
7. White, S.A., "Comb Filter For Digital Servo Controller," IEEE Transactions - Automatic Control, p. 423-424, August 1969.
8. Webb, J.A., "Computation of Voltage and Power Spectra," Proceedings 5th International Aerospace Instrumentation Symposium, Cranfield, U.K., 25 March 1968.
9. Taub, H. and Schilling, D.L., Principles of Communication Systems, McGraw-Hill, 1971.

INITIAL DISTRIBUTION LIST

| | No. Copies |
|---|------------|
| 1. Defense Documentation Center Cameron Station Alexandria, Virginia 22314 | 2 |
| 2. Library, Code 0212 Naval Postgraduate School Monterey, California 93940 | 2 |
| 3. Department Chairman, Code 52 Department of Electrical Engineering Naval Postgraduate School Monterey, California 93940 | 2 |
| 4. Assoc. Professor T.F. Tao, Code 52 TV Department of Electrical Engineering Naval Postgraduate School Monterey, California 93940 | 10 |
| 5. ENS B.R. Freund, USN 1320 NW Forest Lane Corvallis, Oregon 97330 | 3 |



Thesis
F865
c.1

Freund
Implementation of
comb filters by sampled
analog techniques.

26 MAY 76
18 OCT 76

12 NOV 77
19 JUN 78

17 OCT 78
22 NOV 78
15 DEC 79

161485

23472
23512
24671
24670

25268
~~25268~~
24666

23472
23512
24671
24670
25268
~~25268~~
24666

485

ed

Thesis
F865
c.1

Freund
Implementation of
comb filters by sampled
analog techniques.

161485

thesF865

Implementation of comb filters by sample



3 2768 000 98703 6
DUDLEY KNOX LIBRARY